ABSTRACT

Investigations of Dynamic, Higher-Order DNA Polymerase Complexes in Archaea

Matthew T. Cranford, Ph.D.

Mentor: Michael A. Trakselis, Ph.D.

As the blueprint for cellular functions, DNA must be properly maintained and copied. Exposure to DNA damaging agents leads to formation of genomic lesions which cause stalling of high-fidelity (HiFi) DNA polymerases (Pols) during replication. However, the damaged DNA template may still be replicated by specialized Pols which perform translesion synthesis (TLS). Though TLS provides a mechanism of cellular tolerance to DNA damage, it also presents the risk of mutagenesis which must be regulated. Recent investigations have characterized a network of protein-protein interactions among multiple Pols and their accessory factors, highlighting several points of TLS Pol regulation to be explored. This collection of work describes the formation of an archaeal supraholoenzyme (SHE) replication complex on DNA, composed of the HiFi PolB1 and TLS PolY bound to the processivity clamp PCNA123. Formation of this higher-order complex is mediated through individual Pol contacts with PCNA123 and direct contacts between the two Pols. This leads to the hypothesis that DNA is 'handed off' between Pols within a SHE complex, rather than distributively exchanged. Upon encountering a DNA lesion, PolB1 is stalled and must hand off the DNA for TLS by PolY. After bypass of an 8-oxoguanine lesion by

PolY, an intermediate position was identified three base pairs downstream of the lesion. This points to a specific position where PolY passes the DNA back to PolB1 to restore HiFi activity. The coupling of Pols within the SHE complex optimizes their combined activities to promote efficient bypass and extension from the lesion while limiting error-prone TLS activity. This work also reports findings related to alternative higher-order complexes of PolB1, including a homotrimeric PolB1 complex and a heterotrimeric PolB1 associated with two novel binding proteins. Altogether, this work encourages further study of higher-order DNA polymerase complexes in other organisms. By understanding these points of regulation and how DNA is handed off among the various Pols, these mechanisms may be targeted to minimize the adverse effects of TLS.

Investigations of Dynamic, Higher-order DNA Polymerase Complexes in Archaea

by

Matthew T. Cranford, B.S., B.S.

A Dissertation

Approved by the Department of Chemistry and Biochemistry

_____

Patrick Farmer, Ph.D., Chairperson

Submitted to the Graduate Faculty of
Baylor University in Partial Fulfillment of the
Requirements for the Degree
of

Doctor of Philosophy

Approved by the Dissertation Committee

_____

Michael A. Trakselis, Ph.D., Chairperson

_____

Mary Lynn Trawick, Ph.D.

_____

Jung Hyun Min, Ph.D.

_____

Kevin Chambliss, Ph.D.

_____

Bessie Kebaara, Ph.D.

Accepted by the Graduate School

December 2020

_____

J. Larry Lyon, Ph.D., Dean

Page bearing signatures is kept on file in the Graduate School.

TABLE OF CONTENTS

LIST OF FIGURES

LIST OF TABLES

ACKNOWLEDGMENTS

I am incredibly grateful to fellow members of the Trakselis Lab, past and present, for setting a foundation to build from, for carrying this research forward, and for making my time at Baylor University an experience to remember. I have enjoyed working with, learning from, and growing alongside each of you. Thank you to all my friends and family who have supported me along the way. In the trials and the triumphs, your encouragement has motivated me to persevere and to keep moving forward. Finally, my sincerest gratitude goes to Dr. Trakselis. Your guidance, patience, and mentorship has developed me into the researcher I am today and has inspired my continued interest in the field of DNA replication and repair.

DEDICATION

To Laura, for your constant love, continuous support, and for always believing in me

ATTRIBUTIONS

Dr. Aurea M. Chu contributed to the literature review presented in Chapter Two and performed the analytical gel filtration, western blots, and fluorescence resonance energy transfer (FRET) analyses in Chapter Three. Dr. Robert J. Bauer and Joshua K. Baguley contributed to the production of plasmid constructs and purification of proteins used in these studies. Joseph D. Kaszubowski purified proteins, contributed to pre-steady-state assays and fluorescence anisotropy, and assisted in the composition of Chapter Four. Matthew T. Cranford contributed to the literature review in Chapter Two, performed cloning, protein expression and purification, polymerase activity assays, and data analysis in Chapter Three; he also performed and analyzed the data for steady-state and pre-steady-state kinetic assays, as well as fluorescence anisotropy in Chapter Four. Dr. Michael A. Trakselis coordinated the literature review in Chapter Two, assisted with experimental design and composition of Chapters Three and Four, and served as corresponding author for all published manuscripts.

CHAPTER ONE

Introduction

Deoxyribonucleic Acid (DNA)

The chemicals which compose the structural and functional make-up of a cell are classified into four major biomacromolecules: proteins, lipids, carbohydrates, and nucleic acids. Nucleic acids are long polymers of ribo- or deoxyribonucleotides (in RNA and DNA, respectively). The DNA template contains sequences of genes which act as the blueprint of instructions for cellular maintenance. According to the central dogma of molecular biology, these DNA sequences are transcribed into RNA messages, transmitted to the cellular machinery, and translated into the ordered assembly of amino acids into polypeptide chains (**Fig 1.1**). The original DNA blueprint encodes the amino acid sequence

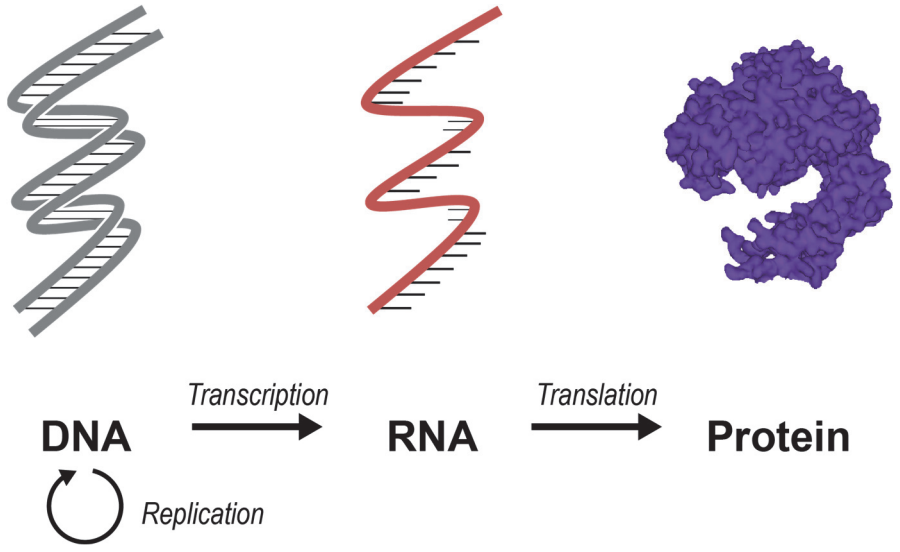

Figure 1.1: Central Dogma of Molecular Biology. Prior to cell division, DNA is replicated to form two identical copies for each daughter cell. The DNA template is transcribed into RNA. This RNA message contains a series of codons which are translated into a protein.

and primary structure of the polypeptide, ultimately dictating its higher-order structure and assembly into a protein. The various proteins which are synthesized then serve as structural components for the cell or act as catalytic enzymes which metabolize and maintain the other biomacromolecules within the cell.

The DNA instructions are encoded in the nitrogenous bases of four deoxyribonucleotides: adenine, thymine, cytosine, and guanine (A, T, C, G, respectively; **Fig. 1.2**). Upon transcription into RNA, thymine is substituted for uracil. The order of bases in an RNA transcript is read in a 3-letter reading frame (or codon) which instructs for one of the twenty natural amino acids to be added to an elongating polypeptide chain. According to this simple genetic language, a 4-letter alphabet (A, T, G, C) forms specific arrangements of 3-letter words (codons) from a dictionary that contains only twenty entries (amino acids). Yet, each organism maintains and expresses its own intricate story, contributing to the immense and diverse body of living literature that composes the biological world.

Discovering, Deciphering, and Duplicating DNA

In the 1860s, DNA was first isolated from cell nuclei and determined to be a novel macromolecule by Friedrich Miescher.[1] Around that time, Gregor Mendel had laid the foundations for understanding the inheritance of observable phenotypes.[2] However, it would take almost another century before the genetic capacity of DNA was identified and linked to the basis of phenotypic inheritance. In 1944, Avery, MacLeod, and McCarty observed that nonvirulent bacterial cells developed a virulent phenotype when exposed to DNA from a virulent strain; they proposed DNA as the "transforming principle."[3] Soon

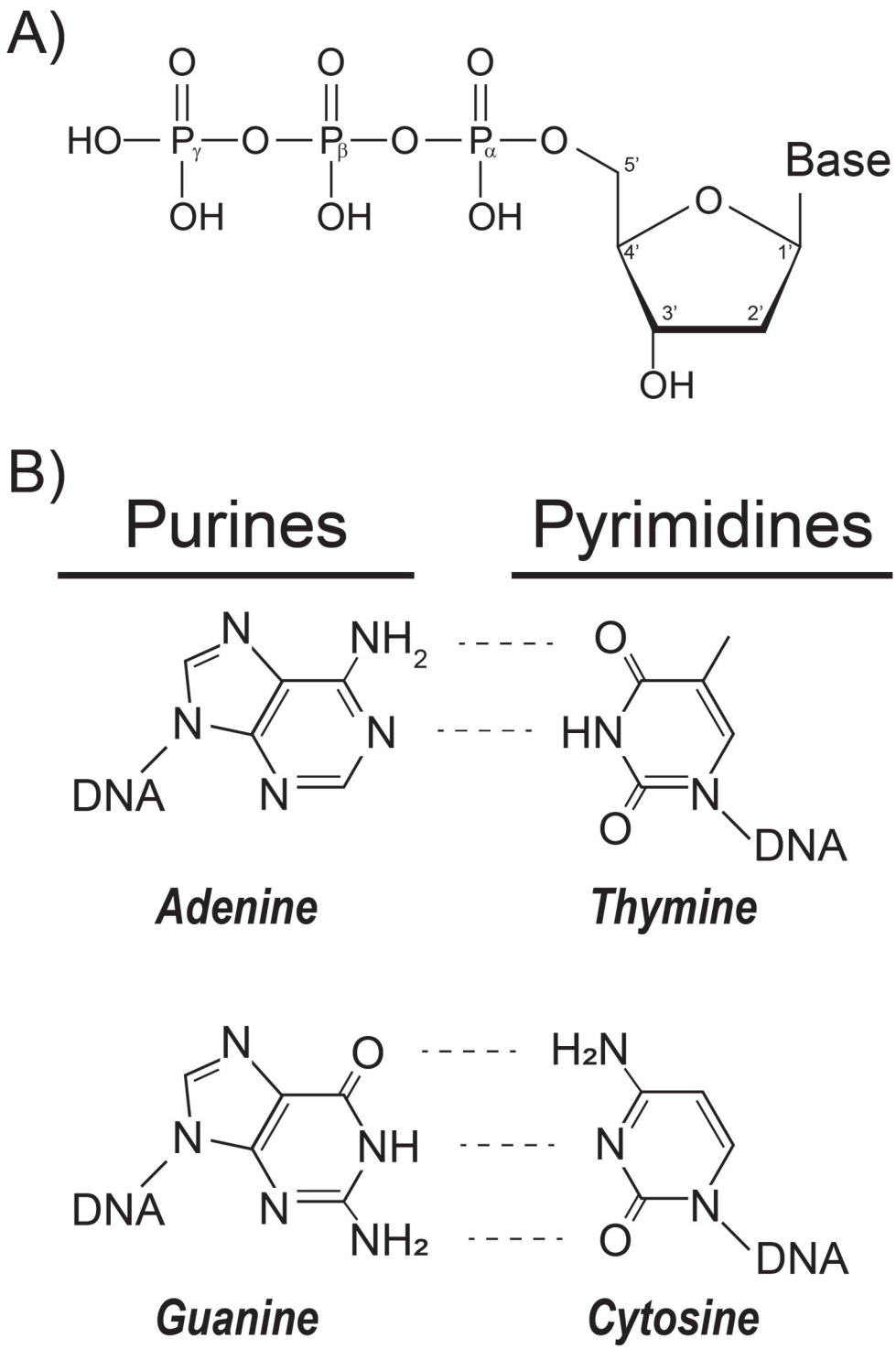

Figure 1.2: Structure of deoxynucleotide triphosphates and the nitrogenous DNA bases. The common structure of a deoxyribonucleotide triphosphate (dNTP), composed of a 2'deoxyribose, a 5' triphosphate group, and a 1' nitrogenous base (A). The DNA bases form complementary pairs, A with T and G with C, through hydrogen bonds (B).

after, Hershey and Chase observed the transfer of radiolabeled DNA from a bacteriophage into a bacterial cell, providing further evidence that nucleic acids were indeed the source of inheritable genetic information.[4] By 1953, x-ray diffraction studies by Franklin and Wilkins provided the foundation for Watson and Crick to solve the molecular structure of DNA.[5, 6] According to their model, two DNA strands with 5'→3' polarity form an anti-parallel double helix which, in agreement with Chargaff's Rules,[7] forms complementary base pairs between A=T and G≡C.

Given that each cell requires a copy of genomic DNA, every round of cell division requires duplication of the genome. Early models described the mechanism of DNA replication by three distinct models: conservative, semi-conservative, and dispersive. By tracking successive generations of DNA containing heavy nitrogen, Meselson and Stahl demonstrated that DNA is replicated in a semi-conservative manner.[8] By this model, the original (or parental) DNA strands are used as templates for synthesis of two nascent strands. As a result, two identical DNA copies are synthesized with each new duplex containing one of the parental strands.

Shortly after the molecular structure of DNA was reported, DNA polymerases (Pols) were identified and characterized as the enzymes which catalyze DNA synthesis. Prior to Pol activity, genomic DNA is unwound by a helicase which separates the duplex into single strands (**Fig 1.3)**. A primase then synthesizes a ribonucleotide primer, providing a 3'-OH group which serves as the starting point for catalysis by the DNA Pol. From this primer terminus, the DNA Pol associates with a processivity clamp which stabilizes the Pol to the DNA substrate. DNA synthesis proceeds as the Pol incorporates incoming deoxyribonucleotide triphosphates (dNTPs) complementary to the template strand,

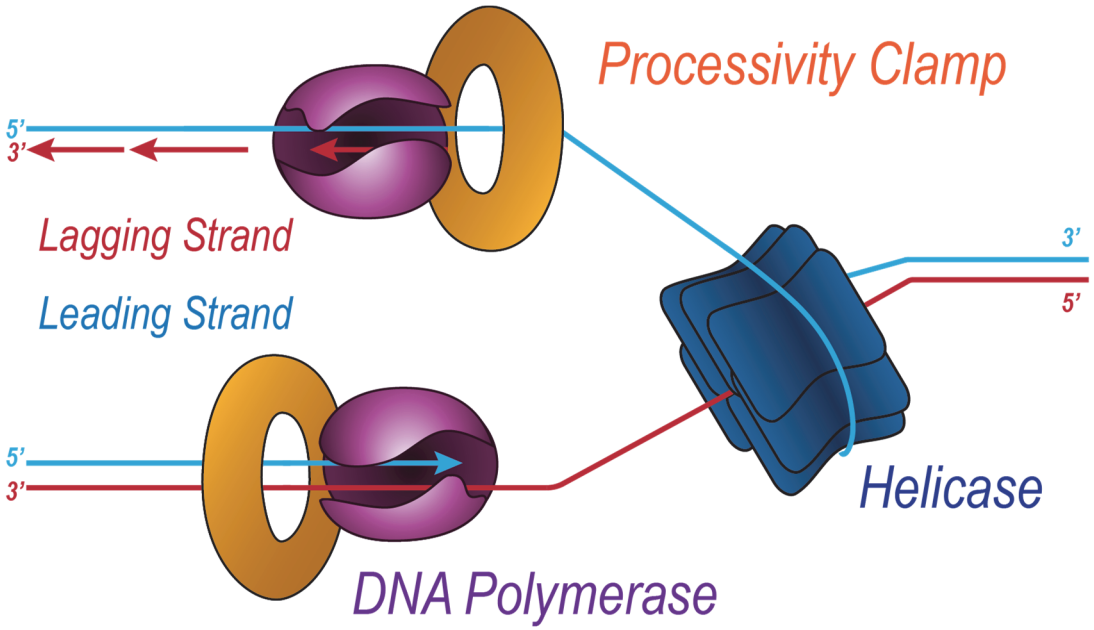

Figure 1.3: Proteins involved in semiconservative DNA replication. Duplex DNA is first unwound into single strands by DNA helicase (blue). Once the template is primed, DNA polymerase (purple) associates with a processivity clamp (orange) to catalyze DNA synthesis in a 5'→3' direction. The directionality of DNA synthesis on anti-parallel strands requires different modes of replication for the leading and lagging strands.

continuously elongating in a 5'→3' direction. From the 5'→3' directionality of DNA synthesis and the anti-parallel nature of the template strands, there is an asymmetry in the way that each strand is replicated. On the 'Leading-Strand,' the nascent DNA is continuously elongated in the 5'→3' direction, following the progression of the helicase. Contrarily, on the 'Lagging-Strand,' synthesis must proceed in the opposite direction of DNA unwinding. This requires synthesis of multiple primers as more of the single-stranded template becomes available. These discontinuous segments, referred to as 'Okazaki fragments,' are then processed to form a continuous DNA strand.

Structurally, the DNA Pols possess a 'right-handed' conformation with Fingers, Palm, and Thumb subdomains (**Fig. 1.4A**).[9] The Thumb tracks along the DNA, while the Fingers facilitate binding of the incoming dNTPs. Upon formation of a proper base pair,

the Fingers and Thumb undergo a conformational change which allows the hand to 'close' on the paired DNA:dNTP substrate.[10] The Pol active site is found in the Palm, where a conserved tricarboxylic core coordinates Mg^{2+} ion cofactors which facilitate nucleotidyl transfer of the dNTP to the elongating 3' DNA end (**Fig 1.4B**). After catalysis and release of pyrophosphate, the hand 'opens' to allow translocation of the Pol to the next template base.

Some DNA Pols also contain an exonuclease domain which catalyzes the removal of nucleotides from the 3' DNA terminus. If an incorrect nucleotide is incorporated, the

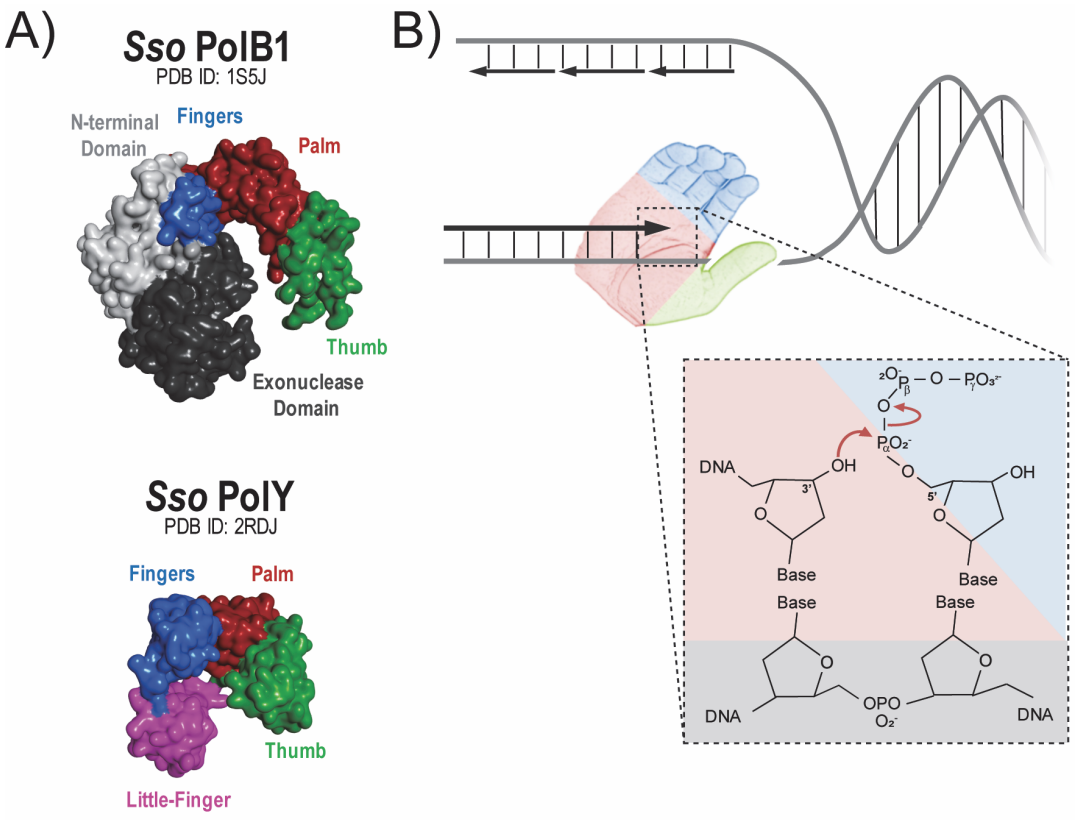

Figure 1.4: DNA Polymerases. PolB1 and PolY are the two major DNA Pols from the model archaeon *Saccharolobus solfataricus* (*Sso*). They adopt the canonical 'right-handed' structure of DNA Pols, described by the fingers (blue), palm (red), and thumb (green) subdomains (A). Pol catalysis is performed in the palm where the 3'-OH of the primer terminus attacks the α-phosphate of an incoming nucleotide (B).

Pol becomes inefficient for additional extension. This allows the 3' DNA terminus to be transferred to the exonuclease domain for degradation. This activity acts as a proofreading mechanism which removes errors made during replication. Together, the stringent active site and proofreading abilities contribute to incredible accuracy and high fidelity (HiFi) of replicative Pols during DNA synthesis.

In the mid-1990s, only a few Pols had been characterized. However, as detailed by Vaisman and Woodgate,[11] recent improvements in biochemical methods have accelerated progress in the field of molecular genetics. In just the last few decades, numerous Pols from all domains of life (and entirely new classes of Pols, in fact) have been identified and demonstrate diverse roles in genomic maintenance (reviewed in Chapter Two). Further, the enzymological basis of DNA Pols has been tailored for breakthrough biotechnological applications such as PCR, genetic sequencing, and directed evolution. Given the recent and rapid expansion of this field, this has only made additional space for continued investigations into the DNA Pols and the roles they play in genomic maintenance.

Responding to Damage in the Double Helix

Cellular exposure to environmental and metabolic agents can lead to chemical modifications and formation of lesions on the DNA bases. This includes oxidative damage, UV-induced crosslinking, methyl adducts, and even loss of the entire base (**Fig. 1.5**). Some estimations have approximated over 70,000 DNA lesions per cell per day.[12] Though numerous pathways have been shown to repair various forms of DNA damage, unrepaired lesions may persist and cause problems during DNA replication. When a Pol encounters a genomic lesion, its active site may be unable to accommodate the damaged base and fails to perform catalysis. Alternatively, the exonuclease domain may sense distortions in the

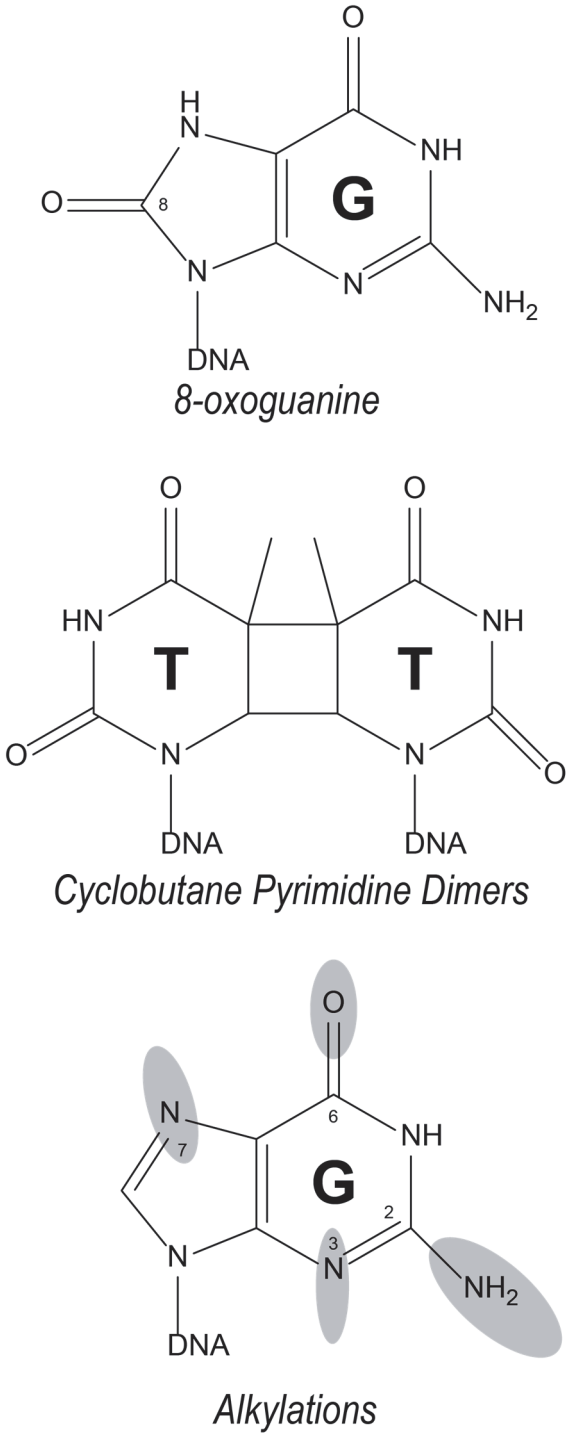

Figure 1.5: Commonly Encountered DNA lesions. Exposure to oxidative agents leads to formation of 8-oxoguanine. UV exposure induces intrastrand crosslinks in the form of cyclobutane pyrimidine dimers. Guanine is also commonly alkylated at multiple positions, as indicated by grey ovals. These lesions disrupt formation of proper base pairs during DNA replication and cause DNA polymerases to stall.

DNA structure and remove nucleotides which are incorporated across a template lesion. This stalling of the replicative Pol halts progression of the replication fork and presents a threat to genomic maintenance. However, this stalling can be relieved by a special class of DNA Pols which perform translesion synthesis (TLS).

The TLS Pols contain a wider, more solvent-exposed active site which can accommodate bulky lesions and distortions in the DNA backbone. This structure allows the TLS Pols to replicate across and bypass DNA lesions. In eukaryotes, each TLS Pol demonstrates efficient and accurate bypass of a specific type of DNA lesion, suggesting that they have divergently evolved to respond to the numerous forms of DNA damage.[11] When a TLS Pol replicates across a genomic lesion, this allow for tolerance of the damage site which must be repaired later.[13] However, on undamaged DNA, the less stringent TLS Pol active site is prone to misincorporations and replication errors. TLS Pols also lack an exonuclease domain, contributing to their reduced fidelity during replication.[14] Instead, the TLS Pols possess a 'Little-Finger' domain which contributes to error-prone lesion bypass activity.[15] Therefore, proper genomic maintenance requires a regulated balance of TLS Pol functions, providing relief to lesion-induced stalling while also limiting the potential for mutagenesis during TLS.

TLS activity requires the recruitment of a TLS Pol to DNA, a process which is still under investigation and is the subject of this current study. At a stalled replication fork, TLS Pols may be recruited through a stochastic, distributive process involving constant and random dissociation and reassociation of Pols at the primer terminus; alternatively, through a more stable, concerted process, multiple Pols may be bound in a higher-order complex during replication (reviewed in Chapter Two). Previously, TLS regulation was

shown to be mediated through transcriptional control and post-translational modifications. However, in all domains of life, a network of interactions has been described among several proteins involved in DNA replication and repair. This suggests the potential for multiple points of TLS Pol regulation which remain to be explored.

In this thesis, a review of relevant literature is presented, followed by the findings of two original research manuscripts and a summary of additional unpublished work on the investigations of dynamic, higher-order DNA polymerase complexes in archaea. These findings report the formation of a 'supraholoenzyme' (SHE) complex composed of both a HiFi and TLS Pol bound to a single processivity clamp, mediated by multiple protein-protein interactions. Formation of this SHE complex allows the DNA substrate to be directly handed off between Pols, optimizing their combined activities for efficient replication and bypass of DNA lesions.

CHAPTER TWO

Coordination and Substitution of DNA Polymerases in Response to Genomic Obstacles

This chapter published as: Trakselis, M.A., Cranford, M.T., and Chu, A.M. (2017) Coordination and Substitution of DNA Polymerases in Response to Genomic Obstacles. *Chem. Res. Toxicol. 30* (11), 1956-1971.

Abstract

The ability for DNA polymerases (Pols) to overcome a variety of obstacles in its path to maintain genomic stability during replication is a complex endeavor. It requires the coordination of multiple Pols with differing specificities through molecular control and access to the replisome. Although a number of contacts directly between Pols and to accessory proteins have been identified forming the basis of a variety of holoenzyme (HE) complexes, the dynamics of Pol active site substitutions remain uncharacterized. Substitutions can occur externally by recruiting new Pols to replisome complexes through an 'exchange' of enzyme binding, or internally through a 'switch' in the engagement of DNA from preformed associated enzymes contained within supraholoenzyme (SHE) complexes. Models for how high fidelity (HiFi) replication Pols can be substituted by translesion synthesis (TLS) Pols at sites of damage during active replication will be discussed. These substitution mechanisms may be as diverse as the number of Pol families and types of damage, however, common themes can be recognized across species. Overall, Pol substitutions will be controlled by explicit protein contacts, complex multiequilibrium processes, and specific kinetic activities. Insight into how these dynamic processes take place and are regulated will be of utmost importance for our greater understanding of the

specifics of TLS as well as providing for future novel chemotherapeutic and antimicrobial strategies.

Introduction

The DNA replication process is an essential and inherent process within cells in all forms of life. Prior to cell division, the genome must be copied precisely to maintain the integrity and fitness of an organism. This responsibility is primarily carried out by DNA polymerases (Pols) that synthesize DNA in the 5'→3' direction, complementary to a DNA template. However, there are a number of enzymatic features and molecular obstacles that can destabilize Pol binding to DNA and allow for enzymatic subunit substitutions during the replication process. Most specifically, damage to the genome in the form of exogenous or endogenous base modifications can impact the ability of high fidelity (HiFi) DNA Pols to replicate past lesions, instead requiring the substitution of specialized translesion synthesis (TLS) Pols for efficient, but potentially mutagenic replication. Most organisms have evolved a number of separate DNA Pol enzymes, each with their own molecular specificities, enzymatic abilities, and preferences for various DNA lesions. This creates a complex multiequilbria nightmare that biochemists need to sort out within the cell.

Most DNA Pols require association with a processivity clamp to maintain contact with the DNA template while repetitively incorporating successive nucleotides over long stretches. This Pol-clamp interaction is just one contact point within a much larger replisome complex that contains a multitude of proteins capable of advancing the replication fork and overcoming DNA damage. This processivity of synthesis is controlled by the inherent affinities of the DNA Pol for both the clamp and the DNA template within a replisome and can be quantified by the probability that the Pol will incorporate an

additional nucleotide rather than dissociate from the DNA template.[16] DNA synthesis was once thought to be a highly processive and elegant process where a single DNA Pol can act on the leading strand, and a separate DNA Pol synthesizes each Okazaki fragment on the lagging strand. However, multiple lines of evidence have identified numerous interactions within replisome complexes that result in a more dynamic and stochastic process at the replication fork.[17-28]

Instead of the traditional view that the replisome can proceed unimpeded in the synthesis of both the leading and lagging strands no matter what lies in its path, plasticity in DNA synthesis, distributive access to the template, directed exchange, or switching can provide mechanisms for a Pol substitution under a variety of molecular circumstances. Even HiFi DNA Pols within active replisomes can act distributively and stochastically.[17, 24, 25, 29, 30] Pol substitutions on DNA templates can occur distributively through an external solution and equilibrium based 'exchange' mechanism or more directly by 'switching' pre-associated and interacting Pols without complete dissociation (**Figure 2.1**). In fact, DNA Pols are generally nonprocessive and act distributively on their own without interactions with processivity factor clamps. Specific known examples requiring a Pol substitution to a TLS DNA Pol capable of bypassing the lesion still have unknown molecular mechanisms for active or passive switching/exchange. The prevailing hypothesis is that a HiFi replication Pol must be temporarily exchanged with a TLS Pol at sites of damage through multiplex contacts with the sliding clamp, PCNA[19, 31], but whether that initial HiFi Pol is utilized afterwards or replaced from solution is not known. Several DNA Pols from different families have been shown to recognize and replicate across various lesions with varying efficiencies, however, the Y-family TLS Pols are the best studied and are thought

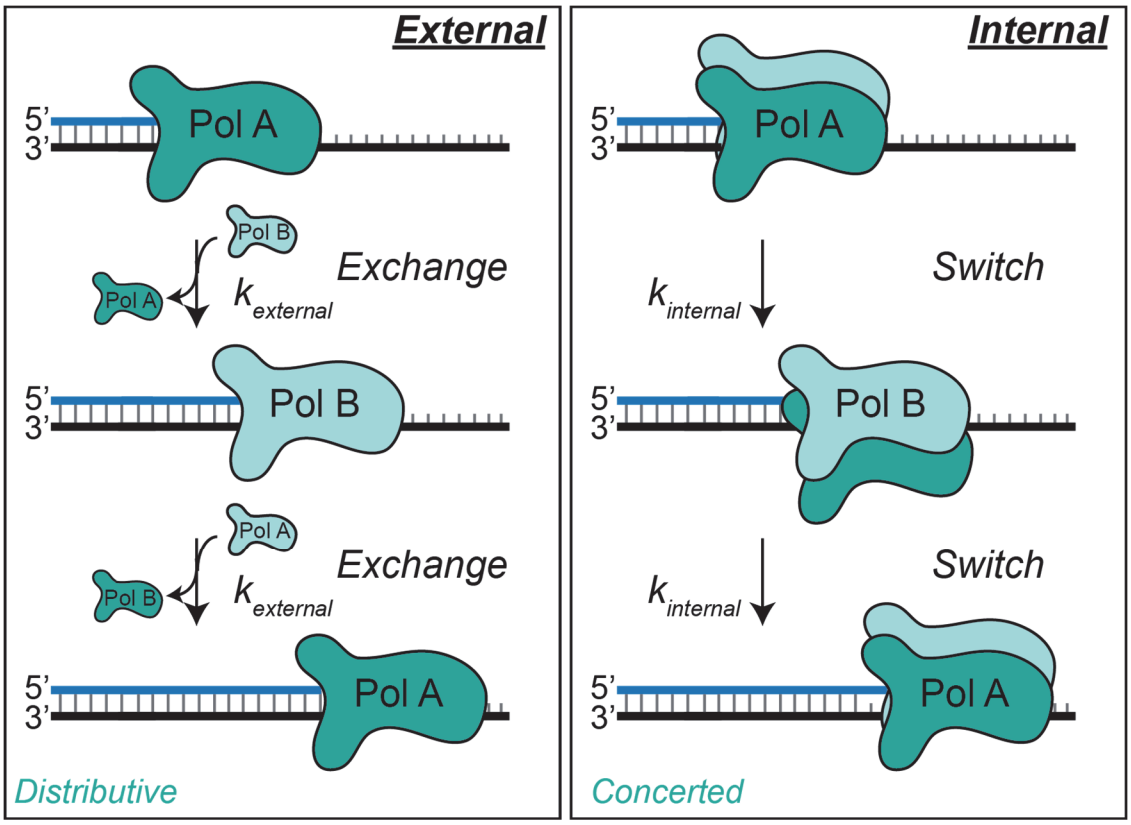

Figure 2.1: General mechanisms for DNA polymerase substitutions
External exchange of Pols arise from solution-based multiequilibrium processes that are dependent on distributive or stochastic molecular events. Internal Pol switching occurs within the confines of specific macromolecular complexes that contain homo- or heteromeric Pols subunits.

to contribute most to the TLS activity in the cell. Although a wealth of structural and kinetic information is known about Y-family TLS Pols across species (reviewed in[32-34]), it is primarily obtained using only conserved and well-structured truncated catalytic core domains in isolation. *In vivo*, Pol selection and recruitment to DNA will depend on mulitiequilbria processes and precise multipoint contacts within the replisome. The substitution of Pol binding to the DNA template can be a stochastic process, an inherent property of DNA Pol holoenzyme (HE) complexes or mediated specifically to overcome molecular obstacles including DNA damage.

DNA Polymerase Families

After the discovery and early characterization of several DNA Pols across many species, structural and functional diversity among these enzymes required a central system of classification. At first, Pols were classified based on their sequence relationship to the well-studied *E. coli* Pols: Pol I, Pol II, and Pol III.[35] Today, the discovery of numerous Pols has demanded an expanded version of that classification system where all DNA Pols are categorized into eight distinct families based on their unique structural arrangements, sequence homology, and specific functions within the cell. These families include A, B, C, D, E, X, Y, RT, and also archaeo-eukaryotic primase (AEP) enzymes that can perform DNA Pol activity (**Table 2.1**).[36-38] Interestingly, while some Pol families are widely conserved, not every family is represented in each domain of life. For example, B-family Pols are found in Bacteria, Eukaryotes, and Archaea, while D & E-family Pols are only found in select phyla of archaea.[39-41] This scattered pattern of Pol families among the domains of life may be the result of early horizontal gene transfer events which have diverged and evolved into the biological roles that we observe today.[38]

Despite sequence and structural diversity, all DNA Pol core domains are characterized structurally as adopting a 'right-handed' conformation consisting of the fingers, palm, and thumb subdomains.[42] The palm region contains the conserved aspartate catalytic residues for coordinating metals in the Pol active site[43, 44] and directly binds the elongating 3' end of the primer terminus.[45] The fingers facilitate binding of the incoming nucleotide to the downstream single-stranded DNA (ssDNA) template, and the thumb tracks the newly synthesized daughter strand. This structural orientation of Pols on DNA has been observed to adopt both an open conformation (when in a binary complex with

Table 2.1: DNA Polymerase Families

Family	Bacteria	Eukarya[4]	Archaea
A	Pol I[2,3]	Pol γ[5] Pol θ	
B	Pol II[2]	Pol α Pol δ Pol ε Pol ζ	PolB1 PolB2 PolB3
C	Pol III[2] PolC[3] DnaE[3]		
D			PolD[6]
E			PolE[7]
X	Pol X[3]	Pol β Pol λ Pol σ Pol μ TdT	
Y	Pol IV[2] Pol Y1[3] Pol V[2] Pol Y2[3]	Pol η Pol ι Pol κ Rev1	PolY
RT		Telomerase	
AEP[1]		PrimPol	PriS/L

[1]Technically the archaeo-eukaryotic primase (AEP) superfamily is classified for DNA primases, however enzymes in this table also exhibit DNA polymerase activities. [2]Examples from Eubacteria (*i.e. E. coli*). [3]Examples from Firmicutes (*i.e. B. subt.*). [4]All known DNA polymerases from eukaryotes are included even though individual species may not have every example listed. [5]In mitochondria only. [6]From euryarchaea phyla of Archaea only. [7]Plasmid encoded.

DNA), as well as a closed conformation (upon binding of an incoming nucleotide) during catalysis.[10] This repetitive Pol opening and closing during successive catalytic events provides a structural basis for DNA binding, translocation, and fidelity of synthesis.[46-48]

HiFi Polymerases

During routine synthesis of DNA, HiFi DNA Pols are utilized for processive and accurate replication and include an exonuclease domain or associated subunit to increase fidelity through proofreading. Phylogenetic, biochemical, and structural analyses have revealed that each domain utilizes different families of replicative Pols for duplicating the genome: Family C in bacteria,[49] Family B in archaea[50] and eukaryotes,[51] and Family D Pols only in archaea.[40] A closer look at the archaeal subdomains reveals that crenarchaea possess only B-family Pols, while euryarchaea and most other species possess both B- and D- family Pols.

In *E. coli*, DNA replication is performed by the multisubunit Pol III HE.[52] This complex is composed of several subassemblies including: i) the Pol III core, which consists of α (catalytic), ε (exonuclease), and θ (exonuclease associated) subunits;[53] ii) the homodimeric β-clamp which acts as a processivity factor for the Pol III core;[54] and iii) the dnaX clamp-loading complex, which is composed of three γ/τ subunits,[55] as well as the δ, δ', χ, and ψ subunits[56] and used to load the β-clamp onto DNA. The fully reconstituted Pol III HE has been demonstrated to simultaneously bind two Pol III cores through interactions with τ,[57] along with two β-clamps which are loaded by the clamp-loader.[58] This assembled HE is capable of rapid and accurate DNA synthesis, as well as coupled leading and lagging strand synthesis. Although this HiFi polymerase is known to carry out the bulk of accurate DNA synthesis, it has also recently been shown to have some TLS activity on its own.[59]

This sets up the possibility that Pol IV and Pol V may be involved instead in gap filling post-replicatively or only acting when severe DNA damage is present.

In eukaryotes, the replicative B-family Pols Pol ε and Pol δ, which act during replication on the leading and lagging strand, respectively,[60, 61] are multisubunit Pol complexes. Pol ε is composed of four different subunits in both yeast[62] and human,[63] while Pol δ is heterotrimeric in budding yeast,[64] and heterotetrameric in other eukaryotes.[65] Though an interaction with PCNA is not required for activity of Pol ε, the processivity clamp along with the rest of the leading strand components stabilizes Pol ε to DNA[66] and is required for Pol ε to achieve its maximal replication rate.[67] Alternatively, the more distributive Pol δ is significantly stimulated and is more processive in the presence of PCNA[68] and is the only known replicative polymerase that can participate in significant strand-displacement synthesis.[69] This activity and coordination provide the foundation for Okazaki fragment maturation.[70]

For archaea, despite their overall nuclear resemblance to bacteria, phylogenetic analyses have shown that they are more closely related to eukaryotes in their DNA processing pathways, such as transcription, replication initiation, and elongation.[71-73] Although early characterization of archaeal Pols suggested that they were monomeric enzymes,[74] the discovery of the D-family of Pols as the replicative Pols in euryarchaea revealed a heterodimeric Pol with a small subunit related to that of the B-family eukaryotic Pol δ.[40] In the crenarchaeaon, *Sulfolobus solfataricus* (*Sso)*, two additional small subunits for *Sso*PolB1 were recently identified as components of its heterotrimeric replicative HE.[75] Taken together, the identification of multisubunit archaeal replicative HEs, in addition to

the homology of origin recognition factors, replicative helicases, and processivity clamps, further strengthens the phylogenetic link between Archaea and eukaryotes.[76]

TLS Polymerases

Despite utilization of different families of replicative Pols, when DNA replication becomes hindered by the presence of DNA damage or other obstacles on the template strand, all domains of life utilize TLS Pols (or non-canonical Pols) to conduct temporary lesion bypass and rescue stalled replication forks. The larger Y-family of TLS Pols was formally classified in 2001,[77] though individual members were initially discovered and characterized earlier including members from the UmuC, Rad30, DinB, and Rev1 subfamilies.[78-80] The UmuC subfamily (*E. coli* Pol V) is found strictly in bacteria, while the Rev1 and Rad30 (Pol η) subfamilies are only found in eukaryotes. However, the DinB subfamily of Y-family Pols (*i.e. E. coli* Pol IV)[80] is the most diverse and is found in all three domains of life and includes *Sso*Dpo4[81] and *Sulfolobus acidocaldarius* Dbh[82] in archaea and Pol κ in eukaryotes.[83] Interestingly, the core structures of DinB Pols from each of the three domains of life are structurally similar (**Figure 2.2A**). Bacterial Pol II, IV and V are induced upon significant DNA damage as a part of a programed SOS response for cellular survival.[84-86] This change in cellular protein concentrations will drastically effect the multiequilibrium for Pols binding to DNA to direct TLS and contribute to an increase in mutation levels as a mechanism for survival.[20, 87]

All Y-family Pols (**Table 2.1**) possess the canonical Pol domain architecture and utilize a conserved Mg^{2+} dependent mechanism of nucleotidyl transfer but also have a few unique structural differences. Y-family Pols characteristically possess a more open, solvent-accessible active site[34, 81, 88-96] with generally smaller thumb and finger domains.[97]

This wider active site allows these non-canonical Pols to accommodate sites of DNA damage (bulky lesions, adducts, or distortions to DNA backbone)[89, 95] which would normally stall and displace the HiFi replicative Pol. The wider active site also affects their ability to make accurate base pairs, allowing Y-family Pols to frequently insert mismatches during synthesis.[89] Y-family Pols also lack an exonuclease domain, and thus lack the ability to excise and proofread any nucleotides they might misincorporate.[98] Uniquely, the Y-family Pols also possess a C-terminal Little-Finger (LF) domain (also called wrist, or Pol associated domains/PADs), which is named according to its spatial orientation relative to the rest of the Pol "hand."[99] Biochemical studies in archaea have also demonstrated the LF domain to have significant contacts with the template DNA, which implicates a role for the LF in the fidelity and activity of the Y-family Pols.[15, 100] The culmination of these unique characteristics provides the structural basis for the lesion bypass capabilities as well as the low fidelity of synthesis observed by these Pols.[14]

Interestingly, the eukaryotic B-family heterodimeric Pol ζ (Rev3 and Rev7), which lacks an exonuclease domain, has also been implicated in mutagenic TLS. Pol ζ has been shown to catalyze limited bypass of DNA lesions but is capable of extending beyond mispaired bases which may result from error-prone lesion bypass of other TLS Pols aided by an interaction with Rev1.[101, 102] Similarly, *E. coli* Pol II is a DNA damage-induced B-family Pol which is moderately active in lesion bypass;[103] yet its cellular role is not fully understood.[20] Alternatively, some members of the X-family Pols (including eukaryotic Pol β, Pol λ, and Pol μ) have been shown to catalyze mutagenic TLS across a variety of lesions.[104] However, these Pols are believed to preferentially participate in base-excision repair (BER) and non-homologous end-joining (NHEJ), suggesting the main cellular role

of X-family Pols to be synthesis for various other DNA repair pathways, rather than for TLS across DNA lesions.[105]

In addition to the numerous X and Y-family TLS Pol in eukaryotic cells, a TLS Pol termed PrimPol has been recently identified.[106] PrimPol contains both primase and a low-fidelity TLS Pol activity, similar to archaeo-eukaryotic type primases (AEP) in archaea and are capable of TLS activity on 8-oxo-deoxyguanosine (8-oxoG), cyclopyrimidine butane dimers (CPDs), and deoxyuracils.[107-111] Numerous reports have suggested that *in vivo*, PrimPol's primary role is to reprime DNA replication downstream of DNA blocks including lesions and stable secondary structures through recruitment by RPA.[110, 112, 113] Because of its extremely low fidelity, it should be tightly regulated to prevent deleterious effects to genomic integrity.

Specificities of Translesion Syntheses

The incorporated nucleotide product of a TLS event can be accurate or mutagenic depending upon the type of lesion encountered, the TLS Pol acting upon the lesion, and the template sequence context.[114] One of the most widespread lesions encountered in genomic DNA is the apyrimidinic/apurinic (AP, or abasic) site, which is caused by the loss of a DNA base along the sugar-phosphate backbone by spontaneous (oxidation, deamination) or catalytic (glycosylase) reactions.[115, 116] Because of a lack of a templating base, HiFi Pols cannot form proper base pairs with an incoming nucleotide, and thus, are stalled at AP sites. When A and B-family Pols do incorporate a nucleotide, it is generally deoxyadenosine (defined as the 'A-rule'), however synthesis past this AP-dA pair is not possible.[117] The basis of this 'A rule' may be explained either by structural specificity of the abasic site itself in the DNA template, or by TLS Pols preferentially binding and

inserting adenine nucleotides. Instead, full extension of the primer past an AP-site requires the substitution of a TLS Pol. TLS Pols also generally follow the A-rule for insertion across from an abasic site,[118, 119] however subsequent extension can utilize either a looped-out adjacent template base, misalignment of the active site, or a specific active site residue to direct catalysis.[92, 120-124] Though abasic sites are considered noninformative DNA lesions, this (mis)insertion pattern across abasic sites for various Pols begs the question as to whether other lesion types have their own rules of lesion bypass.

Products of lesion bypass across other forms of DNA damage in the form of CPDs, 8-oxoG, and bulky alkyl adducts do not seem to follow a particular insertion pattern, but instead depend upon specific Pols acting upon the lesion and the context of the adjacent DNA sequence. *E. coli* UmuD'$_2$C (Pol V) is capable of mutagenic synthesis across a wide variety of lesions and requires interactions with RecA/ssDNA nucleofilaments and SSB for optimal TLS activity.[125, 126] Alternatively, DinB (Pol IV) has varying efficiencies of bypass across different lesions,[126, 127] but is most active on different N^2-deoxyguanine (N^2-dG) bulky adducts.[128-130] Lastly, though its main cellular role remains unknown, Pol II can bypass abasic sites[103] and yields frameshifts when replicating across bulky G-adducts.[131] The archaeal Y-family Pols have been widely studied with respect to the mechanism of nucleotide incorporation, specificity, and structure function relationships and are capable of bypassing a wide variety of lesions.[15, 100, 122, 132-136]

Eukaryotes have evolved multiple TLS Pols each with primary specificities for certain lesions. In most cases, their specific incorporations tend to be accurate despite specific template lesions. The Rev30 homolog, Pol η, can efficiently bypass 8-oxoG and thymine-thymine (TT) dimers almost as fast as undamaged DNA,[137, 138] however, 6-4

photoproducts (6-4 PP) are less efficiently bypassed.[139] For these lesions, Pol ι is proposed to insert (or misincorporate) a nucleotide opposite the 3' template T of the 6-4 PP, but extension past the lesion requires the action of Pol ζ.[101] The eukaryotic DinB homolog, Pol κ, is generally stalled by either UV lesion,[140] yet has moderate fidelity across 8-oxoG,[141] and is accurate across polycyclic hydrocarbon adducts on N^2-dG moieties.[142] The last Y-family Pol, Rev1, has been shown to interact with several other TLS Pols and PCNA through a Rev1-interaction region (RIR) motif.[143, 144] Because these PIP and RIR motifs have overlapping specificities and are capable of binding multiple proteins, it has been proposed that together they all be reclassified as 'PIP-like' motifs.[145] Rev1 has been shown to act as a dC terminal transferase[146] and plays a role in bypass of abasic sites.[147] However, its activity is dispensable for its mutagenic role in TLS,[148] raising the hypothesis that one of its main functions is to recruit other TLS Pols to sites of damage.[22, 149]

When considering the unique structural and kinetic aspects of Y-family Pols, they become the ideal enzymes to carry out a diverse spectrum of translesion syntheses as a convenient or last resort for genomic maintenance. However, when TLS Pols are unregulated or overexpressed artificially or natively in certain cell types or disease states, they can confer an increased hypermutation frequency.[98, 150-153] During conditions of DNA damage, many further Pols are known to localize within foci, presumably contributing to the TLS response.[149, 154-158] Therefore, it is clear that not only the cellular concentration of Pols can change in response to DNA damage, but also the local concentration at the site of damage can drastically change which will effect Pol multiequilibrium, DNA binding, and substitutions. Considering the network of interactions and joint activities of TLS Pols, bypass of lesions or the ability to overcome stable DNA structures or roadblocks may

require a mechanism of coordination of different polymerases, cellular concentrations, and specific contacts to conduct efficient bypass.

Polymerase-Polymerase Interactions Within the Replisome

Early biochemical characterization of Pols focused primarily on individual Pols, their accessory subunits, and the role of other replication components (helicase, processivity clamp, and clamp-loader) on overall replication activity. However, as noted before, organisms possess multiple Pols with specialized functions for replication, lesion bypass, or DNA repair within the cell. Several recent studies of Pols from different organisms have identified and evaluated the roles of different polymerase-polymerase (Pol-Pol) interactions involved in coordination of function at the replisome and have implicated these interactions in regulation between DNA synthesis and lesion bypass.

In bacteria, observations of coordination between *E. coli* Pol V and Pol III led to detection of a direct interaction between both UmuD and UmuD' with the replicative HE.[159-161] In addition, reports of coordination and exchange of activities between Pol IV and Pol III on the β processivity clamp[162, 163] led to identification of the Pol IV T120P mutation which limits TLS-directed lethality by disrupting the proposed contact between Pol IV and Pol III and thereby limiting its access to the replication fork.[164] Lastly, Pol II was shown to exchange with Pol III primarily through interactions with β, but identified direct contacts between polymerases may also contribute.[165] Interestingly, all of these bacterial Pol-Pol interactions described consist of a TLS Pol interacting and exchanging with the replicative Pol III, and no interactions between bacterial TLS Pols have been described to date. However, the observed Pol-Pol interactions are implicated in facilitating

substitutions between the replicative Pol for those that direct lesion bypass, effectively regulating the balance between accurate DNA synthesis and error-prone TLS.

In eukaryotes, novel Pol-Pol interactions were detected by immunofluorescent colocalization between Pol η and Pol ι in damaged and undamaged cells as well as with direct pulldowns independent of other replication components.[158] Additionally, direct interactions were detected between Rev1 and multiple TLS Pols from both mouse[166] and humans,[143] supporting the conclusion that Rev1 acts as a recruiting factor for TLS Pols to sites of DNA damage.[167] Unlike in bacteria or archaea, direct Pol-Pol interactions between the eukaryotic TLS (Pol η, Pol ι, Pol ζ, Pol κ, Rev1) and replicative (Pol ε and Pol δ) Pols have not yet been described. Interactions have been reported between yeast Pol ζ and the accessory subunits of Pol δ (Pol 31 and Pol 32),[168, 169] suggesting a role for the accessory subunits in mediating exchange between replicative and TLS Pols in eukaryotes, however a direct interaction between Pol ζ and the catalytic subunit of Pol δ (Pol3) is not detected. Thus, the interactions between high-fidelity and TLS Pols in eukaryotes remains to be evaluated, however exchange may be controlled and directed through other forms of regulation.

In archaea, homooligomeric interactions by the replicative Pol (PolB1) from *Sso* have been described, where (at higher concentrations) the Pol assembles into a trimeric complex that stimulates activity on DNA.[18] Similarly, Dpo4 can form dimers and tetramers, which as with trimeric PolB1, are stabilized and stimulated at temperatures which are physiologically relevant to thermophilic archaea.[170] A direct interaction was also observed between *Sso* PolB1 and Dpo4.[171] This Pol-Pol interaction, taken together with structural arrangement of the heterotrimeric *Sso* PCNA123,[172, 173] and the exclusive interactions of

PolB1 and Dpo4 with different PCNA subunits,[172, 174-176] has the potential to form a higher order complex.

In fact, we have recently identified the site of interaction between PolY (Dpo4) and PolB1 (YB site) and have confirmed the formation of a supraholoenzyme (SHE) complex in archaea **(Figure 2.2B)**.[177] This conformation may allow for coordination of PolB1 and PolY on DNA through Pol-Pol interactions and specific contacts with the processivity clamp, analogous to the models proposed in bacteria[162, 164] and eukaryotes.[178] Our findings suggest that addition of PolY to a pre-formed PolB1 HE actually stabilizes the entire replication complex and increases its processivity. Interestingly, we have described a mutation which disrupts the YB interaction and prevents SHE formation. This Y122P mutation is strikingly similar to the T120P mutant of *E. coli* Pol IV which hinders its ability to coordinate and exchange with Pol III, ultimately preventing TLS by Pol IV.[164] The addition of newly identified PBP1 and PBP2 subunits with a heterooligomeric *Sso* PolB1[75] also have the potential to fit within this SHE complex to regulate its activity further. Such a complex would allow for coordination of rapid high-fidelity DNA synthesis by PolB1[176, 179-181] with TLS lesion bypass abilities of PolY.[81, 88, 92, 180] Interestingly, the eukaryotic Y-family Pols, η, ι, and κ have inserts within the palm domain that conceal a putative YB-site, potentially evolving further aspects to control Pol interactions that may be necessary for coordinating Pol activities in eukaryotes (**Figure 2.2 A, B, & D**). This has yet to be tested.

Mechanisms for Polymerase Substitutions

The various types of endogenous and exogenous DNA lesions which may arise must be repaired in order to properly maintain the genome for subsequent generations.

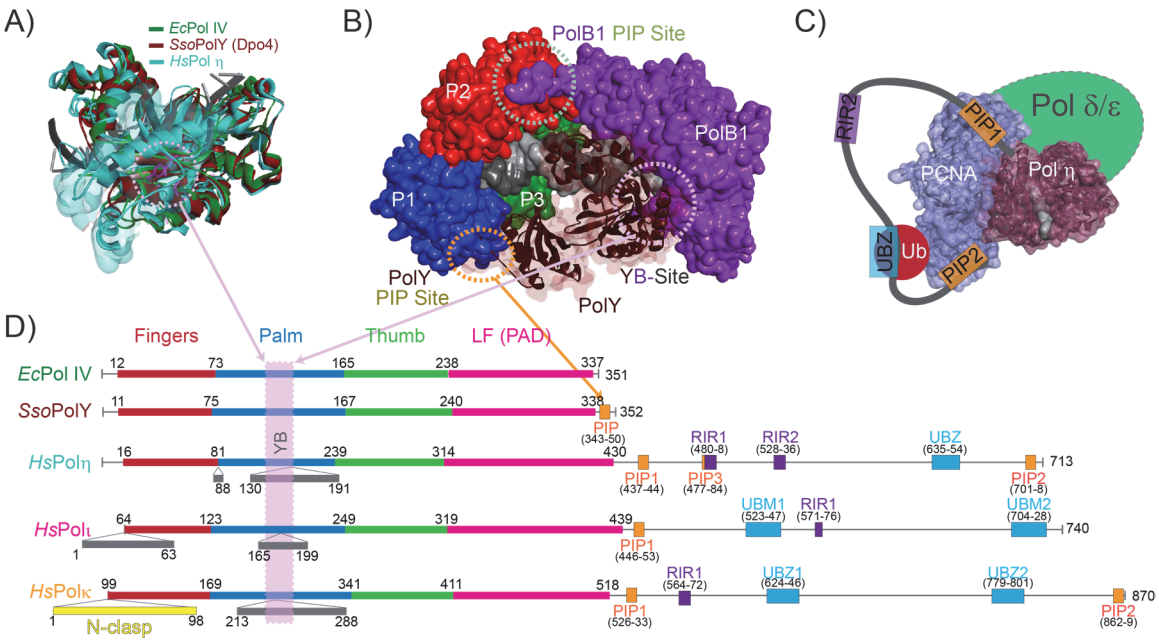

Figure 2.2: Structural Conservation and Formation of a Supraholoenzyme (SHE) Polymerase Complex

A) Superimposition of structures of Y-family Pols from each of the three domains of life: *Ec*Pol IV (bacteria, PDBID:4IR1), *Sso*PolY (Dpo4, archaea, PDBID: 1JXL), and *Hs*Pol η (eukaryotes, PDBID: 3SI8). B) *Sso* SHE model showing specific PIP and YB contacts between PCNA123, PolB1 and PolY in archaea. C) Possible Directed model for *Hs*Pol η bound to PCNA and DNA together with Pol δ or ε. D) Alignment of Y-family Pols showing catalytic domain: fingers, palm, thumb, and little finger (LF); PIP, RIR, and UBZ/UBM sites. *Hs*Pol η, ι, and κ have inserts in the sequence that obscure a putative YB-site.

However, despite the many DNA repair pathways that exist to restore the original DNA sequence, some lesions can escape recognition and repair, and so, are encountered during replication. For example, because CPDs do not dramatically destabilize the duplex, they are repaired by transcription-coupled repaired (TC- NER) in a slower fashion, hence this lesion persists into S-phase.[182] At these lesions, replication forks may stall and become decoupled from the helicase, resulting in replication stress, accumulation of downstream ssDNA, activation of cellular checkpoints, and further DNA damage (reviewed in[183-186]). To overcome these deleterious effects, the cells have evolved further mechanisms including DNA damage tolerance (DDT). During DDT, the stalled replication fork is restarted, and the DNA lesion is temporarily bypassed and remains unrepaired until it may

be corrected by a post-replicative repair pathway. Hence DDT is also prone to increased mutagenesis. Previous studies suggest two strategies on how the cells carry out DDT at template lesions: 1) error-free template switching (TS) involving synthesis across a newly synthesized daughter strand[98, 187-192] and 2) error-prone translesion synthesis (TLS) which replicates over the lesion.[11, 22, 167, 182, 193-196] For the rest of this review, we will focus our discussion primarily on this latter 'on the fly' mechanism for TLS.

TLS involves numerous proteins that associate together in a dynamic, multi-protein complex that is most likely associated with the active replisome. In TLS, the arrested replication fork could be restarted by a temporary Pol exchange (external) or switch (internal) between a HiFi Pol and one or more specialized TLS Pols alone (**Figure 2.1**) or through multiple contacts with PCNA (**Figure 2.2C**). The detailed mechanisms on how the HiFi Pol is substituted with TLS Pol and how the TLS Pol is selected from a cellular pool for a specific DNA lesion are not very well understood**.** Based on the current knowledge, we propose four models for 'on the fly' TLS Pol substitutions **(Figure 2.3)**. In these models, the term 'exchange' is reserved for situations where new Pols are recruited from solution and displace bound enzymes. The term 'switch' is used in cases where two or more Pols are preassociated within a complex and switch active site binding without complete dissociation. Previously, these terms were used interchangeably; instead, we propose specific definitions for each.

Internal switching of active sites for proofreading is common within HiFi Pols[197] and requires movement or rearrangement of the primer from the Pol active site to the exonuclease site, which could cause destabilization of DNA binding of a Pol within a HE.[175, 198] As discussed above, homo or heterooligomeric Pol complexes are also known

to exist,[18, 55, 170, 199] yet whether the DNA primer is exchanged between identical Pol active sites is not known. The external exchange is also known to occur through direct competition of multiple Pols with the template during primer synthesis (from primase to Pol),[200, 201] as well as to bypass DNA damage (lesions) in the template strand.[178, 193, 202] Whether these Pol exchanges are influenced through specific or recruited interactions, intrinsic or inherent destabilization of binding, or from external triggers is not known. Importantly, the molecular architecture, kinetic processes, and diversity is shared evolutionarily among DNA Pol families and their accessory proteins. Knowledge of these mechanistic features is essential to understanding coupled DNA replication and repair at the fundamental level as well as for the design of new cancer therapeutic strategies that target TLS to increase effectivity of current chemotherapeutic agents. Moreover, as TLS is

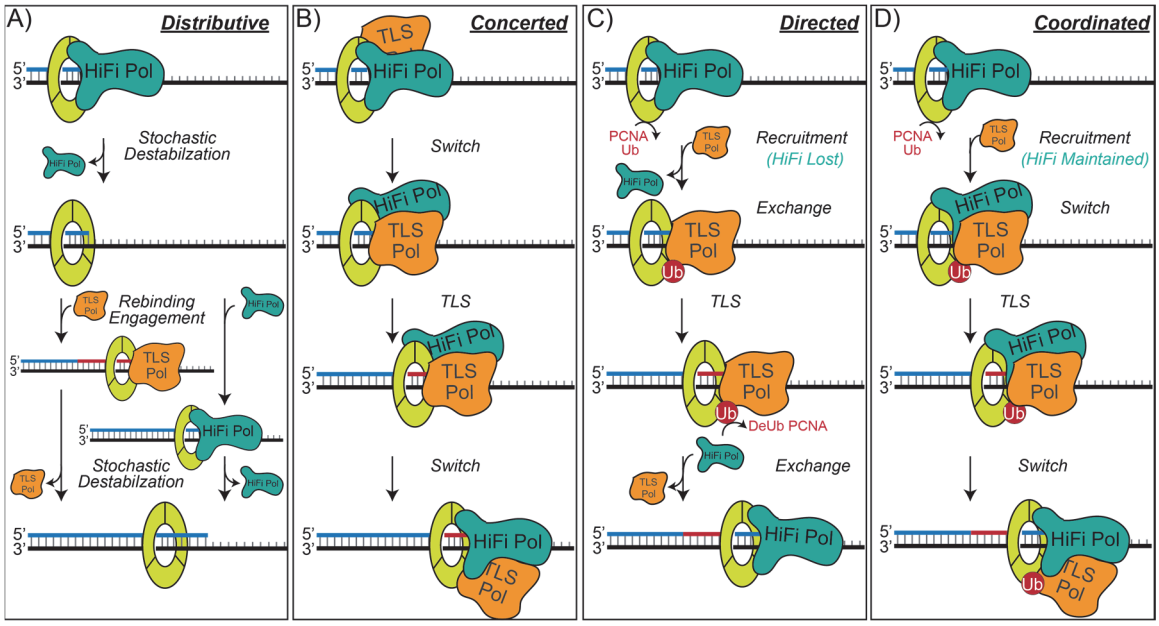

Figure 2.3: Specific Mechanisms for TLS Polymerase Substitutions
A) The Distributive model relies on a stochastic destabilization of the HiFi Pol/clamp complex and Pol recruitment relies on the inherent affinities and inherent solution equilibria. B) The Concerted model includes multiple Pols (HiFi and TLS) within the HE complex that can switch active site engagement of the DNA template without subunit dissociation. C) The Directed model requires ubiquitination of PCNA to exchange HiFi and TLS Pols. D) The Coordinated model also requires the ubiquitination of PCNA to recruit a TLS Pol to the HiFi Pol/clamp complex.

known to generate pathogen adaptation and diversity by promoting mutagenicity,[20, 203-205] knowledge on the mechanism of Pols substitution during TLS may give new insight into the growing problem of bacterial antibiotic resistance.

The Distributive Model

Even under conditions of optimal synthesis, stochastic exchange processes occur within Pol complexes, leading to distributive, yet high fidelity replication. Even though DNA Pol HEs from bacteria were thought to retain a high degree of processivity,[206, 207] this notion has been challenged recently by analyzing stochastic dissociation events in single molecule bacterial replisomes *in vitro*[24, 28] and *in vivo*.[27, 208] Similar Pols within HE complexes characterized in archaea[176] and human[209, 210] systems also appear to act in a more distributive manner. During synthesis, complex multiequilibrium processes and molecular roadblocks directly influence the binding and exchange of Pols on DNA from a multitude of Pols within the cellular pool. In addition to the primary HiFi replication Pol, there are other Pols that have evolved for specialized processes including primer synthesis to initiate or restart replication and those with variable processivities and lower fidelities necessary for lesion bypass. In humans, TLS activity was shown to be dependent on the inherent binding properties of Pol η which enable it to be exchanged with Pol δ on the damage site of the lagging strand.[202] These results suggest that there is an equilibrium and concentration dependent balance for Pol exchange that influences replisome stability.

At issue is the global ability and conserved mechanism used to replicate DNA. Because specificity to the 3'OH of a primer-template DNA is generally shared among Pols, other molecular features must provide discrimination for Pol selectivity. Accessory proteins that promote complex formation do so through specific contacts with the Pol to

generally increase processivity by decreasing the off-rate, however a variety of DNA Pols share common binding sites (*e.g.* PIP site on PCNA). It is probable that HiFi Pol contacts with replication helicases in bacteria[24, 211-213] or eukaryotes[214-217] provide specificity and stability until a lesion or other molecular roadblocks disrupt this association stimulating a distributive exchange mechanism.

The Concerted Model

Early perspectives on TLS Pol coordination was envisioned as a molecular 'tool-belt,' where Pols are recruited to DNA lesions or undamaged primer-template junctions by exclusive interactions with the processivity clamp (β in bacteria and PCNA in archaea/eukaryotes).[22, 167, 218] This Concerted 'tool-belt' configuration leaves open the possibility that the resident Pol remains bound within the complex and can switch back after TLS for continued HiFi synthesis **(Figure 2.2B)**. The 'tool-belt' model was initially validated when the *E. coli* β-clamp was observed to bind Pol III and Pol IV simultaneously, which allows for a concerted switching of Pols as needed within the complex.[162] In support, overexpression of Pol IV was observed to induce a lethal phenotype due to its uncontrolled access to the replisome,[219] presumably by switching contacts with Pol III.[164] Additionally, the engineering of an *E. coli* strain that only expresses the τ_3 form (instead of the truncated γ form of DnaX) of the Pol III HE displays a Pol IV deficiency, suggesting that this form of Pol III (Pol III_3 τ_3 δδ'χψ) lacks the necessary plasticity for exchange and requires at least one subunit of γ for Pol IV recruitment.[220, 221] Moreover, binding of both *E. coli* Pol II and Pol III to the β-clamp allows access to the template and become active within the replisome.[165] Although *E. coli* Pol V can also be bound to the β-clamp through an opposite cleft from Pol III[222] and a direct interaction between Pol III and Pol V has been

noted,[223] the direct exchange of Pol III and Pol V for TLS coordination has not been reported**.** In fact, using single molecule fluorescent microscopy of Pol V in live *E. coli* cells, a rare co-localization of Pol III HE and Pol V mutasome with wild type RecA (*i.e.*, UmuD′$_2$C-RecA$_{WT}$-ATP) was observed after UV irradiation.[224] This may suggest that the direct exchange of Pol III and Pol V for TLS may be limited by molecular mechanisms that limit the amount of time that Pol V has to access DNA.

In archaea, the heterotrimeric PCNA123 clamp allows specific interactions with each Pol (PolB1-PCNA2 and PolY-PCNA1).[172, 174, 180, 225] Our characterization of the SHE complex in archaea consisting of PolB1 and PolY simultaneously bound to PCNA (**Figure 2.2B**) is highly analogous to the 'tool-belt' model in bacteria except that it also adds a direct (YB) interaction between Pols.[177] This conformation may allow for coupling of PolB1 and PolY on DNA through Pol-Pol interactions (discussed above) and individual contacts to the processivity clamp, analogous to the models proposed in bacteria.[162, 164] It will be interesting to test whether this archaeal SHE complex is capable of more efficient TLS activity.

Recent single-molecule experiments with human proteins have demonstrated the formation of a dynamic multi-Pol TLS complex on PCNA, where Rev1 and Pol η are capable of binding either directly to the clamp (tool-belt configuration) or to one another (Pol bridge configuration).[178] Therefore, recruitment of Pols and coordination of their functions may be facilitated by interactions with both the processivity clamp and with other Pols present at the replication fork in all domains of life. A quantitative multisite competitive switch mechanism has been described,[226] where simultaneous binding of multiple low affinity sites can grant stability but also allow for rapid exchange in the

presence of competing proteins.[17, 55, 227-229] This concept can also be utilized to validate the concerted switch mechanism (**Figure 2.1**) associated with dynamic processivity of homo or heterooligomeric Pol complexes in isolation.[17, 18]

The Directed Model

In eukaryotes, the detection of monoubiquitination (mUB) of PCNA in response to DNA damage has suggested a more Directed exchange mechanism at damage sites (**Figure 2.3C**). Stalled replisomes are known to uncouple the HiFi Pol and the helicase activities, causing the build-up of ssDNA coated with RPA downstream of the lesion. This more severe stalling event is believed to signal the recruitment of Rad6/Rad18 which catalyzes the mUB of K164 on PCNA at stalled HEs.[230] In *S. cerevisiae*, Rad18 bound to Rad5 E3 ligase at the blocked replication fork could also polyubiquitinate (pUB) PCNA.[231] pUB of PCNA can induce proteasomal degradation of the clamp, stimulating the error-free TS mechanism over direct TLS substitutions. Interestingly, pUB-dependent proteasomal degradation of yeast Pol η has also been reported;[232] therefore, the pUB of PCNA and/or Pols could serve as important regulatory roles for directing DDT.[22, 190]

Studies on the role of mUB-PCNA on TLS is focused on Pol η, Pol κ, and Pol ι because they contain one or more ubiquitin-binding domains (UBD), UBZ (zinc-finger) or UBM (motif) in addition to PIP sites (**Figure 2.2D**).[22, 32, 34] The presence of both PIP and UBD sites is hypothesized to increase binding specificity and selectivity of TLS Pols (**Figure 2.2C**). The combination of PIP and UBD sites elevates the localization and stability of TLS Pols at the sites of DNA damage[233-235] and increases the resistance to UV sensitization of cells *in vivo*.[236] Efficient Pol exchange of *S. cerevisiae* Pol δ with Pol η requires both the stalling of the HE and mUB-PCNA and is consistent with the faster

kinetic TLS activity observed *in vitro*.[237-239] The removal of mUB moiety from PCNA or other PTMs, like phosphorylation within the Rad51/Mec1 damage response checkpoint pathway,[240] are likely required to resume normal DNA synthesis by HiFi Pol after lesion-bypass. This deubiquitination step may be essential in regulating TLS to keep the mutagenic load low in eukaryotic cells.[241] In mammals, mUB-PCNA was required for maximal TLS activity, however when mUB of PCNA was inhibited, TLS activity could proceed with a lower efficiency.[242] More globally, the fork protection complex (FPC) (Tof1 and Csm3 in budding yeast;[243] TIM and TIPIN in mammals[244]) is responsible for ensuring consistent fork progression and stabilization of the replisome at sites of DNA damage[245, 246] by inhibiting activity of the MCM helicase complex (CMG) and initiating intra-S phase checkpoint (Chk1) to slow progression and allow DNA repair to proceed (reviewed in[247-250]).

In mammals, there is extensive evidence showing that TLS activity can be independent of PCNA monoubiquitination involving a more passive 'on the fly' exchange mechanism[202, 251, 252] more similar to the Distributive model (**Figure 2.3A**). So, the role of mUB-PCNA in human TLS Pol exchange remains unclear. In fact, some *in vivo* evidence suggests that there is no direct interaction between mUB-PCNA and Pol η during human TLS. For example, human Pol η co-localizes with PCNA at DNA replication foci even in the absence of DNA lesions and this co-localization does not require the mUB of PCNA but instead the UBD of Pol η.[235] Additionally, other groups reported that accumulation of Pol η into replication foci after UV irradiation is both independent of PCNA monoubiquitination[251, 253] and the UBD site within Pol η.[236] It was concluded that the inherent binding properties of Pol η enable it to be exchanged with Pol δ at the damage site

on the lagging strand, and it does not require mUB of PCNA.[202] It was also shown that Pol η or κ could substitute with Pol δ stalled at common fragile sites and this process is neither stimulated by PCNA, nor through mUB of PCNA.[252] The latter supports the idea that PCNA can be unloaded from a stalled replication fork possibly in a pUB dependent fashion.[254-256] It is still unclear whether the presence of Pol η or any other TLS Pol directs the substitutions. Therefore, the TLS substitution mechanism in humans may be different from that in yeast. The emerging idea is that for yeast, mUB of PCNA is required to recruit TLS Pols on the damage site, while in humans this may be a more dynamic or redundant feature.

The Coordinated Model

As the mUB of PCNA seems to be influential in some TLS situations (especially in yeast), the question remains whether the original HiFi Pol is retained (*i.e.* switch) or exchanged within the complex. The Coordinated model (**Figure 2.3D**) relies on the mUB of PCNA, however, it leaves open the possibility that multiple Pols can be retained within a SHE complex. The X-ray structure of mUB-PCNA shows that recruitment of a TLS Pol occurs on the back face and may allow simultaneous binding with a HiFi Pol.[237] A solution SAXS structure of mUB-PCNA and Pol η also allows for the possibility of simultaneous binding of a HiFi or other Pol,[257] consistent with a two-polymerase PCNA mechanism.[258] Even if not directly coordinated by bimodal binding to mUB-PCNA, binding of a single Pol to PCNA through a variety of motifs can then retain a second Pol through direct Pol-Pol interactions as in the case of Pol η and Rev1 or Pol δ.[259, 260] Additional structures or biochemical data for mUB-PCNA mediating the binding of multiple Pols will be required to validate the Coordinated model.

Other Molecular Obstacles for Polymerases

Besides template lesions, DNA Pols encounter a number of other external obstacles including downstream duplex DNA, bound proteins, complex DNA structures, and transcription conflicts that aim to derail this processive process (**Figure 2.4**). The PCNA/HiFi Pol HE complex may also coordinate the exchange of enzymatic activities in these situations as well. In fact, some of the best characterized 'tool-belt' models include not just Pols but also enzymes involved in Okazaki fragment maturation including Fen1 and DNA ligase.[225, 261-264] Although biochemical Okazaki maturation is stimulated in some of these arrangements, other experiments show no functional advantage and instead suggest a sequential switching mechanism[265] or a more stochastic process where bound primase complexes can stimulate HE dissociation.[25] The recently described stochastic behavior of leading and lagging strand synthesis[24, 25] may also argue against a coordinated 'tool-belt' model for Okazaki fragment maturation where instead distributed enzymatic action is utilized to complete the intact lagging strand.

Other impediments or replication fork barriers (RFBs) to DNA Pol progression (**Figure 2.4**) will include stably bound proteins such as Tus bound termination sites (Tus-Ter) in bacteria[266] or stably bound transcription repressors such LacI or TetR,[267, 268] although it may be more likely that these proteins block the replication helicase preferentially.[269] In fission yeast, DNA binding proteins associated with imprinting[270] or 3' ends of rRNA genes[271] cause unidirectional DNA Pol stalling. Replication stalling at highly transcribed regions of the genome is also very prevalent.[272] Difficult to replicate DNA including G-quartets,[273] repetitive sequences,[274] and inverted repeats[275] are also known to cause fork stalling and may require the substitution of TLS Pol or recruitment of

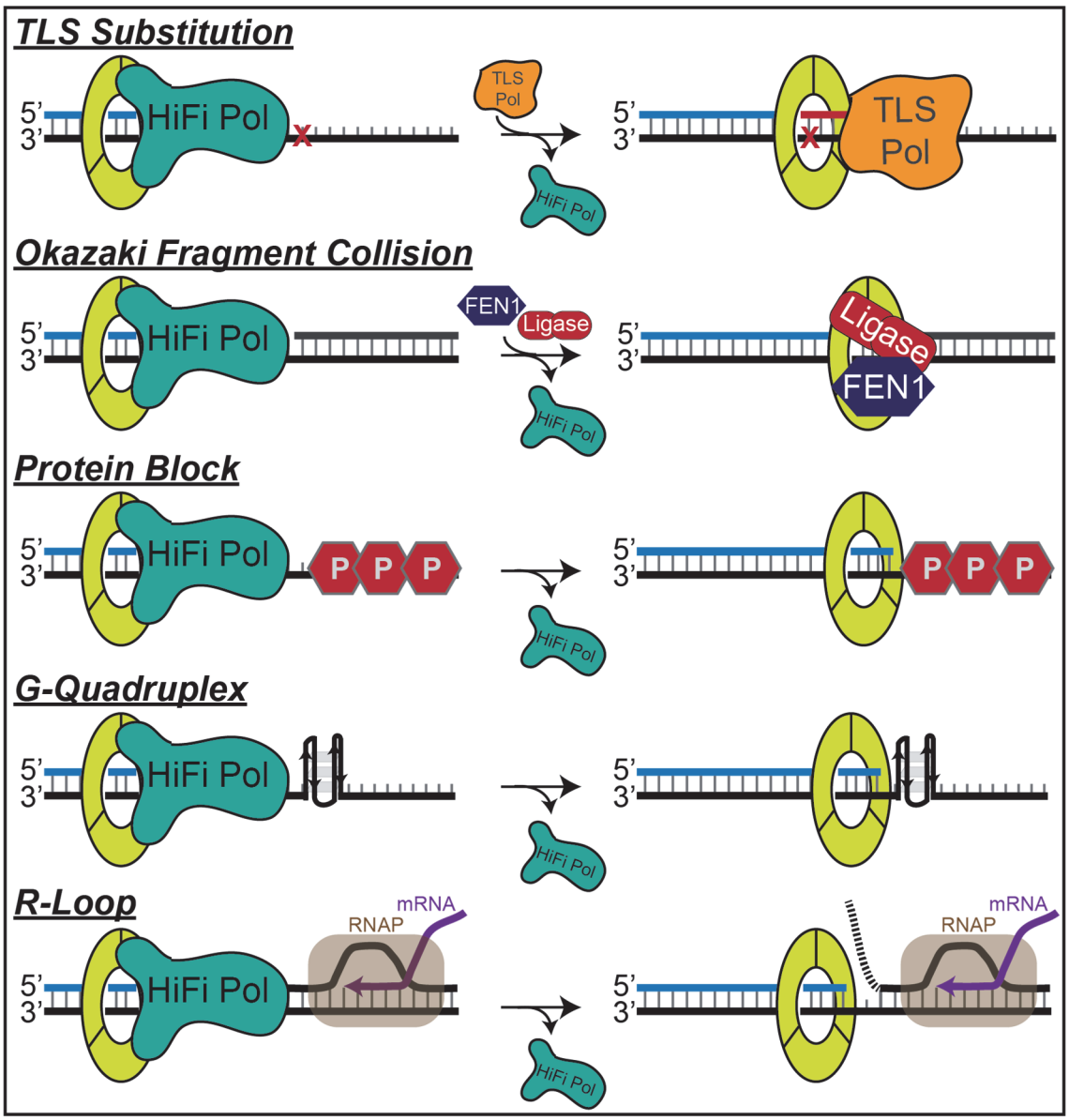

Figure 2.4: Molecular Roadblocks for Polymerase Activity
Events that destabilize DNA Pol binding and influence substitutions or dissociations.

accessory helicases to overcome.[272, 276-279] However, some of the strongest impediments to replication fork progression are head-on transcription R-loop structures that are either active or stalled and backtracked producing very stable complexes.[185, 280-282] There is a wealth of research activity trying to understand the mechanism of these collisions as well as their cellular consequences and we should have a better idea of the role of Pol substitutions over the next couple of years.

Conclusions

Clearly, the molecular process of overcoming damage to the genome is quite complex. However, the DDT that occurs when the replisome encounters damage in the template strand happens during the most vulnerable times within the cell cycle *i.e.* when there are significant amounts of ssDNA. Therefore, it is not surprising that there are cellular checkpoint proteins and pathways that constantly survey the genome for the buildup of ssDNA to initiate repair before they become double strand breaks.

The plethora of DNA Pols in most organisms seems to be not only a benefit but also somewhat of a curse. The evolution of individual TLS Pols that preferentially target specific lesions allows for more accurate nucleotide incorporation despite the lesion. However, the more DNA Pols available in a cellular pool creates competition and a highly complex multiequilibrium for binding to a singular 3'-OH DNA primer-template target. With many Pols available, controlling access of singular Pols to the primer template will become more important for maintaining genomic integrity. As discussed in this review, cellular multiequilibrium, Pol concentrations, kinetic activities, active site selection, specific interactions, and posttranslational modifications all contribute to that selection.

Development of our understanding for how these processes impact TLS activity in humans compared with other species is only just being started.

Although this review focused primarily on mechanisms for 'on-the-fly' TLS substitutions, there are many more instances in which TLS activity will be carried out post-replicatively involving other mechanisms of switching and exchange that are also not well described. TS avoids the lesion or obstruction altogether by utilizing the newly replicated sister strand to crossover and synthesize past an undamaged region on the complementary strand.[98, 283] How the recombination dependent TS process is initiated or regulated or whether new Pols are recruited needs to be determined. Finally, replication repriming and restart downstream is a *bon a fide* mechanism of lesion bypass that leaves unreplicated stretches of ssDNA that can be replicated and repaired later.[187, 284] How Pols are recruited or selected for substitutions needed for post-replicative TLS are also not known. Presumably, Pols act similarly on these short stretches of DNA for accurate TLS across lesions only to have the template lesion repaired later by alternative base or nucleotide excision repair (BER or NER) mechanisms. If TLS activity occurs prior to BER or NER, the possibilities for mutagenicity are greatly increased.

Even with all these possible static models for TLS Pol substitution, what is generally missing is direct kinetic or dynamic monitoring of the actual switch or exchange. Dynamic single molecule or ensemble fluorescence experiments monitoring the overall process will be needed to nail down differences between the various TLS contexts. Other complications include the very real probability that TLS action is mediated by multiple protein contacts with differing and variable specificities. Care will be needed to not only detect the strongest of those interactions but also to dissect how multiequilibrium processes

can influence some of the slightly weaker contacts to occur under certain cellular circumstances.

CHAPTER THREE

Characterization of a Coupled DNA Replication and Translesion Synthesis Polymerase Supraholoenzyme from Archaea

This chapter published as: Cranford, M.T., Chu, A.M., Baguley, J.K., Bauer, R.J., and Trakselis, M.A. (2017) Characterization of a coupled DNA replication and translesion synthesis polymerase supraholoenzyme from archaea. *Nucleic Acids Res. 45*(14), 8329-8340.

Abstract

The ability of the replisome to seamlessly coordinate both high fidelity and translesion DNA synthesis requires a means to regulate recruitment and binding of enzymes from solution. Co-occupancy of multiple DNA polymerases within the replisome has been observed primarily in bacteria and is regulated by posttranslational modifications in eukaryotes, and both cases are coordinated by the processivity clamp. Because of the heterotrimeric nature of the PCNA clamp in some archaea, there is potential to occupy and regulate specific polymerases at defined subunits. In addition to specific PCNA and polymerase interactions (PIP site), we have now identified and characterized a novel protein contact between the Y-family DNA polymerase and the B-family replication polymerase (YB site) bound to PCNA and DNA from *Sulfolobus solfataricus*. These YB contacts are essential in forming and stabilizing a supraholoenzyme (SHE) complex on DNA, effectively increasing processivity of DNA synthesis. The SHE complex can not only coordinate polymerase exchange within the complex but also provides a mechanism for recruitment of polymerases from solution based on multiequilibrium processes. Our results provide evidence for an archaeal PCNA 'tool-belt' recruitment model of

multienzyme function that can facilitate both high fidelity and translesion synthesis within the replisome during DNA replication.

Introduction

To ensure accurate and faithful DNA synthesis, the DNA replisome must maintain a certain plasticity, such that enzymes can be exchanged to overcome any obstacles to replication. Although the bulk of DNA synthesis is performed by high fidelity B-family (archaea & eukaryotes) or C-family (bacteria) DNA polymerases that ensure genomic integrity, DNA damage encountered in the template strand is replicated using lower fidelity Y-family translesion (TLS) DNA polymerases.[77, 95] In eukaryotes, multiple TLS polymerases have evolved to provide specificity and accuracy of DNA synthesis across a broad range of lesions in spite of the type of damage.[32, 285] However, bacteria and archaea generally contain one or two translesion DNA polymerases with broader lesion specificity.

In both archaea and eukaryotes, the processivity clamp, PCNA, interacts with many protein partners that contain a PCNA interacting peptide (PIP) motif that binds to a hydrophobic pocket on the front face of PCNA.[286] This common interaction site on PCNA is utilized to localize proteins not only for DNA replication but also for translesion synthesis, mismatch repair, nucleotide excision repair, chromatin remodeling, and cell cycle control, making PCNA an important localization point for many DNA related processes.[287, 288] In eukaryotes, although specific mechanisms may differ between yeast and mammals, optimal TLS activity includes the monoubiquitinylation (mUb) of PCNA.[235, 242] The hypothesis is that the combination of mUb and PIP binding provides greater binding specificity and selectivity for TLS polymerases. Eukaryotic Y-family TLS polymerases, pol η, pol κ, pol ι, all contain both PIP sites and ubiquitin binding domains

(UBD).[32, 34] mUb-PCNA has been shown to not only increase the localization of these TLS polymerases to sites of damage,[233, 234] but it also aids in the resistance to UV sensitization of cells.[236] These *in vivo* results are validated by the increased kinetic polymerization ability of TLS polymerases with mUb-PCNA compared to unmodified PCNA.[237, 238] Therefore, the combination of PIP and UBD sites increases the localization and stability of TLS polymerases at sites of DNA damage in eukaryotes.

Although bacteria and archaea also possess multiple DNA polymerases including Y-family TLS polymerases, the processivity clamps in these organisms do not seem to be modified with ubiquitin or any other posttranslational modifications. Instead, the PIP binding site (in archaea)[173, 289] or the equivalent hydrophobic patch on the β-clamp (in bacteria)[290] are the primary interaction sites for both high and low fidelity DNA polymerases within both domains. In addition to clamp binding, direct contacts between polymerases (Pol III and Pol II or Pol IV) have been identified that are important for polymerase switching and translesion synthesis in bacteria.[164, 165] Although an initial interaction between PolB1 and PolY has been identified in archaea,[171] its mechanistic role in polymerase exchange or TLS has not been described making comparisons with either the bacterial or eukaryotic domain impossible. However, homoligomeric contacts within single archaeal DNA polymerases have been described,[18, 170] providing a potential for heteroligomeric polymerase contacts. Barring these secondary interaction sites, there would be direct competition and thermodynamic equilibria/competition for individual polymerase molecules binding to PCNA and DNA, potentially impacting processivity and fidelity of DNA synthesis.[170, 291]

Because the eukaryotic DNA processing components seemed to have emerged from a common ancestor in archaea,[292, 293] the archaeal DNA replication enzymes are a *de facto* relevant model system for understanding mechanism of action within the replisome. In fact, *Sulfolobus solfataricus* (*Sso*) Dpo4 (PolY) has been one of the most intricately studied DNA polymerases with regards to its structure/function, kinetics, and template lesion bypass specificities.[15, 81, 89, 92, 100, 122, 132-136] The heterotrimeric *Sso*PCNA123 clamp can provide for more specific interactions of proteins with individual subunits in a 'tool-belt' configuration,[172, 225, 294] similar to that described for the bacterial system.[162] *Sso*PolB1 is considered to be the main DNA replication polymerase and interacts specifically with *Sso*PCNA2,[172, 180] while *Sso*Dpo4 (PolY) is the primary TLS polymerase and interacts specifically with *Sso*PCNA1.[174] In addition, direct contacts between PolB1 and PolY have also been observed but not functionally characterized.[171] Therefore, the potential for a coordinated PolB1/PolY/PCNA123 supraholoenzyme (SHE) in *Sso* is possible and would provide valuable insight into the polymerase exchange mechanism in archaea.

In this report, we have not only detected the presence of a *Sso* SHE complex using analytical gel filtration and presteady-state stopped flow FRET, but we have also validated the activity and polymerase exchange using both kinetic replication and processivity assays. Interaction between PolB1 and PolY within the SHE occurs at both PIP sites on PCNA2 and PCNA1, respectively, as well as a novel YB binding site directly between PolY-PolB1 polymerases. Addition of PolY stabilizes the SHE complex on DNA and increases processivity of DNA synthesis. Although direct polymerase solution equilibrium competition occurs for binding to DNA, the presence of both the PIP and YB interaction sites in the SHE increases the ability to directly exchange and regulate polymerase contacts

with the primer-template. Altogether, this work identifies the presence of a novel YB interaction site that is important in coordinating polymerase switching for low and high fidelity synthesis within a novel supraholoenzyme complex, providing significant implications for polymerase recruitment and lesion bypass during replication.

Materials and Methods

Materials

Oligonucleotides used (**Table 3.1**) were purchased from IDT (Coralville, IA). Fluorescently labeled DNA was HPLC purified by IDT. ATP was from Sigma-Aldrich (St. Louis, MO). ^{32}P-γ-ATP was from PerkinElmer (Waltham, MA). Alexa Fluor 488 ® (A^{488})

Table 3.1: DNA Sequences

DNA	Sequence (5'-3')
Primer 21	5'-GCTGTGCTCTCGCCGCGTGCC
Template 31	5'-TATCTTCTATGGCACGCGGCGAGAGCACAGC
Template 31*	5'-TATCTTCTATGGCACGCGGCGAGAGCACAGC^{488}
PolY cat$^-$ QC FWD	5'-GAGAAGATCGAGATTGCAAGTATAGCTGCAGCTTATCTTGATATCTCAGACAAAG
PolY cat$^-$ QC REV	5'-CTTTGTCTGAGATATCAAGATAAGCTGCAGCTATACTTGCAATCTCGATCTTCTC
PolY PIP$^-$ QC FWD	5'-TTTATTGAAGCAATAGGATTAGACAAGGCAGCTGATACTTAAGGATCCGAATTCGAGCTC
PolY PIP$^-$ QC REV	5'-GAGCTCGAATTCGGATCCTTAAGTATCAGCTGCCTTGTCTAATCCTATTGCTTCAATAAA
PolY L126N QC FWD	5'-TCAGAGATTATAGAGAGGCATATAACCTAGGTAACGAGATTAAGAACAAAATACTTGAAA
PolY L126N QC REV	5'-TTTCAAGTATTTTGTTCTTAATCTCGTTACCTAGGTTATATGCCTCTCTATAATCTCTGA
PolY I163N QC FWD	5'-CGAAAATTGCTGCTGATATGGCCAAGCCAAATGGAAACAAAGTTATTGATGATGAAGAAG
PolY I163N QC REV	5'-CTTCTTCATCATCAATAACTTTGTTTCCATTTGGCTTGGCCATATCAGCAGCAATTTTCG
PolY Y122P QC FWD	5'-CAGACAAAGTCAGAGATTATAGAGAGGCCCCTAATCTAGGTTTGGAGATTAAGAACAAAA
PolY Y122P QC REV	5'-TTTTGTTCTTAATCTCCAAACCTAGATTAGGGGCCTCTCTATAATCTCTGACTTTGTCTG
PolY Y122A QC FWD	5'-GACAAAGTCAGAGATTATAGAGAGGCAGCTAACCTAGGTTTGGAGATTAAGAACAAAATA
PolY Y122A QC REV	5'-TATTTTGTTCTTAATCTCCAAACCTAGGTTAGCTGCCTCTCTATAATCTCTGACTTTGTC

^{488} – Alexa 488

and Alexa Fluor 594 ® (A^{594}) C5 maleimides were from ThermoFisher (Pittsburgh, PA). All other chemicals, buffers, and media were analytical grade or better.

Cloning and Protein Purification

Sso PolB1, RFC, and PCNA123 and their mutants were purified as described previously.[176] *Sso*PolY mutants were created using a standard Quikchange protocol from pET11-Dpo4[81, 170] using KAPA DNA polymerase (Kapa Biosystems, Wilmington, MA). Primers are listed in **Table 3.1**. Mutations were confirmed by DNA sequencing (ICMB, UT Austin). PolY WT and mutants were purified essentially as described previously[170] using autoinduction[295] in Rosetta 2 cells (Novagen EMD Millipore, Billerica, MA) followed by HiTrap MonoQ, Heparin, and Superdex S-200 columns on a AKTA Pure FPLC chromatography system (GE Healthcare Life Sciences, Marlborough, MA). All PolY mutants retain near wild-type activity on their own and within a PolY HE complex (data not shown).

Analytical Gel Filtration

Analytical gel filtration experiments were conducted using a Superdex 200 10/300 GL column (GE Healthcare Life Sciences) equilibrated in Buffer A (20 mM HEPES-NaOH (pH 7.0), 50 mM NaCl, 10% β-mercaptoethanol). Calibration of the Superdex 200 10/300 GL column was performed by running molecular ruler standards consisting of Thyroglobulin (165 kDa, Sigma), Conalbumin (75 kDa, GE Healthcare Life Sciences), Albumin (43 kDa, Sigma), Myoglobin (17.6 kDa, Sigma) and Vitamin B12 (1.4 kDa, Sigma). The standard calibration curve was created by plotting retention volume data against the logarithm of the molecular weights of the calibration proteins and was fitted by

linear least squares. Five hundred microliters samples consisting of 5 μM of each indicated component (PolB1, PolY, PCNA123, RFC, DNA21/31) and 1.6 mM ATP were mixed, nutated at room temperature for 10 min, and injected in the Superdex column (4°C). Protein elution was monitored at 280 nm and fractions collected at regular intervals.

Western Blot Analysis

Analytical gel filtration fractions of SHE and PolY HE were separated in 10% SDS-PAGE, transferred onto PVDF membranes, and probed with antibodies against PolB1 or PolY (1:4000). Proteins of interest were detected with HRP-conjugated anti-rabbit (1: 5000) and visualized with the Pierce ECL Western blotting substrate (Thermo Scientific, Rockford, IL), using ImageQuant LAS 4000 (GE Healthcare Life Sciences) according to the manufacturer's instructions.

Protein Fluorescent Labeling

Proteins were fluorescently labeled at a single accessible cysteine residue with either A^{488} or A^{594} maleimides as described previously.[176] PolB1 has three native cysteines: C538 and C556 in a disulfide bond and a single solvent accessible Cys 67. C67 was mutated to Ser in favor of moving the labelling position towards the C-terminus (C67S/S740C). Single cysteines were introduced into *Sso*PCNA subunits [PCNA1 (S191C), PCNA2 (S92C)] and labelled similarly. *Sso*Dpo4 (PolY) was labelled at a single native C31.[296] Proteins were dialyzed into their storage buffer free of β-mercaptoethanol before adding 1.2- to 5-fold molar excess dye. Reactions were allowed to proceed for 2 hours at room temperature or overnight at 4 °C. Labelled proteins were separated from free dye using a 1 mL G-25 column (GE Healthcare Life Sciences), and/or extensive dialysis in labeling

buffer. Labeling efficiencies were calculated from a ratio of concentrations (dye: protein) using the extinction coefficients and generally exceeded 95%.

Steady-State FRET

Steady-state fluorescence spectroscopy was performed on a FluoroMax-4 spectrofluorimeter (HORIBA Jobin Yvon). WT or Y122P PolY labeled with A^{488} at 20 nM was titrated at room temperature with increasing concentrations of PolB1 labeled with A^{594} as indicated in the figure legends. The fluorescence emission spectra (505 to 650 nm) were collected with an excitation wavelength of 485 nm and 4 nm slits after each PolB1 addition. $PolB1^{594}$ titrations in the presence of unlabeled PolY were also performed similarly and subtracted from the donor/acceptor spectra. The quenching at 517 nm normalized to the donor-only intensity (v) was plotted as a function of PolB1 concentration and fit to the following equation:

$$v = 1 - \frac{\Delta F \times [PolB1]}{K_d + [PolB1]} \qquad \textbf{(Equation 3.1)}$$

where ΔF is the change in fluorescence amplitude, $[PolB1]$ is the protein concentration, and K_d is the dissociation constant calculated using KaleidaGraph (v4.5, Synergy Software). Multiple titrations were performed and averaged included with standard error before fitting.

Presteady-State FRET

Stopped-flow fluorescence experiments were performed on an Applied Photophysics (Leatherhead, UK) SX.20MV in fluorescence mode at a constant temperature of 22 °C. Template DNA (31mer) was labeled at the 3′ end with A^{488} by IDT. A 21 base primer was annealed and complementary to the 3′ end of the template. Final concentrations

of components after mixing were PolB1 (0.4 μM), RFC (0.4 μM), DNA (0.2 μM), ATP (0.3 mM), and PolY (0.4 μM), unless indicated otherwise. The samples were excited at 490 nm, and a 590-nm-cutoff filter was used to collect 4000 oversampled data points detecting only A^{594} emission over single or split-time bases. The slits were set at 3 mm for both excitation and emission. At least seven traces were averaged for each experiment and performed multiple times and on multiple occasions. The observed averaged traces were fit to one, two, or three exponentials using the supplied software. Below is the equation for a double exponential fit:

$$v = a_1 \cdot e^{-k_1 t} + a_2 \cdot e^{-k_2 t} + C \qquad \textbf{(Equation 3.2)}$$

where *a* is the amplitude change, *k* is the exponential rate, *t* is time, and *C* is a constant for the amplitude.

In Vitro Replication and Processivity Assays

Polymerase replication and processivity assays were performed as previously described,[176] with the following modifications. PolB1 (0.2 μM), PCNA (2 μM), RFC (0.4 μM), and ATP (0.2 mM) were loaded onto primed M13mp18 DNA (18 nM) to form the PolB1 HE. A M13 primer was 5' end labelled with ^{32}P-γ-ATP (PerkinElmer, Waltham, MA) using Optikinase (Affymetrix, Santa Clara, CA) according to manufacturer's instructions. PolY was added (at indicated concentrations) and incubated for 5 minutes, before initiating the reaction with 0.2 mM dNTPs. Single-turnover processivity assays were simultaneously initiated with 0.2 mM dNTPs and a 5000-fold excess salmon sperm DNA trap (3 mg/mL). DNA products were separated on either a 0.8% or 2.5% alkaline agarose gel depending on expected product length and dried under vacuum at 80 ºC for 1 hour. Gels were exposed to a phosphorscreen (GE Healthcare Life Sciences) for a minimum of

4 hours, imaged using a Storm 820 Phosphorimager (GE Healthcare Life Sciences), and the data analyzed using ImageQuant software (v.5.0, GE Healthcare Life Sciences). Quantification of the lane profiles from multiple experiments were calibrated to the 1kb DNA ladder (Promega, Madison, WI) to determine DNA product lengths.

Results

Detection of the Supraholoenzyme (SHE) Complex

As a means to follow composition and stability of the DNA polymerase holoenzyme complexes, we utilized analytical gel filtration chromatography (**Fig. 3.1A**). The heteropentameric *Sso* clamp-loader (RFC), consisting of four subunits of RFCS (small) and 1 subunit of RFCL (large), alone elutes around 12 mL with a total molecular weight 197,760 g/mol. RFC-directed loading of PCNA (individual subunits 1, 2, & 3) onto DNA is apparent at 10.5 mL. The broad spread of signal from 10-14 mL most likely indicates dynamic loading/dissociation of PCNA on DNA and interactions with RFC as well as RFC and PCNA123 alone. Formation of the PolY HE complex includes PolY/PCNA123/DNA at 10.6 mL with RFC dissociated from this complex. Similarly, the PolB1 HE consisting of PolB1/PCNA123/DNA forms at 10.5 mL (**Fig. 3.1B**) with RFC dissociated as also indicated previously.[176] Interestingly, addition of PolY to the PolB1 HE shifts the main peak to 9.7 mL indicative of a higher order SHE complex consisting of both PolY and PolB1 bound to PCNA and DNA. A western blot of the gel filtration fractions shows the shift and presence of PolY in the earlier eluting fractions within the SHE complex (**Fig. 3.1B-C**).

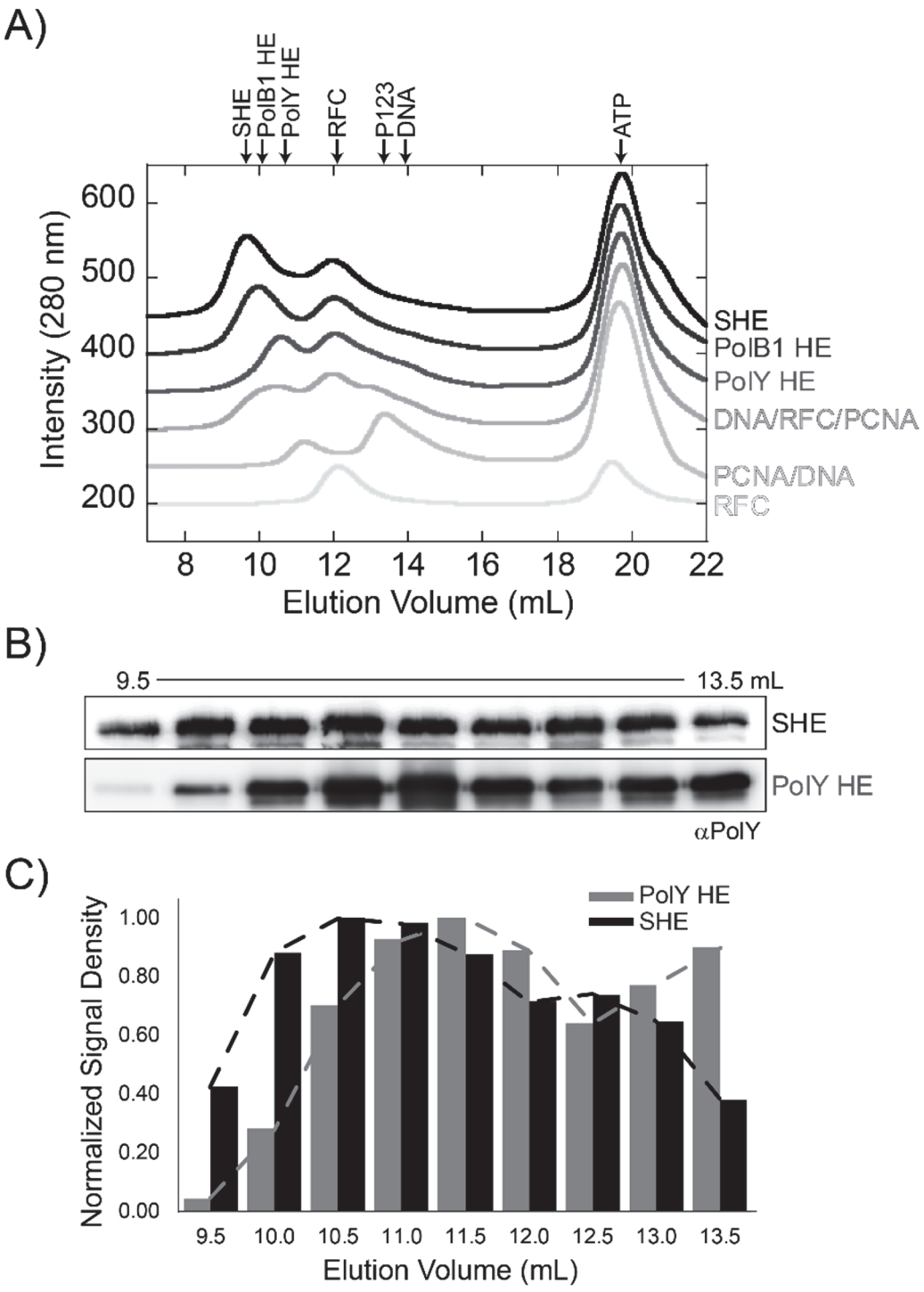

Figure 3.1: Detection of Supraholoenzyme (SHE) Complex by Analytical Gel Filtration. A) Size exclusion chromatography profile of the different protein/DNA complexes performed as described in Materials and Methods. PolY holoenzyme (PolY HE) consists of PolY/ DNA/RFC/PCNA123. PolB1 HE consists of PolB1/DNA/RFC/PCNA123. SHE consists of PolB1HE/PolY. ATP was included in all reactions for RFC-directed HE formation as well as an internal standard to account for drift in the elution profile. B) Western-blot analysis of αPolB1 and αPolY in SHE and PolB1 or PolY HE fractions. C) Relative quantification of PolY compared between SHE and PolY HE.

In order to directly monitor interactions between PolB1 and PolY by fluorescence resonance energy transfer (FRET), we labelled single cysteine positions on both proteins with fluorescent dyes. All proteins were active after labeling and were able to stimulate the activity of the respective PolB1 and PolY holoenzymes (data not shown). Titration of PolY labelled at C31 with Alexa 488 (A^{488}) with PolB1 labelled at C740 with Alexa 594 (A^{594}) showed fluorescence quenching and acceptor sensitization of the donor fluorescence consistent with an interaction between these two polymerases (**Fig. 3.2A**). Steady-state FRET experiments were also performed in reverse ($PolY^{594}$ titrated into $PolB^{488}$) with similar results and K_d (data not shown). Quantification of the normalized donor quenching at 517 nm as a function of [$PolB1^{594}$] was fit to **Equation 3.1** to give a $K_d = 0.14 \pm 0.02$ μM (**Fig. 3.2B**).

The interaction between PolB1 and PolY was also monitored by presteady-state FRET using a stopped-flow instrument. Rapid mixing of equal molar $PolB1^{488}$ and $PolY^{594}$ (0.4 μM final) shows a biphasic fluorescence increase consistent with a direct interaction between polymerases (**Fig. 3.2C**). Doubling or quadrupling the concentration of $PolY^{594}$ does not significantly affect the observed rate constants, k_1 and k_2, consistent with second order conformational change processes. Importantly, these experiments formed the basis for directly monitoring PolB1-PolY interactions within a SHE complex by FRET.

Recruitment of PolY to form the SHE Complex

Previously, we have shown assembly of the *Sso*PolB1 DNA polymerase holoenzyme (PolB1 HE) using presteady-state FRET.[176] Assembly included a complex multiple step pathway to form the PolB1 HE complex. Although PolB1 has specificity for PCNA2 and PolY has specificity for PCNA1, we can also monitor binding to the

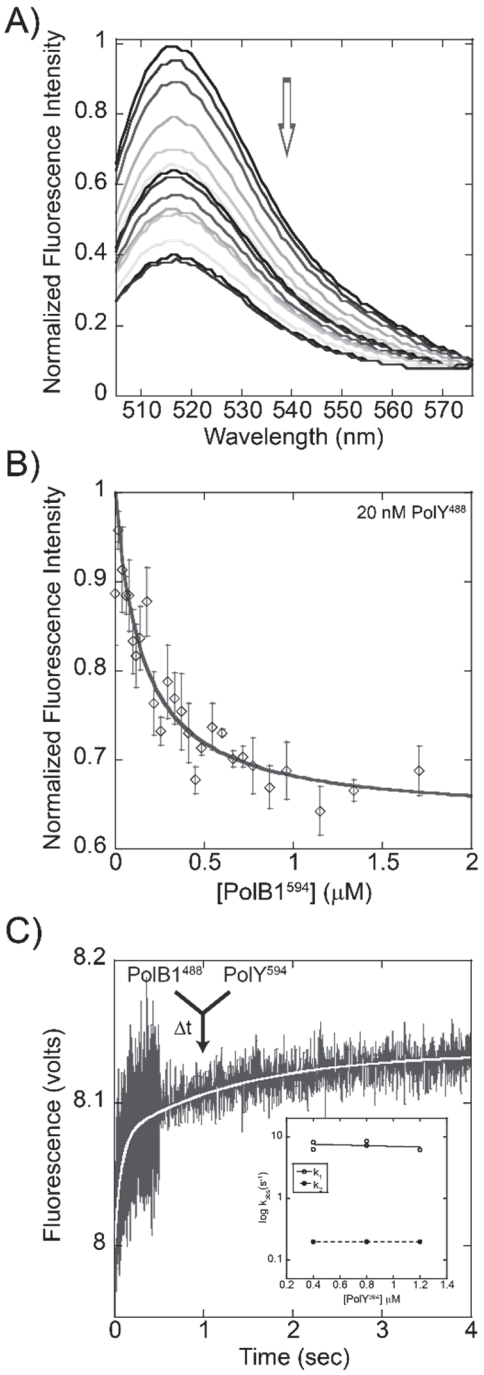

Figure 3.2: Direct Interaction of PolB1 and PolY Monitored by FRET
A) Steady-state FRET quenching 20 nM PolY labeled with Alexa 488 ($PolY^{488}$) with PolB1 labeled with Alexa 594 ($PolB1^{594}$) at room temperature (22 °C). Reported spectra were corrected for dilution and for the intrinsic fluorescence of buffer components and unlabeled PolY. Spectra were normalized to 1.0 by using the donor only as a reference. B) The fluorescence maximum (@ 517 nm) was plotted as a function of [$PolB1^{594}$] and fit to **Equation 3.1** to give $K_d = 0.14 \pm 0.02$ μM. Error bars represent the standard error from five independent titrations. C) Presteady-state FRET of $PolB1^{488}$ interacting with $PolY^{594}$ (0.4 μM final) shows a biphasic curve. The observed rates (k_1 and k_2) from ten experiments consisting of at least seven averaged traces each were plotted as a function of [$PolY^{594}$] indicating second order rate constants (inset).

heterotrimer PCNA123 and assembly of the complexes from either labelled position (**Fig. 3.3A&B**). Larger FRET is observed when there is a preformed PCNA123 heterotrimer with the label at either PCNA1 or PCNA2 subunit. From the clamp-loaded state (DNA/PCNA123/RFC), we have now monitored the recruitment of PolY to form the PolY TLS holoenzyme complex (YHE) using specifically fluorescently labelled proteins (**Fig. 3.3C**). The averaged stopped-flow FRET trace fit best to a double exponential consistent with two conformational change steps (k_1^{obs} and k_2^{obs}) after association. YHE assembly can be monitored from either donor labelling of PCNA1, or PCNA2 with similar rate constants although labelling at PCNA2 ensures interaction FRET measurements with the PCNA123 trimer instead of direct interactions between PolY and PCNA1. Doubling or halving the PolY concentration did not significantly affect the observed rates (data not shown) indicating that we are monitoring second order conformational steps after binding.

When the PolB1 HE complex is preformed, addition of PolY to form the SHE complex can be monitored by FRET from multiple vantage points (**Fig. 3.4A**). Specific labelling of DNA, PCNA1, PCNA2, or PolB1 with A^{488} within the PolB1 HE can be used as donor positions to follow an incoming PolY labeled with A^{594}. Interestingly, although the fluorescence amplitude changes as a function of labelling efficiency and relative spatial position within the SHE complex, the observed rates (k_1^{obs} and k_2^{obs}) are similar for binding of PolY (**Fig. 3.4B&C**). This suggests that PolY binds the PolB1 HE complex independent of any one protein and that no single protein is displaced upon binding PolY. The DNA concentration in this experiment is limiting (0.2 μM final) as higher concentrations of DNA show vastly greater rates when DNA is labelled with A^{488}, more consistent with direct binding of PolY to free DNA. Changing the concentration of PolY while keeping the

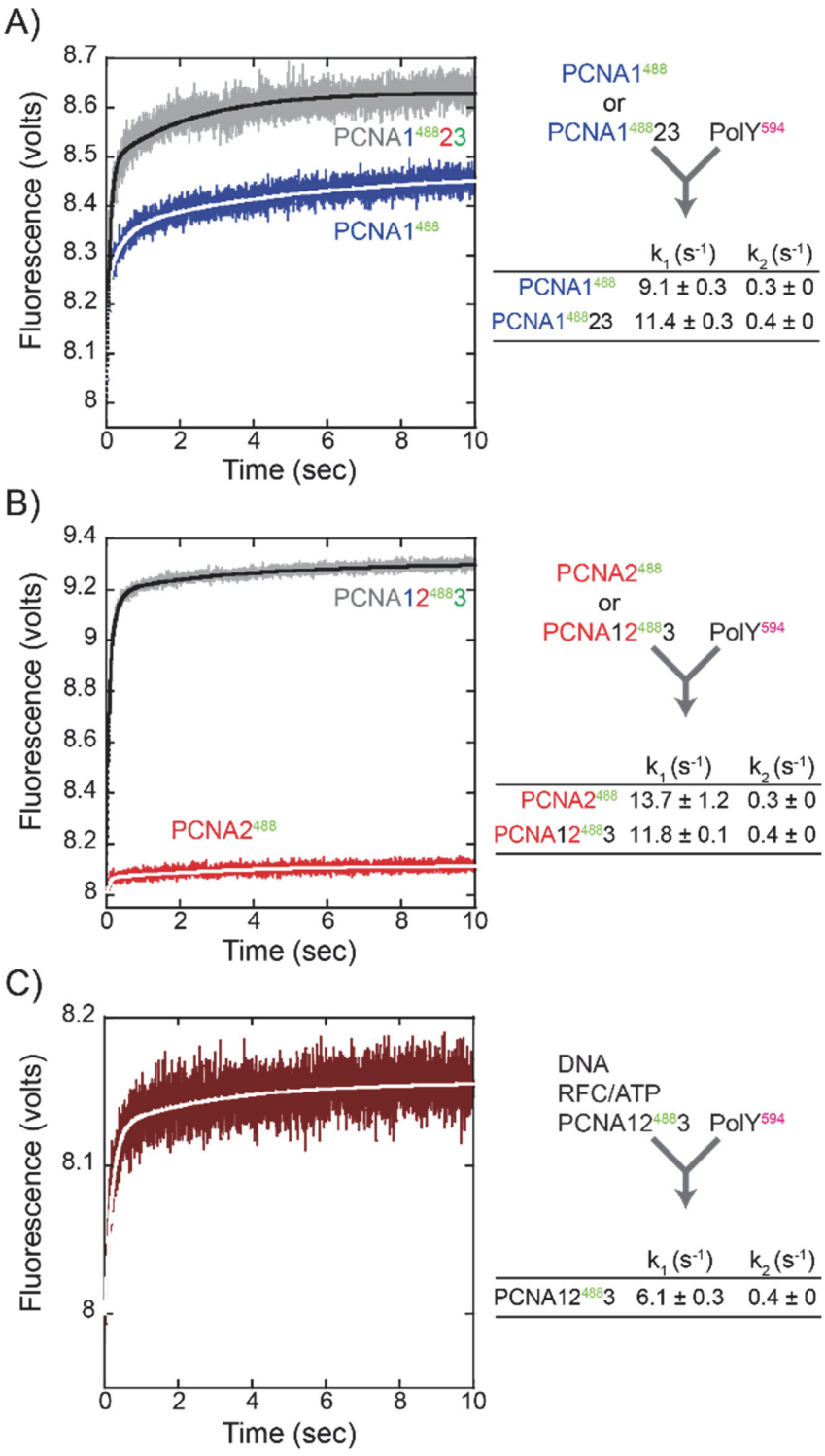

Figure 3.3: PolY Specificity for PCNA Alone and Within PolY HE
Specificity of A) PCNA1^{488} or B) PCNA2^{488} alone or within a heterotrimeric complex (PCNA123) for PolY^{594} followed by presteady-state FRET (0.4 μM final). C) Presteady-state interaction of PolY^{594} to a preloaded PCNA12^{488}3/RFC/DNA (0.4 μM final) complex in the presence of ATP (0.3 mM). Double exponential rates derived from fitting to **Equation 3.2** are shown adjacent to the plots.

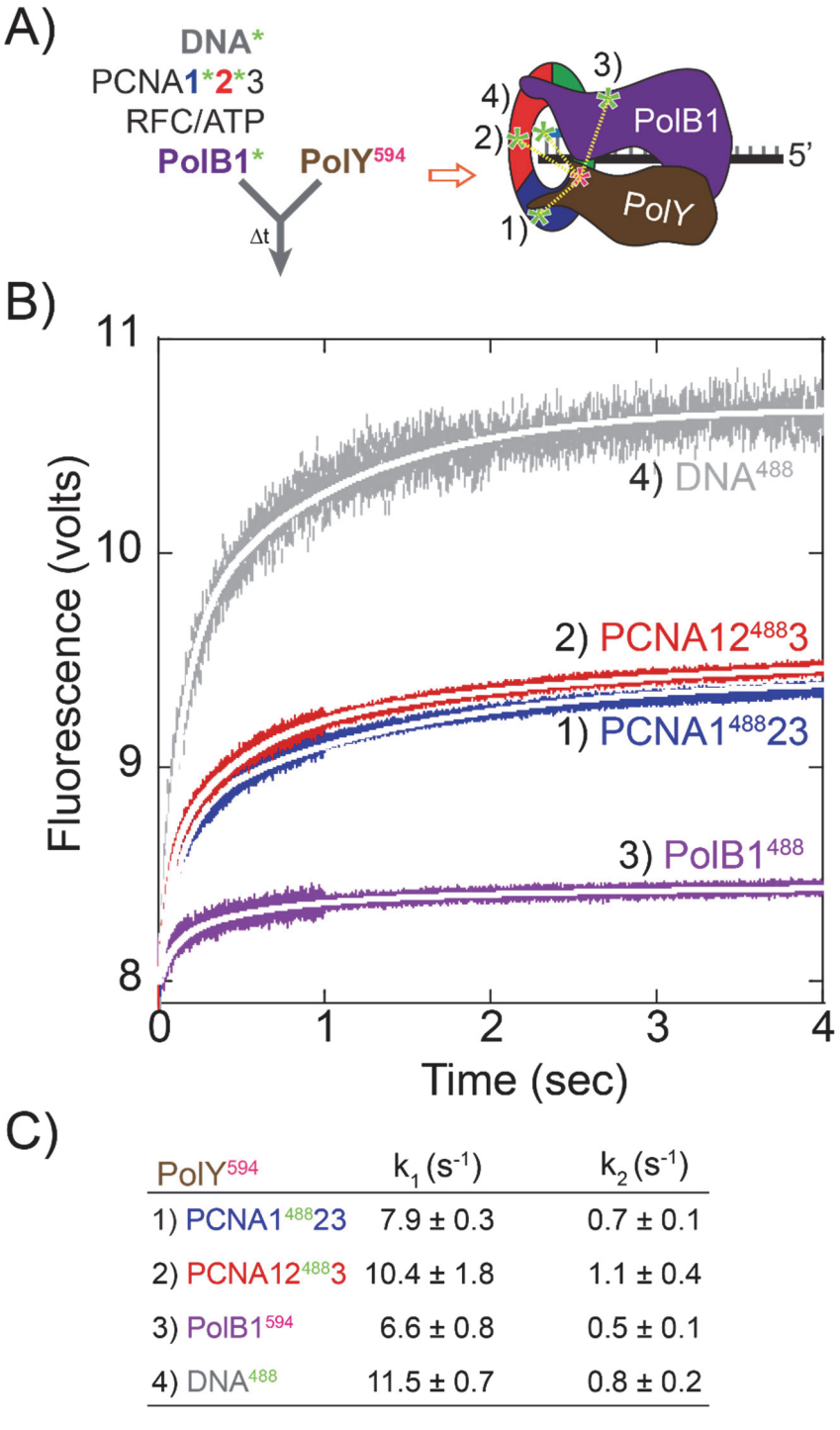

C)

PolY594	k_1 (s^{-1})	k_2 (s^{-1})
1) PCNA1488 23	7.9 ± 0.3	0.7 ± 0.1
2) PCNA12488 3	10.4 ± 1.8	1.1 ± 0.4
3) PolB1594	6.6 ± 0.8	0.5 ± 0.1
4) DNA488	11.5 ± 0.7	0.8 ± 0.2

Figure 3.4: Presteady-state FRET Assembly of the SHE
A) Presteady-state FRET traces monitoring interactions of PolY^{594} (0.4 μM final) to specific components of a preformed PolB1 HE complex. In each experiment, only one PolB1 HE component was fluorescent labeled with Alexa^{488} (*): DNA* (grey), PCNA2* (red), PCNA1* (blue), or PolB1* (purple) in separate experiments. B) Fluorescence traces were adjusted to 8.0 and plotted together for more direct comparison of the C) rates fit from a double exponential increase (**Equation 3.2**). Error values indicate the standard error from three independent experiments consisting of at least seven averaged traces each.

concentration of the PolB1 HE components the same does not alter the observed rates indicating that we are monitoring a first-order conformational change process (**Fig. 3.5**). Building on the kinetic assembly pathway from PolB1/PCNA123/DNA^{G} published previously,[176] formation of the SHE complex proceeds through an equilibrium binding step (H) followed by two additional fluorescently observed conformational states (I-J).

In order to confirm that the PolB1 HE stays intact when PolY binds to form the SHE, we instead assembled a PolB1 HE labelled with both a donor and acceptor dye as a FRET complex from three different perspective and then mixed with unlabeled PolY (**Fig. 3.6A**). In this experiment, should PolY displace the binding of any single PolB1 HE component, the FRET signal would decrease. However, for the three different experiments with donor and acceptor labels on different proteins or DNA, double exponential increases in fluorescence were observed (**Fig. 3.6B&C**) that mirror the rates from direct FRET monitoring of SHE formation (**Fig. 3.4B**). Therefore, PolY not only binds to form the SHE complex, it also stabilizes and/or rearranges the overall conformation.

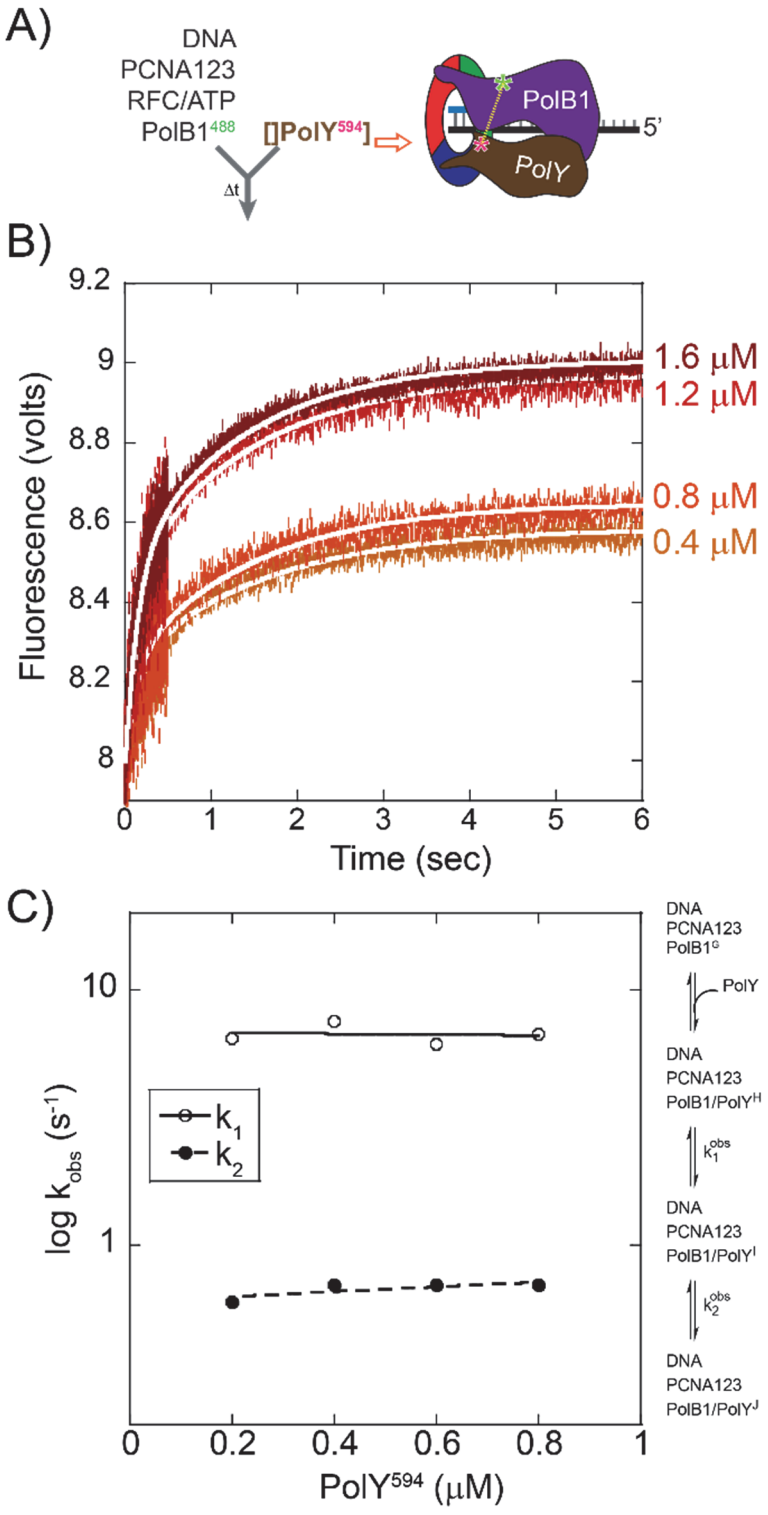

Figure 3.5: Effect of [PolY] on SHE Formation
A) Presteady-state FRET traces monitoring interactions of PolY^{594} at different concentrations to a preformed PolB1 HE complex labeled at PolB1^{488}. Fluorescence traces were adjusted to 8.0 for more direct comparison. B) The observed double exponential rates (k_1 & k_2) for PolY binding and SHE formation were plotted monitoring two second order steps.

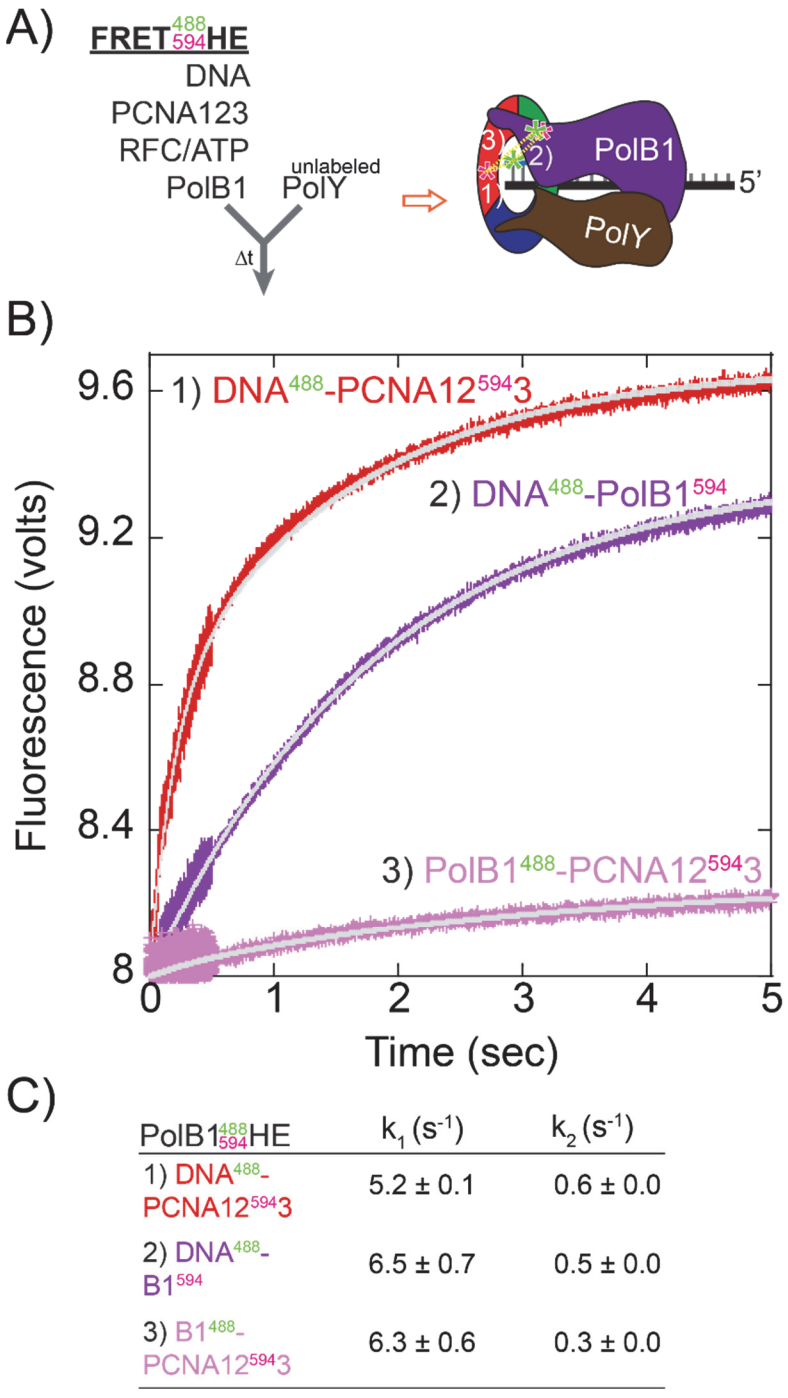

C)

PolB1 488/594 HE	k_1 (s^{-1})	k_2 (s^{-1})
1) DNA488-PCNA125943	5.2 ± 0.1	0.6 ± 0.0
2) DNA488-B1594	6.5 ± 0.7	0.5 ± 0.0
3) B1488-PCNA125943	6.3 ± 0.6	0.3 ± 0.0

Figure 3.6: Addition of PolY Stabilizes the SHE Complex
A) Preformed PolB1 HE with two of the components labeled was mixed with unlabeled PolY in a stopped-flow instrument and the FRET signal was monitored. B) Presteady-state FRET traces of a preformed FRET PolB1 HE complex showing the fluorescence enhancement and stabilization upon addition of unlabeled PolY (0.4 μM final). Fluorescence traces were normalized to 8.0 for more direct comparison. Schematic representation of the FRET experiments is shown inset. C) Double exponential rates (**Equation 3.2**) of the interactions fit for each FRET increase. Error values indicate the standard error from three independent experiments consisting of at least seven averaged traces each.

Polymerase Exchange is Directed by PIP Interactions

Previously, we described how the *Sso* replicative holoenzyme achieves high rates of replication through a process of rapid polymerase re-recruitment, rather than processive single enzyme synthesis.[176] This mechanism may also allow for the rapid exchange of the PolB1 replication polymerase with a TLS polymerase, PolY, opportunistically or specifically when needed. However, whether this is directed by contacts within a SHE complex or polymerase exchange occurs preferentially from solution is not known. Therefore, we titrated PolY constructs aimed to test interactions with PCNA into a PolB1 HE primer extension reaction (**Fig. 3.7**). PolY has a slower global polymerization rate because of its low processivity;[180] therefore, if it exchanges with PolB1, the product length will be shorter than as seen with WT (lanes 2-5). The reduction in product length occurs at stoichiometric or higher concentrations compared with PolB1. Mutation of the PIP site in PolY (PIP$^-$) eliminates an interaction with PCNA1 specifically and shuts down DNA synthesis even more than WT (lanes 6-9) suggesting that either direct exchange from solution is favored or the PIP site interaction coordinates exchange within a SHE complex.

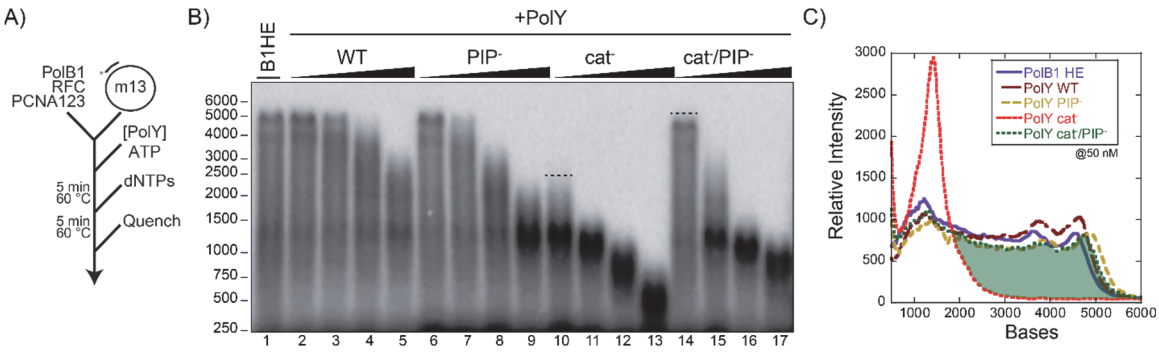

Figure 3.7: PolY PIP contacts are important for SHE action and exchange
A) Experimental scheme showing PolY variants titrated to a 200 nM PolB1 HE before initiation with dNTPs to follow DNA synthesis length after five minutes at 60 °C. B) PolY WT, PIP$^-$, cat$^-$, or cat$^-$/PIP$^-$ were added at increasing concentration (50, 100, 200, 400 nM). The dashed lines (lanes 10 and 14) indicate C) the 50 nM [PolY] that are directly compared (cat$^-$ vs. cat$^-$/PIP$^-$) by difference shading (green) in quantification of the product lengths.

Mutation of the active site of PolY (cat$^-$) reduces product length further (lanes 10-13), consistent with both direct PolY exchange and with PCNA directed exchange within SHE. Interestingly when the cat$^-$/PIP$^-$ PolY mutant was titrated, there was a partial rescue in product length (lanes 14-17) compared to cat$^-$ alone (lanes 10-13) (**Fig. 3.7B&C**), suggesting that PolY-PCNA1 contacts are important but not solely required for effective polymerase exchange. DNA synthesis was not inhibited until higher concentrations of the cat$^-$/PIP$^-$ polymerase were titrated compared to the cat$^-$ PolY (**Fig. 3.8**). However, full length DNA products were not restored to WT lengths for cat$^-$/PIP$^-$ and were even greater than cat$^-$ products, indicating that other interaction sites for PolY may exist within the SHE to mediate exchange. The combined data indicates that PolY is able to replace PolB1 from solution and that exchange is facilitated when PolY interacts with PCNA1, but importantly, there is also evidence for direct contacts between PolB1 and PolY within a SHE complex during active replication.

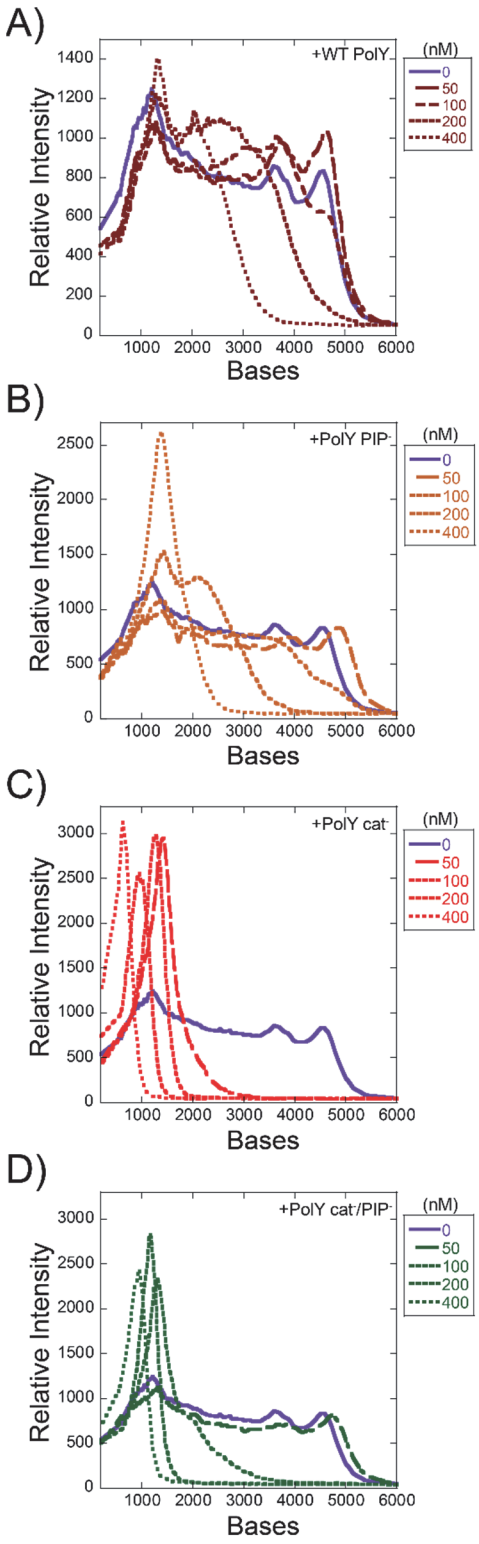

Figure 3.8: Quantification of the DNA Product Distribution from Figure 3.7
Lane profiles for DNA products synthesized when PolY A) WT, B) PIP$^-$, C) cat$^-$, or D) cat$^-$/PIP$^-$ (50, 100, 200, 400 nM) was added to a 200 nM PolB1 HE. The lane profile for the PolB1 HE alone is included (purple) for comparison.

Novel PolB1-PolY (YB) Interaction Site Identified Within the Supraholoenzyme

In order to probe a potential PolB1-PolY interaction on DNA synthesis ability and exchange, we identified residues (Y122, L126, I163) within a hydrophobic patch on the surface of PolY (**Fig. 3.9A-B**). This patch was identified first through molecular modelling of a SHE complex that fixed the PIP site of PolB1 to PCNA2 and the PIP site of PolY to PCNA1 bound to a primer template DNA. We then utilized PolB1 truncation data that mapped PolY binding to the central region on PolB1 (residues 482-617)[171] to limit the potential interaction site of PolY contained with the SHE. Coincidently, these residues in Archaeal PolY are homologous to residues in the TLS polymerase, Pol IV, from *E. coli* identified from a genetic mutant screen sensitive to DNA damage (**Fig. 3.9C**).[164]

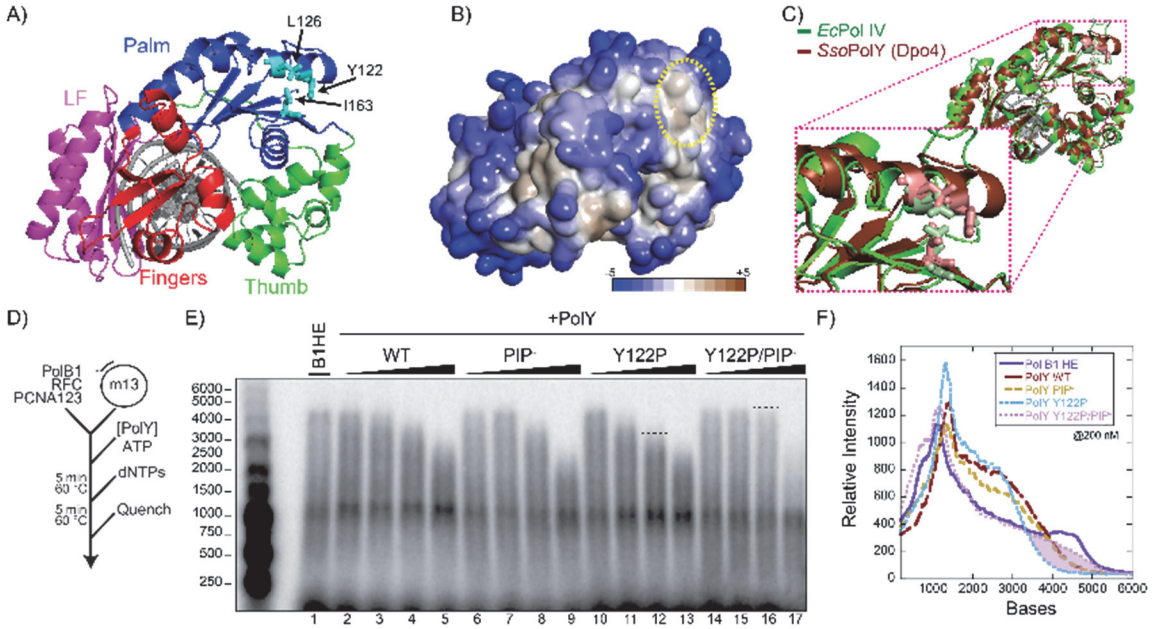

Figure 3.9: PolY YB contacts are also important for SHE action and exchange
A) Crystal structure of *Sso*PolY(Dpo4)/DNA (PDBID: 1JXL) identifying residues (Y122, L126, & I163) within a B) hydrophobic patch on the back of the palm domain. C) Structural overlay of *Ec*Pol IV (PDBID: 4IR1) (green) with *Sso*PolY (brown) highlighting homologous Pol IV residues (T120, Q124, & Q161). D) Experimental scheme showing PolY variants titrated to a 200 nM PolB1 holoenzyme before initiation with dNTPs to follow DNA synthesis length after five minutes 60 ºC. E) PolY WT, PIP$^-$, Y122P, Y122P/PIP$^-$ were added at increasing concentration (50, 100, 200, 400 nM). The dashed lines (lanes 12 and 16) indicate F) the 200 nM [PolY] that are directly compared (Y122P vs. Y122P/PIP$^-$) by difference shading (lilac) in quantification of the product lengths.

Again, we designed primer extension assays to test the ability of these PolY mutants (Y122A, Y122P, L126N, I163N) to direct exchange within the SHE complex and slow synthesis to affect product length. The absence of an interaction of PolY with PolB1 from a specific mutation would abrogate this polymerase exchange ability and result in longer products than with wild-type PolY. Mutation of PolY (Y122P) decreases the quenching and binding affinity for PolB1 measured in steady-state FRET assay (**Fig. 3.10**). In fact when each of the PolY mutants was titrated into a PolB1 HE primer extension assay, only in combination with the PIP$^-$ mutation did the PolY-YB/PIP$^-$ mutants restore more full length product at the higher concentrations, indicating the exchange had been affected (**Fig.**

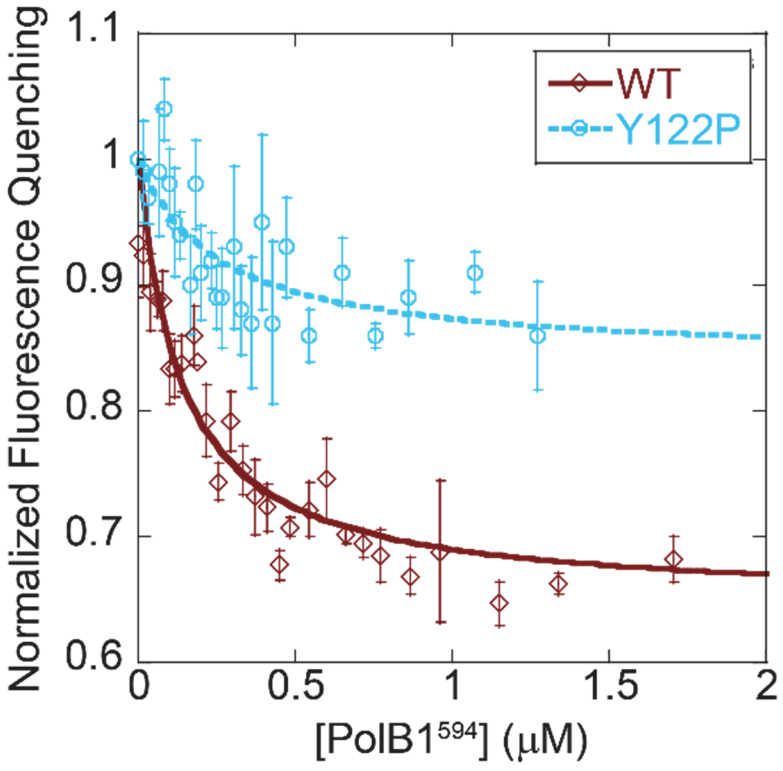

Figure 3.10: Reduced Affinity for PolB binding to PolY (Y122P)
Steady-state FRET quenching 20 nM PolY [WT (brown) or Y122P (azure)] labeled with A^{488} titrated with PolB1^{594} at room temperature (22 °C). Spectra were corrected, normalized, and fit as in **Figure 3.2** to give K_d = 0.26 ± 0.13 μM for PolY (Y122P) compared to 0.14 ± 0.02 μM for WT. Error bars represent the standard error from multiple titrations.

3.11). Directly comparing stoichiometric concentrations of PolB1 and PolY in this assay for Y122P and Y122P/PIP$^-$ mutants show only a restoration of product length when both contact sites in PolY are mutated (lanes 14-17) (**Fig. 3.9D-F**). Quantification of the product length as a function of concentration of each PolY construct shows modulation in the product length, especially for Y122P/PIP$^-$ (**Fig. 3.12**). Therefore, PolY requires at a minimum interactions with both PCNA1 (PIP) and PolB1 (YB) to direct exchange from solution and within the SHE complex.

Based on the stabilization of the SHE complex noted above with the stopped-flow FRET (**Fig. 3.6**) and the YB contacts identified to be important for complex formation, we next tested the ability of the SHE complex to increase processivity of DNA synthesis (**Fig. 3.13**). Previously, we had shown that the PolB1 HE alone has low processivity and instead acts distributively during synthesis, repetitively recruiting PolB1 to replicate long stretches of DNA.[176] Addition of WT PolY to the PolB1 HE (forming the SHE) increases the processivity of DNA synthesis by a few hundred bases (lanes 3 vs. 4) (**Fig. 3.13B)**. In these processivity assays, a high concentration of ssDNA is added with the dNTPs to initiate synthesis while at the same time trapping any polymerases that dissociate from the DNA template during the course of the reaction to measure length of DNA synthesis from a single processive event. Both PIP$^-$ and Y122P PolY constructs also increase the processivity significantly over PolB1 HE alone (**Fig. 3.13B,** lanes 5-6 **& C**). However, when both PIP$^-$ and Y122P mutations are combined, the processivity is reduced to PolB1

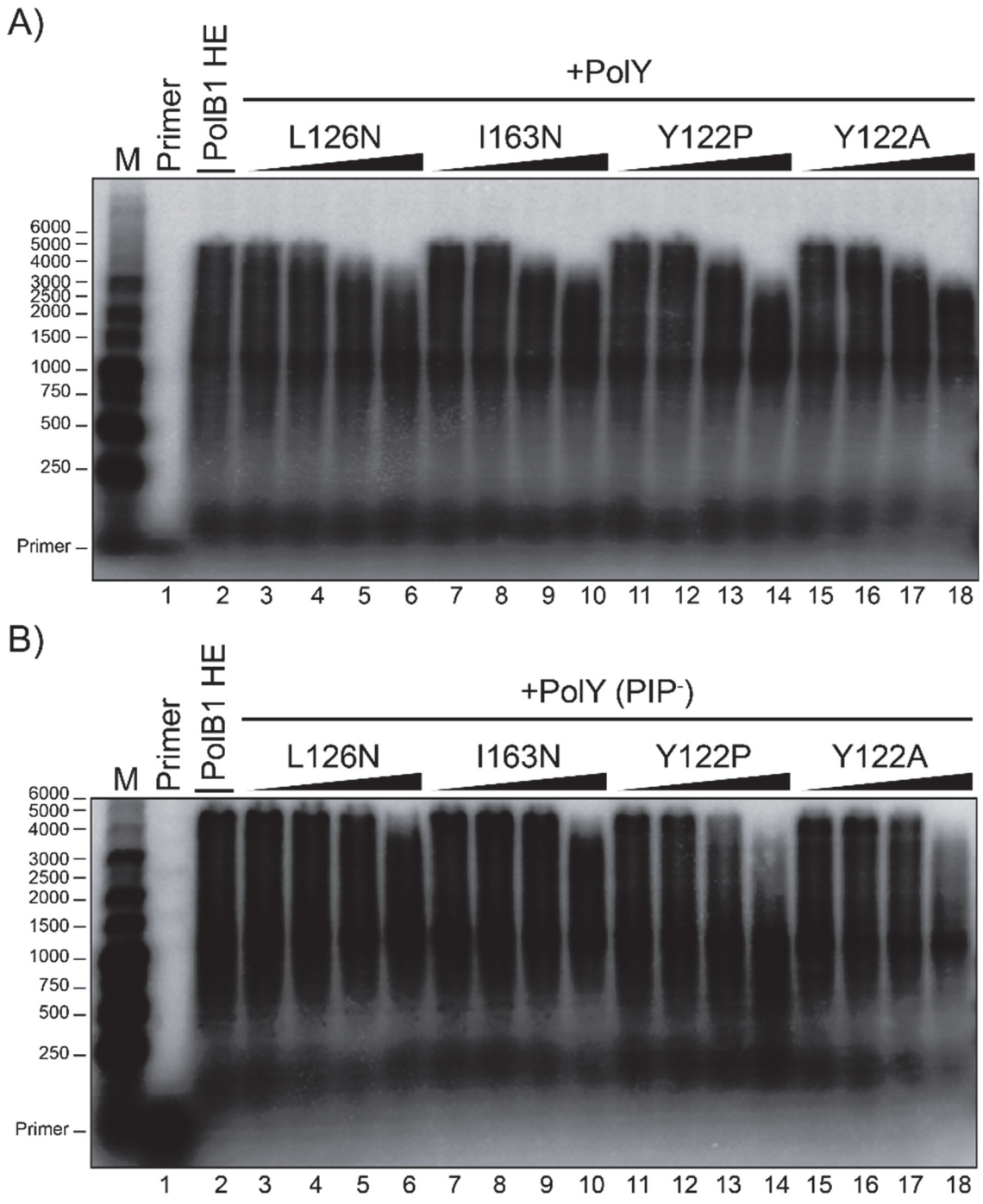

Figure 3.11: Effect of YB mutants of the PolB1 HE activity
A) Pol Y YB mutants (L126I, I163N, Y122P, or Y122A) or B) YB PIP- mutants (50, 100, 200, 400 nM) added to a 200 nM PolB1 holoenzyme before initiation with dNTPs to follow DNA synthesis length after five minutes.

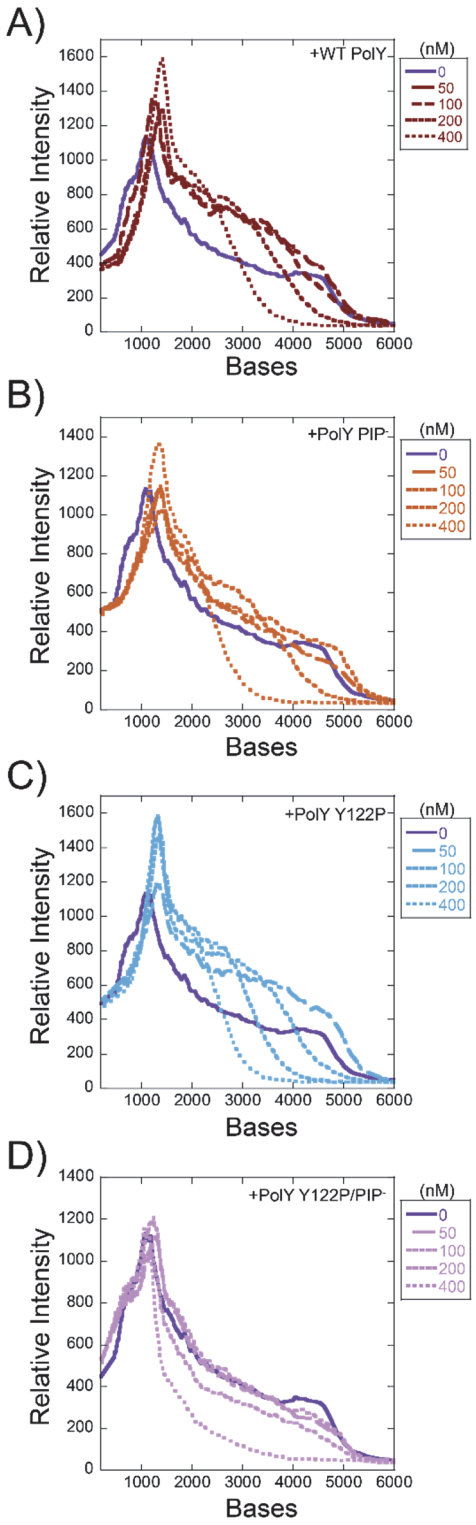

Figure 3.12: Quantification of the DNA Product Distribution from Figure 3.9
Lane profiles for DNA products synthesized when PolY A) WT, B) PIP$^-$, C) Y122P, or D) Y122P/PIP$^-$ (50, 100, 200, 400 nM) was added to a 200 nM PolB1 HE. The lane profile for the PolB1 HE alone is included (purple) for comparison.

HE level (lanes 3 vs. 7) implicating both sites for the stabilization of the SHE complex on DNA.

Presteady-state stopped-flow FRET experiments were used again to follow the impact of the Y122P on interaction within the PolB1 HE. PolY Y122P interacts similarly to WT with PCNA123 labelled at P1 or P2 in isolation (**Fig. 3.14**). When PolB1^{488} was preloaded on DNA in a HE complex and rapidly mixed with PolY^{594} (WT or Y122P), there

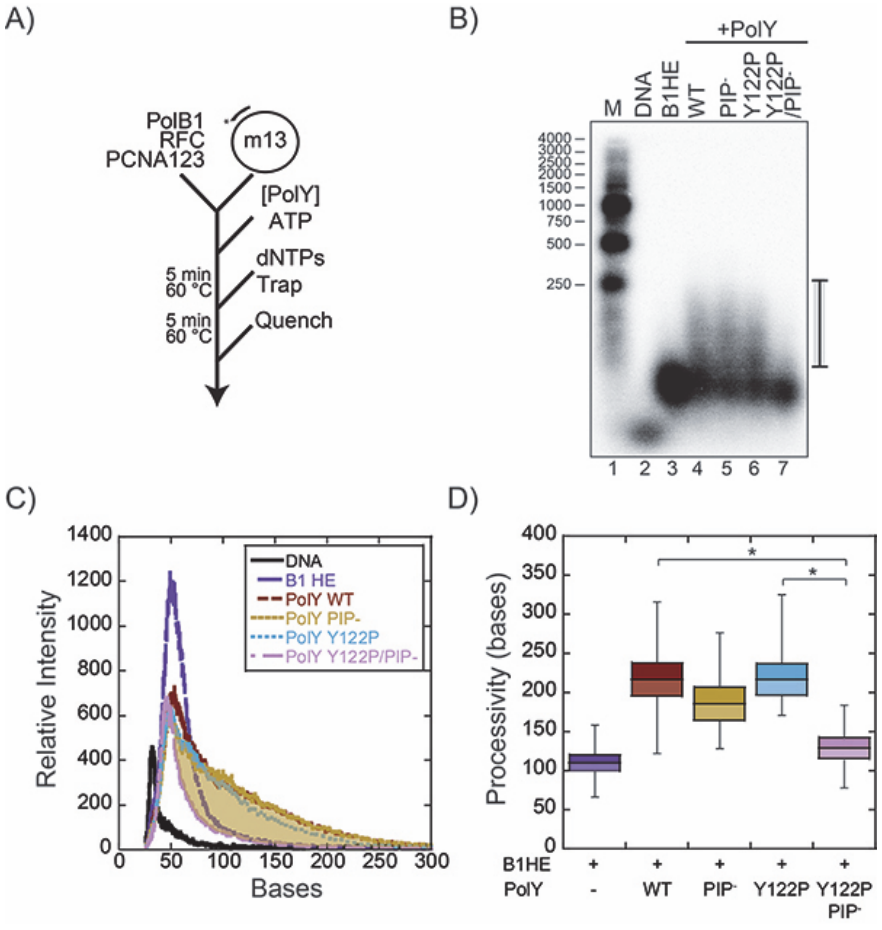

Figure 3.13: Addition of PolY Increases the Processivity of the PolB1 HE
A) Experimental scheme showing B) 200 nM PolY variants [WT (brown), PIP$^-$ (maize), Y122P (azure), Y122P/PIP$^-$ (lilac)] added to a 200 nM PolB1 HE before initiation with dNTPs and 3 mg/mL ssDNA trap to follow processivity of DNA synthesis. C) Quantification of the DNA product lengths and difference shading (maize) of Y122P/PIP$^-$ compared to PIP$^-$. D) Plot of the mean, standard error, and range of processivity values for SHE combinations from eight independent experiments. Significance and p-values are indicated (* < 0.5).

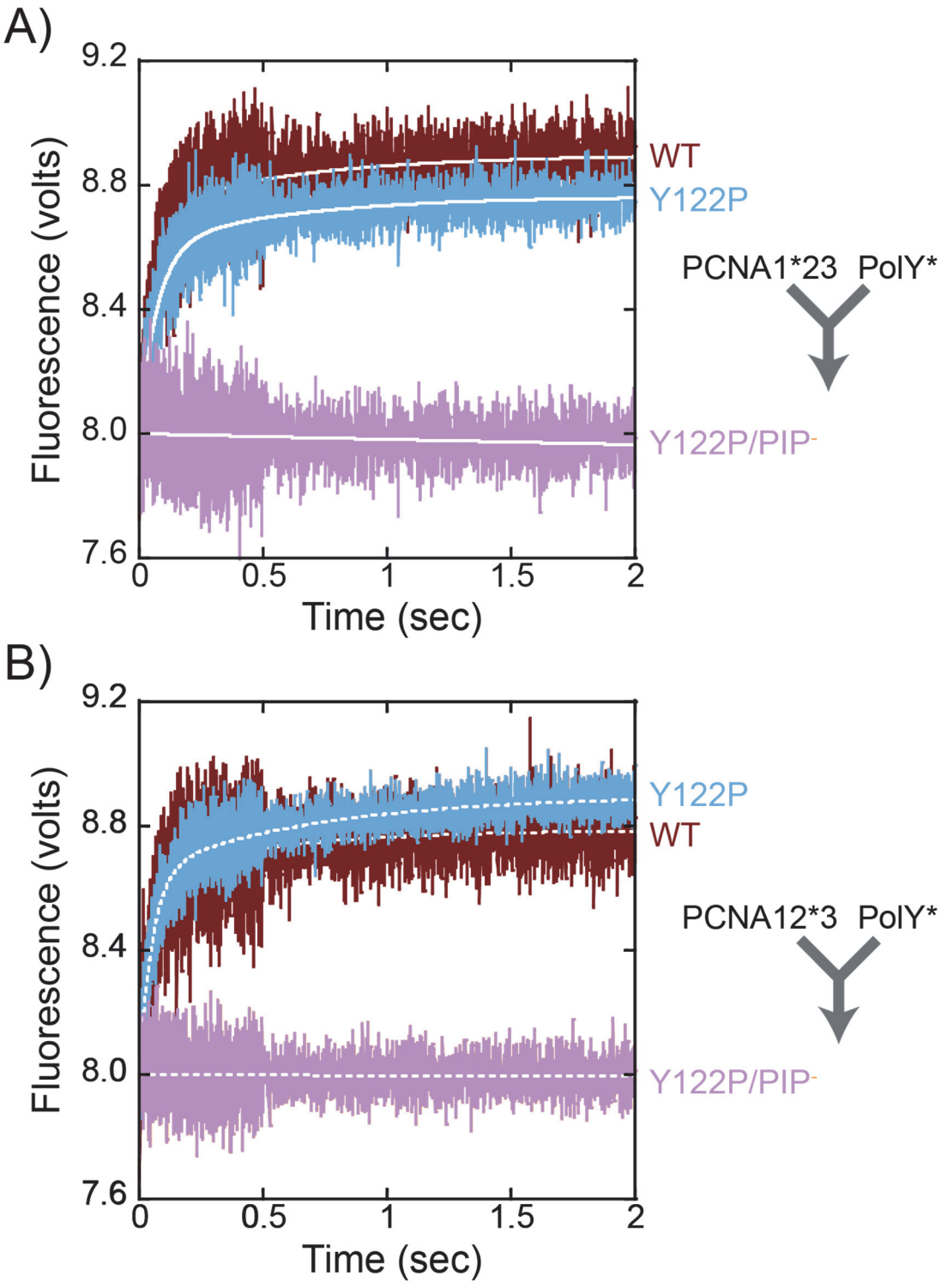

Figure 3.14: Y122P Mutation Does not Disrupt PolY Interaction with PCNA
Presteady-state FRET was used to monitor the interaction between A) PCNA1^{488}23 or B) PCNA12^{488}3 subunit versus PolY^{594} (WT, Y122P, or Y122P/PIP^{-}).

were similar double exponential increases observed (**Fig. 3.15**). The amplitude is consistently larger for Y122P over WT, which may indicate a slightly different final conformation for this mutant within the SHE complex. Mutation of PIP^- in PolY reduces the FRET signal considerably but without significantly affecting the rate, suggesting a reduction in the formation of the SHE complex. The combination of Y122P and PIP^- mutations in PolY virtually abrogate the entire FRET signal, clearly implicating both the PIP and YB sites in formation of the SHE complex.

Discussion

In this study, we have identified interactions between the B-family replication polymerase and the Y-family TLS polymerase in *Sso* that contribute to formation of a supraholoenzyme (SHE) complex. For this, we utilized a combination of biochemical techniques aimed at first identifying direct interactions between polymerases first by analytical gel filtration and FRET and second examining the mechanism of polymerase exchange that occurs during DNA synthesis. Known PIP binding sites to PCNA1 as well as a newly identified YB interaction site between polymerases are together required for maintaining the SHE complex. The YB site is a conserved hydrophophic patch on the back of the palm domain of PolY. Binding of PolY to the PolB1 HE occurs through concerted interactions with the PIP interaction site on PCNA1 and a YB interaction site with PolB1. The presence of PolY within the SHE stabilizes the entire complex, effectively increasing processivity of DNA synthesis. Direct polymerase exchange with the DNA template can occur within the confines of the SHE complex during DNA synthesis repetitively switching high and low fidelity polymerases. At higher concentrations of PolY, polymerase exchange

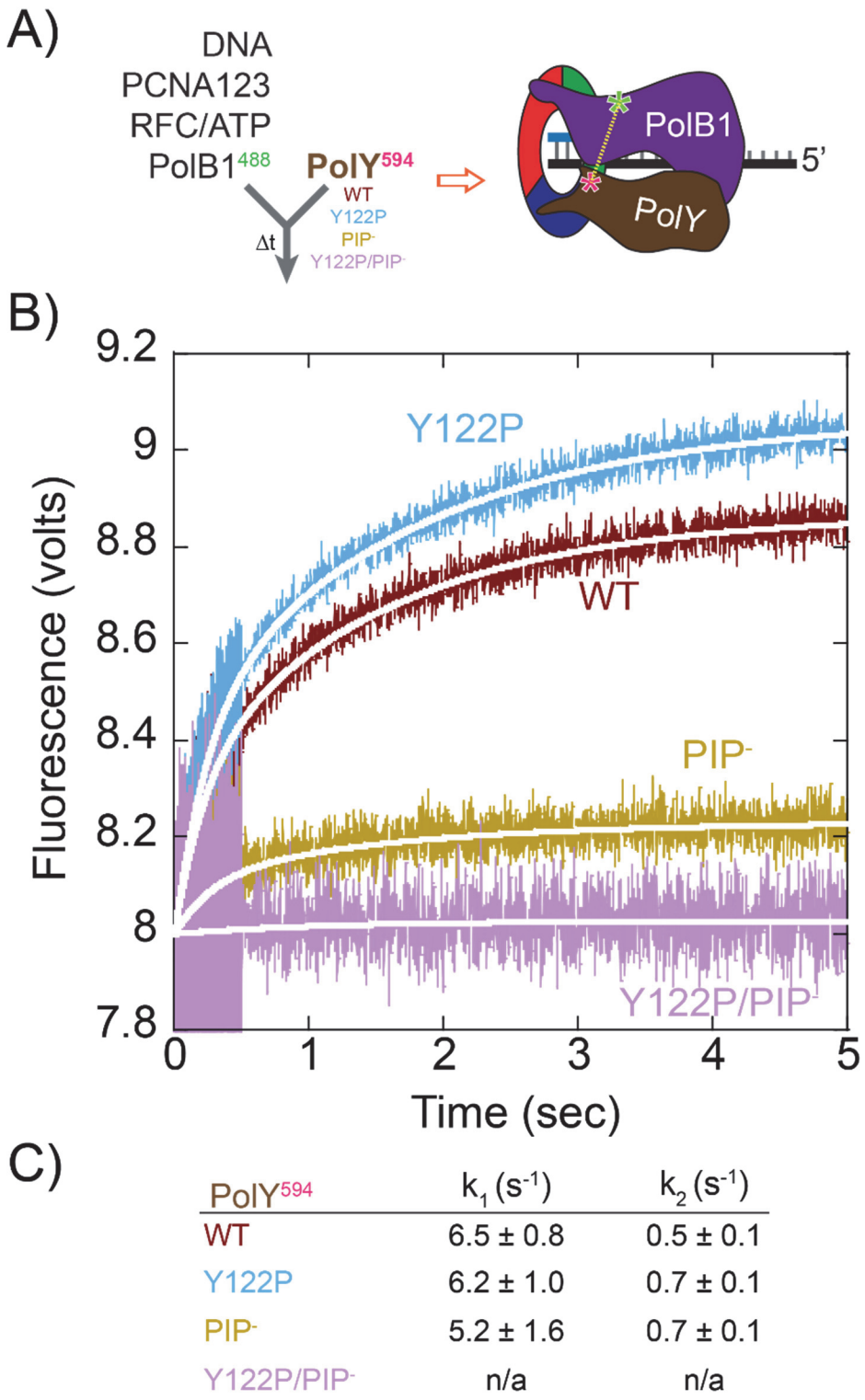

PolY^{594}	k_1 (s^{-1})	k_2 (s^{-1})
WT	6.5 ± 0.8	0.5 ± 0.1
Y122P	6.2 ± 1.0	0.7 ± 0.1
PIP$^-$	5.2 ± 1.6	0.7 ± 0.1
Y122P/PIP$^-$	n/a	n/a

Figure 3.15: SHE Formation is Dependent on Both PIP and YB Sites
Presteady-state FRET traces showing the interactions of PolY^{594} [WT (brown), PIP$^-$ (maize), Y122P (azure), Y122P/PIP$^-$ (lilac)] to Pol B1^{488} HE. Fluorescence traces were normalized to 8.0 for more direct comparison and fit to a double exponential (**Equation 3.2**) and reported in B). Error values indicate the standard error from three independent experiments consisting of at least seven averaged traces each.

from solution predominates, displacing the PolB1 HE or SHE. Identification of the SHE complex expands our understanding of concerted DNA polymerase exchange within the complex as well as provides a plausible mechanism for recruitment of PolY from solution for coordination of high fidelity and translesion DNA synthesis.

PCNA is known to interact with many protein partners through the PIP binding site, however, how the trimeric protein coordinates binding and regulates activity is still not known. The availability of three binding sites on the trimer could allow up to three different protein partners to be contained and their activities coordinated towards the DNA substrate in a 'tool-belt' configuration. Increasing local concentrations of proteins or providing contacts for recruitment by simultaneous binding to PCNA can effectively increase the rate of processing. For example, Okazaki fragment maturation requires the sequential action of DNA polymerase, flap endonuclease, and DNA ligase. In archaea, it has been shown that an Okazakisome consisting of the co-occupancy of these three proteins to the heterotrimeric *Sso*PCNA123 can exist to promote joining of Okazaki fragments.[225, 261] However, although a similar Okazaki fragment maturation complex can exist in eukaryotes, engineered single binding site PCNA molecules are fully capable of directing lagging-strand processing through a sequential switching process[70, 265] calling into question the absolute utility of the 'tool-belt'.

Perhaps some of the most well characterized 'tool-belt' activity and coordination comes from work with the β-clamp and various DNA polymerases in bacteria. Both the high-fidelity Pol III and lower-fidelity TLS Pol IV can be contained on the β-clamp[162] and a secondary binding site can regulate Pol IV engagement and Pol III dissociation at the site of a lesion.[19, 163, 297, 298] In the absence of Pol IV or on undamaged DNA, Pol III

preferentially engages the DNA template for active and processive DNA synthesis. Further work identified a functional interaction between residues in Pol III and Pol IV from a genetic screen[164] that are homologous to the YB site identified here (**Fig. 3.9C**). In addition to Pol IV, the cryptic activity of the TLS Pol II has also been shown to form a 'tool-belt' complex with Pol III and the beta clamp that can rapidly exchange binding to the DNA template, although the disruptive activity is less than for Pol IV.[165] The third TLS polymerase in bacteria, Pol V, can also be bound to the beta clamp through an opposite cleft from Pol III, however, genetic experiments show that a single cleft is capable of supporting coordinated TLS synthesis implicating other binding sites within this complex.[222] Pol V – Pol III directed exchange and TLS coordination has yet to be shown experimentally *in vitro*.

It is interesting that different laboratories have independently identified common polymerase interaction sites (YB) in two highly divergent domains of life: bacteria and archaea. The amino acid residues in this area are not highly homologous across domains or even within related species. However from the limited x-ray structures available, there is a strong hydrophobic surface on the back of the palm domain of all these polymerases. As well as providing for an interaction with PolB1 (YB) within a SHE complex, this hydrophobic patch may also be important for recruiting PolY to additional DNA damaged sites through interactions with other proteins such as single-strand binding protein or other DNA repair factors.

PolY's primary interaction site is with the clamp protein, *i.e.* PCNA1 in *Sso*. The co-occupancy of two polymerases on the clamp (especially Pol III and Pol IV) has been shown to be dynamic, with both polymerases switching access to the DNA template and

influencing the dissociation of the other.[19, 163] The consequences of co-occupancy of polymerases must include having at least two conformational states: DNA engaged and unengaged. High fidelity proofreading polymerases must also have at least two additional engaged conformational states for polymerase and exonuclease activities. The dynamics and coordination of all of these conformational states are not entirely clear, however, archaeal *Pyrococcus furiosus* PolB has been visualized by EM in different conformation states identifying additional interactions with PCNA that position it in a 'standby' state that is unengaged from DNA.[175, 198] Moreover, hinges in *Sso*PolY (Dpo4) have also been shown to influence the conformation of PolY bound to PCNA/DNA complex indicating at least three conformational states that regulate the activity and accessibility to DNA.[174] These alternative conformational states could allow for binding of both *Sso* PolB1 to PolY in the SHE complex and allow for 'tool-belt' – like polymerase switching to occur that seamlessly replicates undamaged DNA and bypasses lesions.

In eukaryotes, stalled DNA polymerases at DNA lesions will cause an increase in the amount of ssDNA created, and the buildup and persistence of RPA-coated DNA which is a signal for the Rad6/Rad18 dependent monoubiquitination (mUb) of PCNA.[230, 299, 300] Whether this later stage temporal process is what actually directs TLS activity or just upregulates the global DNA damage response (DDR) in severe cases is still being determined. For example, the human Y-family pol η is known to colocalize with DNA replication foci even in undamaged conditions,[235] and the ubiquitination of PCNA is not required for the localization of pol η in foci.[251] Although in humans there is no current evidence for a SHE-like complex, translesion synthesis can occur 'on the fly' and without mUB through a passive exchange mechanism with pol δ.[202, 230, 301] This passive exchange

mechanism relies on the inherent dissociation property of pol δ at a lesion site allowing for pol η to bind in its place. Whether pol η or any other Y-family pol influences this dissociation or exchange is still being studied. Therefore, the emerging view is that 'on the fly' TLS activity can be coordinated within the progressing replisome with associated Y-family pols, while more extreme stalling or replication re-start may require mUB of PCNA for more stable recruitment of Y-family pols. This is similar in principle to the archaeal SHE complex identified here.

In conclusion, our study identifies and characterizes a PCNA 'tool-belt' configuration of high fidelity PolB1 and TLS PolY polymerases simultaneously contained within a SHE complex in archaea. This novel YB interaction site between polymerases and in combination with the PIP sites are important for the processivity of the entire complex and exchange processes that occur both within the SHE complex as well as from solution. The implication of the SHE complex provides a mechanism for coordinating and localizing replication and TLS activities at the replication fork. It still remains to be seen how this polymerase coordination actually contributes to efficient TLS activity both *in vitro* and *in vivo* and whether similar mechanisms exist in eukaryotic systems or whether archaea and bacteria share sole homology for this process.

CHAPTER FOUR

A Hand-Off of DNA Between Archaeal Polymerases Allows High-Fidelity Replication to Resume at a Discrete TLS Intermediate Three Bases Past 8-Oxoguanine

This chapter accepted as: Cranford, M.T., Kaszubowki, J.D., and Trakselis, M.A. (2020) A hand-off of DNA between archaeal polymerases allows high-fidelity replication to resume at a discrete TLS intermediate three bases past 8-oxoguanine. *Nucleic Acids Res.*

Abstract

During DNA replication, the presence of 8-oxoguanine (8-oxoG) lesions in the template strand cause the high-fidelity (HiFi) DNA polymerase (Pol) to stall. An early response to 8-oxoG lesions involves 'on-the-fly' translesion synthesis (TLS), in which a specialized TLS Pol is recruited and replaces the stalled HiFi Pol for lesion bypass. The length of TLS must be long enough for effective bypass, but it must also be regulated to minimize replication errors by the TLS Pol. The exact position where the TLS Pol ends and the HiFi Pol resumes (*i.e.* the length of the TLS patch) has not been described. We use steady-state and pre-steady-state kinetic assays to characterize lesion bypass intermediates formed by different archaeal polymerase holoenzyme complexes that include PCNA123 and RFC. After bypass of 8-oxoG by TLS PolY, products accumulate at the template position three base pairs beyond the lesion. PolY is catalytically poor for subsequent extension from this +3 position beyond 8-oxoG, but this inefficiency is overcome by rapid extension of HiFi PolB1. The reciprocation of Pol activities at this intermediate indicates a defined position where TLS Pol extension is limited and where the DNA substrate is handed back to the HiFi Pol after bypass of 8-oxoG.

Introduction

Accurate replication of genomic DNA is an elaborate cellular process which is essential to the propagation of life. The double helix is first unwound to form a replication fork where the two strands are primed for replication. A high-fidelity (HiFi) DNA polymerase (Pol) then associates with a processivity clamp to form a replicative holoenzyme (HE) complex which utilizes the single strands of the DNA substrate as a template for accurate duplication of the genome. At times, the molecular information of the template DNA is exposed to damaging agents and becomes chemically modified to form a variety of DNA lesions. DNA repair pathways (including nucleotide-excision repair and base-excision repair) allow for correction of these genomic lesions, yet, excess exposure to DNA damaging agents allows lesions to persist and then be encountered during replication. These template lesions cause HiFi Pols to stall, leading to genomic instability.

However, a specialized set of evolutionarily conserved Pols can perform translesion synthesis (TLS) by incorporating deoxynucleotides (dNTPs) across template lesions.[302] Although these TLS Pols are prone to errors during replication,[14] they provide a pathway for DNA damage tolerance and allow replication to proceed in the presence of unrepaired DNA lesions. Previous studies have implicated two DNA damage tolerance pathways which involve TLS Pols: by 're-priming,' a new primer is synthesized downstream of the replication-stalling lesion.[109, 303, 304] This allows the HiFi Pol to skip the lesion and continue synthesis downstream. However, this discontinuous process creates a single-stranded gap which must be resolved by either template-switching homology-directed gap repair (a TLS-independent pathway) or post-replicative gap filling by TLS Pols.[305] Alternatively, TLS may occur 'on-the-fly,' in which a TLS Pol is recruited directly to a stalled replication fork

to perform lesion bypass prior to a re-priming event.[182] Recent *in vitro* studies have suggested that this continuous 'on-the-fly' TLS pathway is an early response to replication stalling lesions, whereas re-priming serves as a slower mechanism which is likely utilized during conditions of excessive DNA damage.[306-308]

The model for 'on-the-fly' TLS presents two distinct events where the DNA substrate is 'handed-off' between the HiFi and TLS Pols. Upon encountering a lesion, a HiFi Pol stalls one template base prior to the lesion (-1) as a result of competing polymerase and exonuclease activity.[309] From this stalled position, the DNA must be handed-off from the stalled HiFi Pol to a TLS Pol, allowing for bypass of the template lesion. The mechanism of this hand-off may occur indirectly by distributive 'exchange,' where an active Pol fully dissociates from the DNA prior to equilibrium-driven recruitment of the next Pol from solution;[24] or, the DNA may be passed directly through a 'switch' within a coupled supraholoenzyme (SHE) complex consisting of multiple Pols bound to a single processivity clamp (*i.e.* the tool belt model).[19, 177, 178, 310] The TLS Pol synthesizes a nascent segment of DNA which bypasses the lesion and extends to an intermediate position downstream. However, the exact length of this TLS patch and the position of the second hand-off (to resume synthesis by the HiFi Pol) has not been investigated in archaea. It is understood that the length of the TLS patch must be long enough to prevent lesion recognition and exonucleolytic degradation by the HiFi Pol, but continued extension beyond the lesion by low-fidelity TLS Pols must be limited to minimize error-prone synthesis.[20] Limitations to TLS Pol extension may indeed be explained by their characteristically low processivity,[32] but the complex multieuilibria of the cell provides multiple factors which may regulate the TLS Pol. A previous study demonstrated that a

TLS patch length of 5 nucleotides beyond an acetylaminofluorine adduct was sufficient for HiFi *E. coli* Pol III to resume replication; however this is not implicated as the position of the second hand-off, as TLS Pol V is capable of much longer processive stretches of synthesis.[311] In eukaryotes, synthesis of this TLS patch is more intricate, involving posttranslational modifications of PCNA[312] and additional hand-offs among the various TLS inserter and extender Pols which possess unique activities for inserting across and extending beyond different types of DNA lesions, respectively.[95] This is further complicated by a recent study revealing competition between Polδ and Polη in a stalled replisome that is decoupled from the CMG, even on a leading-strand lesion.[308] Nevertheless, the extent of combined TLS Pol activity beyond the lesion is not fully understood. This current knowledge gap encourages additional investigation into the molecular mechanisms which limit error-prone TLS extension after lesion bypass and restore accurate HiFi replication.

PolY (also referred to as Dpo4) acts as the TLS Pol in the archaeon *Saccharolobus solfataricus* (*Sso*).[81] This model enzyme has been well studied structurally[89, 313-315] and kinetically,[134, 313, 316] and its legacy has provided a basis for our current understanding of the various eukaryotic TLS Pols.[11] PolY adopts the canonical 'right-handed' Pol structure with 'Fingers,' 'Palm,' and 'Thumb' subdomains.[9, 89] As a Y-family polymerase, PolY also contains the unique Little-Finger (LF) domain which plays a central role in TLS activity.[15, 89] In response to 8-oxoguanine (8-oxoG) lesions, PolY is remarkably efficient and accurate for non-mutagenic insertion of dCTP.[134, 313] Other Pols are prone to incorrect insertion of dATP across 8-oxoG by formation of a Hoogsteen base pair, resulting in G-to-T transversion mutations.[317] However, R332 (in the LF of PolY) stabilizes the *anti*-

conformation of 8-oxoG in the PolY active site, allowing accurate Watson-Crick base pairing and efficient insertion of dCTP.[313, 314, 318]

Downstream of 8-oxoG, PolY is capable of extension activity.[134, 313] However, the extent of PolY's catalytic role beyond the lesion in the presence of other replisome components has not been investigated fully, which prompts investigation into how these 'right-handed' Pols 'hand-off' the DNA in response to lesions. One previous kinetic study included PolB1 (the HiFi Pol in *Sso*) to evaluate its role in extension after PolY bypass of 8-oxoG,[134] albeit in the absence of the heterotrimeric processivity clamp PCNA123[172, 173] and clamp loader complex RFC.[319, 320] PolB1 polymerase and exonuclease activities were unperturbed by the template 8-oxoG lesion on a DNA substrate with a primer terminus that was extended 1 base pair downstream (+1) of the lesion. This +1 position is highlighted as a kinetically favorable location for the second Pol hand-off. However, the authors ultimately conclude that inclusion of PCNA123 may alter the balance of bypass and extension activities by PolY and PolB1, and this mediation may dictate the position where the DNA is handed off between Pols after bypass of 8-oxoG.[134]

Building upon this kinetic framework, we have determined that PolY performs lesion bypass across 8-oxoG and extends to a position three base pairs beyond the lesion (+3). Additional extension by PolY from this position is inefficient, leading to accumulation of a +3 intermediate product. Within a SHE complex (composed of PolB1, PolY and PCNA123), accumulation of the +3 intermediate is reduced as a result of a second hand-off to resume rapid extension activity of PolB1. Collectively, this identifies a specific position for the second Pol hand-off where HiFi replication resumes after TLS bypass of an 8-oxoG lesion during 'on-the-fly' TLS.

Materials and Methods

Protein Expression and Purification

Wild type *Sso* PolB1,[18] PolY,[177] and RFC[176] were expressed and purified as previously described. The wild-type PolB1 was used in these studies, as exonuclease deficient PolB1 has been shown to bypass 8-oxoG lesions.[134] His-tagged subunits of heterotrimeric PCNA123 were expressed and purified individually and reconstituted into the heterotrimer complex as previously described.[176]

The DNA sequence for PolB1 binding protein 1 (PBP1; SSO0150) and PBP2 (SSO6202) were amplified from *Sso* genomic DNA (primer sequences in **Table 4.1**). The amplified genes were cloned into pET30a using XhoI and NdeI restriction sites. The proteins were expressed in Rosetta2 DE3 *E. coli* cells by autoinduction in ZYP-5052 media,[295] followed by lysis and purification of the PBPs as previously described.[75]

Steady-State Lesion Bypass and Extension Assays

DNA primers (Sigma) were radiolabeled at the 5'-end with ^{32}P using the manufacturer recommended protocol for T4 PNK (New England Biolabs) and ATP [g-^{32}P] (Perkin Elmer). Radiolabeled primers were individually mixed with the DNA template containing an 8-oxoG lesion at the 23rd base from the 3' end (t52$_{8;}$ **Fig. 4.1A** and **Table 4.1**). Substrates were annealed at a 1.2:1 primer:template ratio in a thermocycler (BioRad) by incubation for 10 minutes at 95 ºC, followed by a decrease to 20 ºC at a rate of 1 ºC/min. Annealed substrates were pre-loaded with different Pol HE complexes in reaction buffer (20 mM Tris-OAc (pH 7.5), 100 mM KOAc) with PCNA123, RFC, PolB1 and/or PolY. ATP was added, followed by incubation at 60 ºC for 5 min to promote loading of PCNA123

Table 4.1: DNA substrates used in this study

Name	Sequence (5'-3')
p18	GCGAGGCGAGCGCGAGCG
p22	GCGAGGCGAGCGCGAGCGATAC
p23	GCGAGGCGAGCGCGAGCGATACC
p24	GCGAGGCGAGCGCGAGCGATACCG
p25	GCGAGGCGAGCGCGAGCGATACCGC
p26	GCGAGGCGAGCGCGAGCGATACCGCG
p41	GCGAGGCGAGCGCGAGCGATACCGCGATCGAGTGCAAGCTT
FAM-p22	FAM-GCGAGGCGAGCGCGAGCGATAC
FAM-p26	FAM-GCGAGGCGAGCGCGAGCGATACCGCG
$t52_{Und}$	CGTCCAACATGAAGCTTGCACTCGATCGCGGTATCGCTCGCGCTCGCCTCGC
$t52_{8}$	CGTCCAACATGAAGCTTGCACTCGATCGC8GTATCGCTCGCGCTCGCCTCGC
$t52_{AP}$	CGTCCAACATGAAGCTTGCACTCGATCGC_GTATCGCTCGCGCTCGCCTCGC
$t52_{Alt8}$	CGTCCAACAT8AAGCTTGCACTCGATCGC8GTATCGCTCGCGCTCGCCTCGC
SsoPBP1+NdeI FWD	ATTACATATGTCAACGAGATGGCTACCTAAG
SsoPBP1+XhoI REV	ATTACTCGAGTTACTCCTCTTCACTTTCTTCTTCAC
SsoPBP2+NdeI FWD	ATTACATATGAATACTGGATTAATATATCTTATGTCTGTTAATC
SsoPBP2+XhoI REV	ATTACTGCAGTCACTTCTTGTCAGTAGATTTCCTCAC

"8" - 8-oxoguanosine; "_" - abasic site

to the DNA substrate. Reactions were initiated upon addition of dNTPs, $Mg(OAc)_2$, and salmon sperm DNA (spDNA; Invitrogen) as an enzyme trap, followed by quenching with 100 mM EDTA after 3 minutes. The final reaction concentration of each component is indicated in **Figure 4.1A**.

Reaction products were resolved by denaturing polyacrylamide gel electrophoresis (PAGE) through either a 10 cm gel (20% polyacrylamide/6M urea/25% formamide/1x TBE) or a 38 cm DNA sequencing gel (15% polyacrylamide/6M urea/25% formamide/1x TBE). Resolved products were exposed to a phosphor screen for a minimum of 4 hours and scanned with a Storm 820 phosphorimager (GE Healthcare Life Sciences). The product signals were quantified using ImageQuant software (v5.0, GE Healthcare Life Sciences).

Pre-Steady-State Lesion Bypass and Extension Kinetics Assays

For pre-steady-state lesion bypass kinetics assays, reactions were performed using a DNA substrate containing the 8-oxoG damaged template ($t52_8$) annealed to primer p22

(-1). This 'stalled' DNA substrate was pre-mixed with reaction buffer, PCNA123, and RFC. ATP was added followed by incubation for 2 minutes at 60 ºC and loading into sample loop A of an RQF-3 rapid-quench instrument (KinTek). The RQF-3 was connected to a circulating water bath at 40 ºC. This temperature was chosen based on temperature limitations recommended by the instrument manufacturer [316]. Reactions were initiated upon addition of dNTPs and $Mg(OAc)_2$ from sample loop B, followed by quenching with EDTA from syringe C after indicated time points. PolY and PolB1 were introduced into lesion bypass kinetics assays from different syringe positions as outlined by pre-loading *Schemes i - iv*. Final concentrations of all reaction components are the same as outlined in **Fig. 4.1A**. Products were resolved by denaturing PAGE, exposed, and scanned as described above. In order to obtain the observed rate constant for lesion bypass, the normalized signals for total bypass products were fit to according to **Equation 4.1**:

$$\text{Normalized Product} = A[1 - \exp^{(-k_{obs}\, t)}] \qquad \textbf{(Equation 4.1)}$$

where A is the reaction amplitude, k_{obs} is the observed rate constant, and t is reaction time (Kaleidagraph, v4.5). Signals of other reaction intermediates (defined by brackets) were also plotted and fit to smooth traces for visual comparison of intermediate signal magnitudes.

For pre-steady-state extension kinetics assays, reactions were performed using a DNA substrate containing an 8-oxoG damaged ($t52_8$) or undamaged G ($t52_{Und}$) DNA template annealed to primer p26 (+3). Where indicated, single nucleotide incorporation assays were performed by initiating extension reactions with various concentrations of dATP. PolY and/or PolB1 were introduced to the extension kinetics assays from different

syringe positions as outlined in pre-loading *Schemes i - vi*. Products were resolved by denaturing PAGE, exposed, scanned, and quantified for total extension activity as above.

Fluorescence Anisotropy DNA Binding Assay

HPLC purified and fluorescently labeled primers (p22-FAM or p26-FAM) (Sigma-Aldrich) were annealed to either damaged or undamaged templates ($t52_8$ and $t52_{Und}$; **Table 4.1**). Fluorescence anisotropy experiments were performed essentially as described previously.[18] Fluorescence was excited at 483 nm, and the emission at 517 nm was monitored during a 2 second integration and an average of three measurements at room temperature using a CaryEclipse (Agilent) fluorimeter with automatic polarizers. Slit widths were set at 10 nm, and the PMT was 700 V. The G-factors (*G*) were automatically calculated and corrected, and anisotropy (r) was calculated according to **Equation 4.2** using the included Agilent software:

$$r = \frac{I_{VV} - G I_{VH}}{I_{VV} + 2 I_{VH}} \qquad \textbf{(Equation 4.2)}$$

where I_{VV} and I_{VH} are the intensity of the vertically or horizontally polarized light, respectively. PolY was then titrated into the indicated DNA substrates (4 nM), mixed, and incubated for 90 seconds prior to measuring anisotropy values. Anisotropy values were plotted as a function of PolY concentration to obtain the binding curve and fit to **Equation 4.3** to obtain the dissociation constant, K_d:

$$Fraction\ Bound = B_0 + (B_{max} * [PolY]^{n_h}) \,/\, ({K_d}^{n_h} + [PolY]^{n_h}) \qquad \textbf{(Equation 4.3)}$$

where B_0 is the fraction bound at 0 nM PolY, B_{max} is the fraction bound at saturation, n_h is the Hill slope, and K_d is the dissociation constant for PolY binding to DNA. Reported K_d values are the average of three independent titrations.

PolY and PolB1 have Complementing Activities for Bypass of and Extension from an 8-oxoG Lesion

To measure lesion bypass activity, different Pol HE complexes were assembled by pre-loading PolB1 and/or PolY with PCNA123 on a damaged DNA substrate containing an 8-oxoG lesion. Primers of progressing length were utilized in order to monitor lesion bypass or extension activities from different starting positions relative to the site of the template lesion (**Fig. 4.1A**). Reactions were initiated upon addition of dNTPs, Mg^{2+}, and an excess amount of non-specific salmon sperm DNA (spDNA) as a trap to alter the multiequilibria of polymerase 'exchange.' As a pre-trapping control, spDNA was pre-

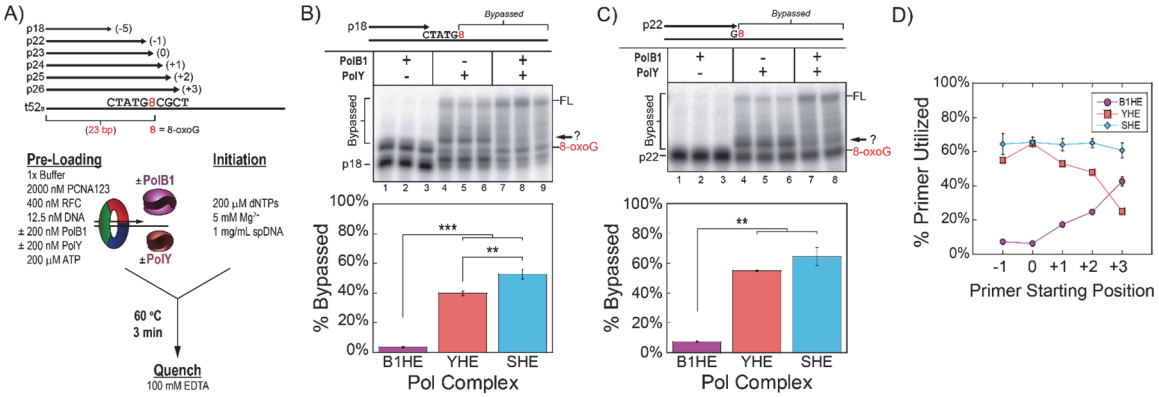

Figure 4.1: PolY and PolB1 have complementing activities for bypass and extension from an 8-oxoG lesion.
A) A 52-mer DNA template containing an 8-oxoG lesion at position 23 (from the 3' end) was annealed to primers of progressing lengths. DNA sequences for each oligo are listed in **Table 4.1**. Steady-state lesion bypass assays were performed by pre-loading the indicated DNA substrate with different replication subassemblies at indicated (final) concentrations (see Materials and Methods). Lesion bypass reactions performed on B) the running start substrate and C) the stalled substrates were resolved by low-resolution denaturing PAGE. The "?" highlights an intermediate product of undefined length formed by YHE downstream of 8-oxoG. Products formed by the indicated Pol complex were quantified for percentage of 'Bypassed' products beyond the lesion position. D) Steady-state extension assays were performed on substrates with longer starting primers. Products quantified for the percentage of primer that was utilized by each Pol complex (B1HE, purple -●-; YHE, red -■-; SHE, blue -♦-). Gel images are in **Fig. 4.3**. FL indicates the position of full-length product, and arrows indicate an intermediate product downstream of 8-oxoG. Error bars represent the standard deviation from three independent replicates.

incubated with the DNA substrate prior to reaction initiation (**Fig. 4.2**). At 1 mg/ml of spDNA, pre-trapped Pol complexes are not completely trapped in solution, suggesting that this concentration of spDNA does not abolish but slows the rate of distributive Pol exchange from solution. On the running start primer p18 (-5), synthesis takes place prior to encountering the 8-oxoG lesion. However, to compare lesion bypass activity, only the signal of 'Bypassed' products beyond the position of the lesion were quantified (**Fig. 4.1B**, brackets). From the running start position, the PolB1 holoenzyme (B1HE; lanes 1-3) is completely stalled at the 8-oxoG lesion with negligible signal beyond the lesion (purple). As expected, reactions with the PolY holoenzyme (YHE, lanes 4-6) demonstrate lesion bypass activity with 39.8 ± 1.5% of products extended beyond the lesion (red). Upon examining the gel image, the distribution of lesion bypass products by the YHE appear to be enriched at an intermediate position downstream of the lesion (**Fig. 4.1B**, arrow). This indicates that PolY is capable of TLS, but it exhibits poor processivity and limited

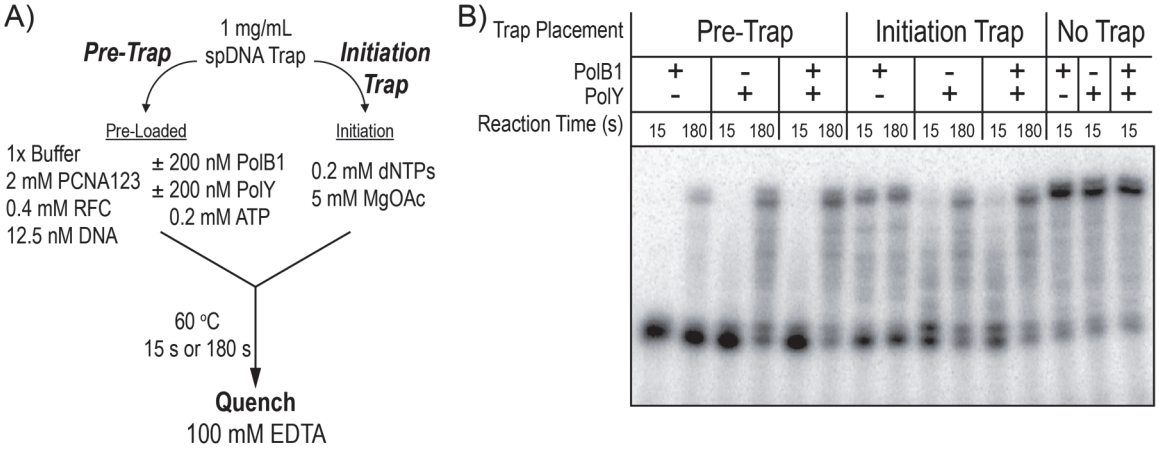

Figure 4.2: Pre-trapping with 1 mg/mL of spDNA still allows for distributive Pol activity.
A) 1 mg/mL of spDNA was introduced to the steady-state polymerase assay either by pre-mixing with the indicated Pol complex and undamaged T DNA substrate ('Pre-Trap'), added upon initiation with dNTPs and Mg^{2+} ('Initiation Trap'), or in the absence of trap ('No Trap'), and quenched at indicated time points. B) All 'Pre-Trap' Pol complexes demonstrate time-dependent activity, indicating that this concentration of trap still allows for distributive exchange of Pols from solution through an altered multieuilibria.

extension beyond the 8-oxoG lesion. Lastly, formation of the SHE complex, containing both PolB1 and PolY (lanes 7-9), yields significantly more (52.6 ± 3.3 %; blue) lesion bypass products compared to the YHE. Additionally, the intermediate observed in the YHE reactions is not apparent in the lesion bypass products for the SHE, and more products are elongated to FL.

We repeated this lesion bypass assay on a DNA substrate simulating a stalled position using primer p22 (-1; **Fig. 4.1C**). Again, the B1HE (lanes 1-3) is stalled by 8-oxoG (purple), while the YHE (lanes 4-6) is capable of lesion bypass (55.0 ± 0.5 %, red). As observed in **Fig. 4.1B**, most of the lesion bypass products by the YHE are concentrated at a position beyond the lesion (**Fig. 4.1C**, arrow). Finally, though the SHE (lanes 7-8) does not yield a significant increase in total bypassed products (64.3 ± 6.0 %, blue) relative to the YHE, most of the bypassed products are extended to the end of the substrate and the observed intermediate disappears. Thus, in response to 8-oxoG, bypass and extension from the lesion are most efficient when both PolB1 and PolY are present.

We continued these lesion bypass assays for each Pol complex using DNA substrates with progressively longer primers and quantified the percentage of primer that was utilized for each substrate (*i.e*. extended by at least one base pair; **Fig. 4.1D,** gel images in **Fig. 4.3**). In this way, we can compare the activities of each Pol complex on substrates with different starting positions relative to the 8-oxoG lesion. Activity of the B1HE is negligible on primers p22 and p23, which start before (-1) or at (0) the site of the lesion. However, activity of the B1HE gradually increases on primers further downstream of the lesion (purple circles). Remarkably, products from the YHE exhibit the opposite trend; activity is elevated on primers before or at the lesion and gradually decreases on primers

which require extension from the lesion (red squares). Finally, activity of the SHE consistently yields about 65% of extension on all primers (blue diamonds). Unlike reactions with individual Pol HEs, the magnitude of primer extension by the SHE complex is independent of starting primer length.

The apparent inverse in activities relative to the 8-oxoG position by the YHE and B1HE highlights the complementing roles for PolY and PolB1. This is further supported

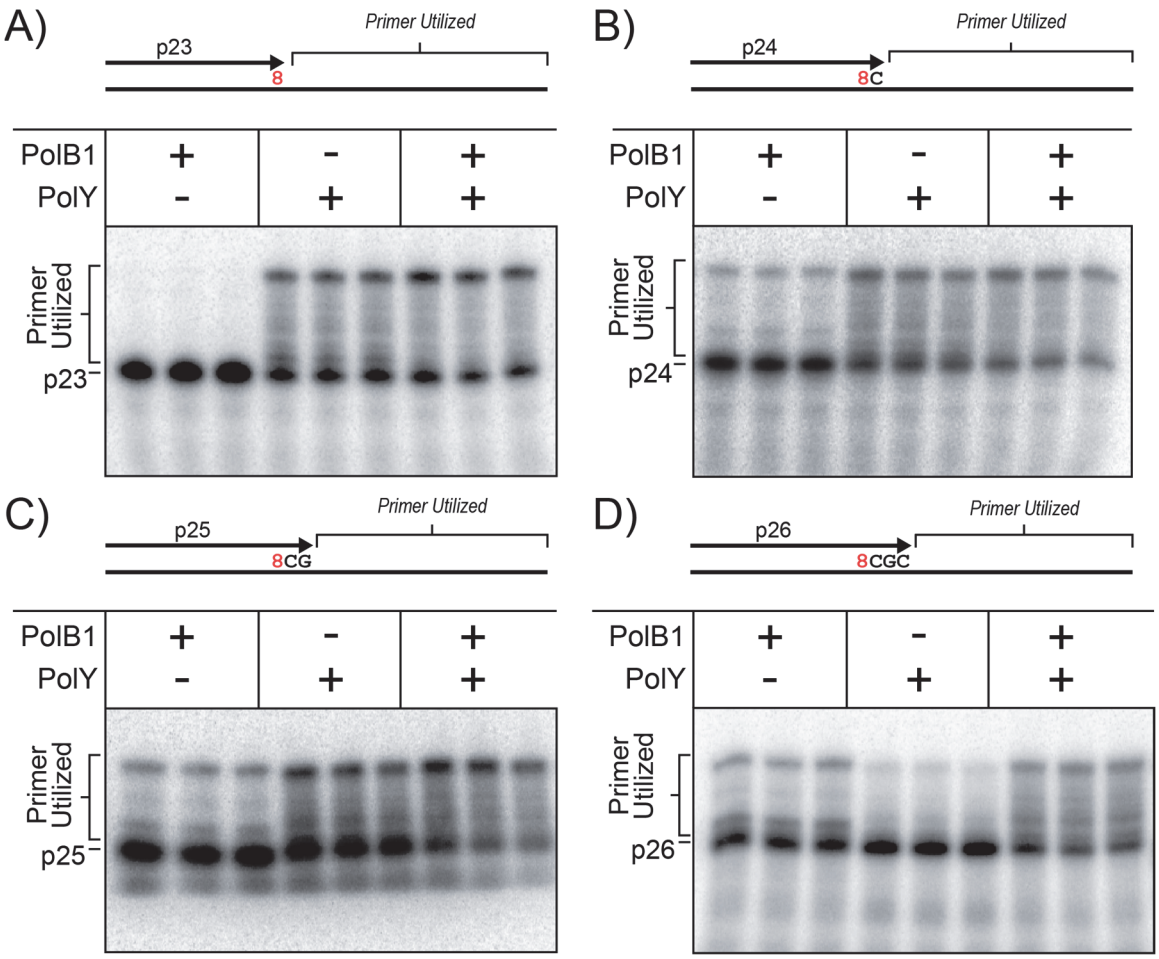

Figure 4.3: Gel images of steady-state lesion bypass by each Pol complex on progressively longer primers

Reactions described in **Figure 4.1A** were performed on 8-oxoG damaged DNA substrates containing progressively longer primers A) p23, B) p24, C) p25, and D) p26. Products were quantified as a percentage of primer utilized (brackets) and plotted in **Figure 4.1D**.

by the SHE reactions, where the combined Pol activities yield increased levels of bypass and extension. These data also point to a position where the substrate is handed off between the Pols in the SHE reactions. The reciprocation of Pol activities occurs on a primer terminus positioned 3 base pairs downstream of the lesion. This leads us to hypothesize that the +3 position is the site of the second hand-off, from TLS PolY to HiFi PolB1, after bypass of an 8-oxoG lesion.

Lesion Bypass by PolY Yields a Major Intermediate 3 Base Pairs Downstream of the 8-oxoG Lesion

In order to visualize discrete lesion bypass intermediates, representative products from the previous reactions were resolved by high-resolution denaturing PAGE (**Fig. 4.4A**). This gel image depicts the same activity trends summarized in **Figure 4.1D**, but it also grants a more precise examination of lesion bypass and extension products formed by each Pol complex. Notably, lesion bypass products by the YHE are specifically enriched at the +3 position, regardless of the primer starting position (**Fig. 4.4A**, arrow). The consistent position of this enriched YHE intermediate indicates that it is not a product of an ordinary processive step by PolY. If so, the position of the enriched intermediate would shift along the substrate in relation to the primer starting length. This observation indicates a specific perturbation in polymerase activity of PolY when positioned 3 base pairs downstream of an 8-oxoG lesion.

As previously noted, lesion bypass with the SHE yields an apparent decrease in the intermediate observed in bypass by the YHE complexes and an apparent increase in products extended to FL. In order to compare the relative amount of +3 intermediate formed on each substrate, the signal of the +3 intermediate product bands (**Fig. 4.4A**,

arrow) from the YHE and SHE reactions were normalized to their respective lanes (**Fig. 4.4B**). When compared, the magnitude of the +3 intermediate signals from the SHE reactions (blue) is reduced by approximately half relative to the YHE reactions (red) on corresponding DNA substrates. Additionally, upon comparing the normalized fraction of extended products (**Fig. 4.4A**, bracket), the SHE reactions (blue) yield about twice as much

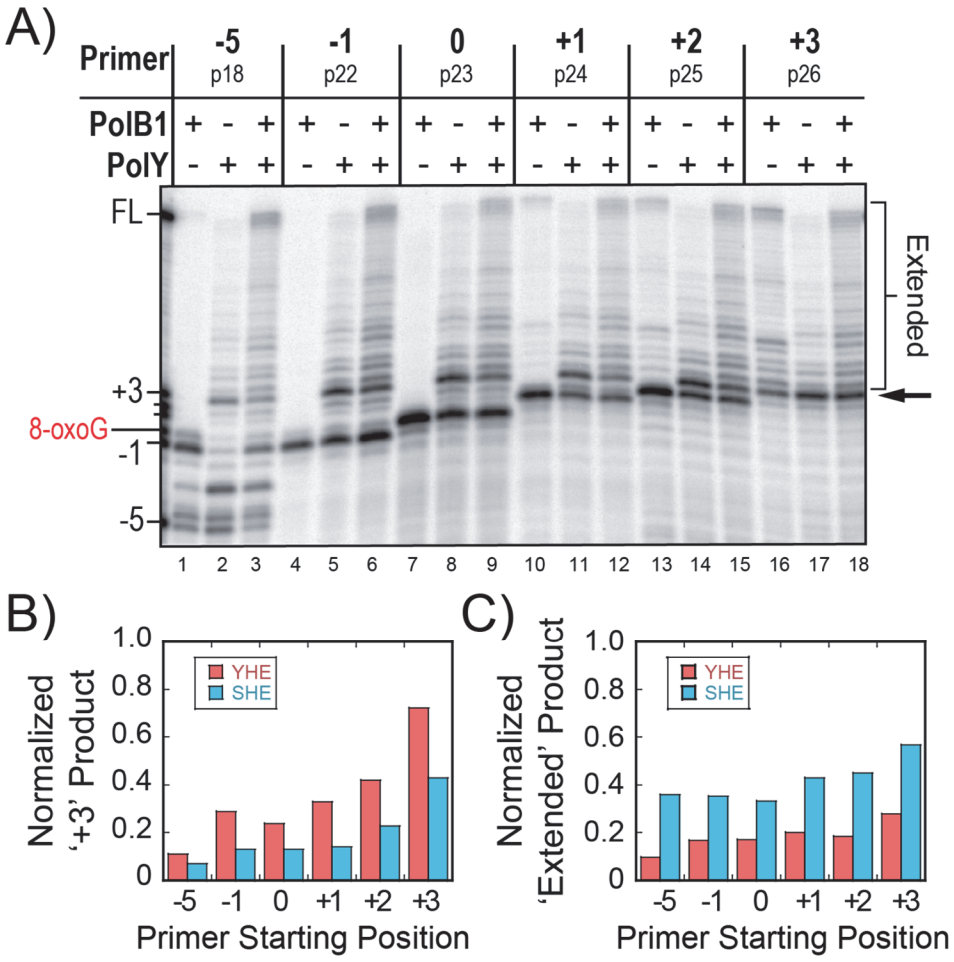

Figure 4.4: Lesion bypass by PolY yields a major intermediate 3 base pairs downstream of the 8-oxoG lesion.
A) Representative lesion bypass and extension products by different Pol complexes (from **Fig. 4.1 and Fig. 4.3**) were resolved by high-resolution denaturing PAGE. The arrow indicates the intermediate product 3 base pairs beyond (+3) the 8-oxoG lesion, and 'Extended' indicates all products beyond the +3 position. The normalized fraction of B) '+3' product bands and C) 'Extended' products for the YHE (red) or SHE (blue) were plotted from indicated primer starting positions.

product that is extended beyond the +3 position relative to the YHE (red; **Fig. 4.4C**). Altogether, these data indicate that PolY conducts bypass of an 8-oxoG lesion and is disrupted at a position 3 base pairs downstream, and the presence of PolB1 promotes extension from this intermediate position.

Kinetics of Lesion Bypass Intermediates Demonstrate Reduced Accumulation of the +3 Intermediate upon Formation of the SHE

After recognizing the +3 position as a major intermediate for PolY, we examined the direct kinetics of the intermediate without altering the equilibria by spDNA. In order to acquire faster time points, reactions were operated through an RQF-3 (KinTek) rapid quench instrument at 40 ºC. PolY was introduced to the reaction by either syringe A or B (**Fig. 4.5A**, *Schemes i* or *ii*). By changing the position where PolY is introduced to the reaction, we can evaluate how the observed rate of lesion bypass changes under different pre-loading conditions. Any products which extend from this primer were quantified as 'Total Bypass' (**Fig. 4.5B**, left bracket), as the 8-oxoG lesion is the first templating base from the stalled primer p22 (-1) terminus. Further, all extension products were classified into three categories of intermediates: '0 to +2,' '+3,' and 'Extended.' (**Fig. 4.5B**, right brackets). The signal of each intermediate category was then quantified and fit to smooth traces to observe these intermediate signals over time.

In reactions where PolY is pre-loaded with the DNA substrate and accessory factors (**Fig. 4.5C**, *Scheme i*), total bypass proceeds with a k_{obs} of 0.81 ± 0.11 s^{-1}. This rate is representative of the catalytic rate of pre-loaded PolY across 8-oxoG. When PolY must first be recruited to the stalled DNA substrate upon initiation (**Fig. 4.5C**, *Scheme ii*), the

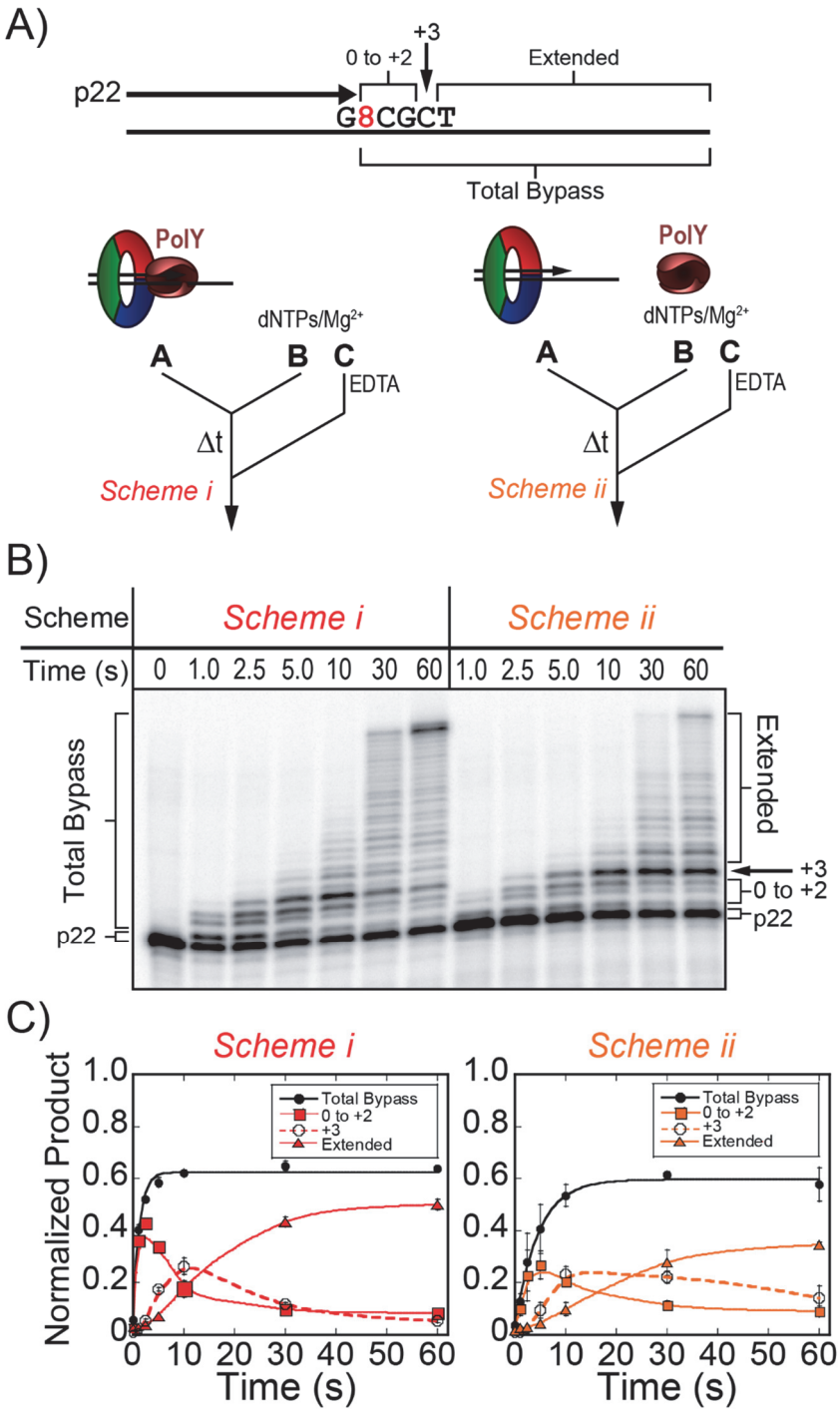

Figure 4.5: Kinetics of lesion bypass by the YHE complexes demonstrate accumulation of the +3 intermediate.

A) Pre-steady-state lesion bypass assays were performed on substrates containing the stalled primer, p22 (-1), by *Schemes i* (red) and *ii* (orange). B) Products were resolved by denaturing PAGE and C) quantified for 'Total Bypass' (black -●-, solid line fit to **Equation 4.1**), or '0 to +2' (-■-, smoothed solid line), '+3' ' (-○-, smoothed dashed line), and 'Extended' (-▲-, smoothed solid line) intermediates. Error bars represent standard deviation from three independent replicates of each time point.

apparent rate of bypass is slowed 4-fold, with a k_{obs} of 0.22 ± 0.02 s^{-1}. This observed rate is likely limited by the rate of association of PolY to DNA:PCNA123 prior to the catalytic step. In these YHE schemes, the kinetic trace of the +3 intermediate accumulates (**Fig. 4.5C**, dashed traces) and reaches a maximal normalized product of over 0.20 (at 10 seconds), suggesting that extension by the YHE complexes is impaired at the +3 position. When lesion bypass reactions are performed by *Scheme i* using abasic and undamaged DNA templates, this intermediate is not apparent (**Fig. 4.6A**). Also, on an alternative 8-oxoG template containing a different sequence context beyond the lesion (8TAC vs

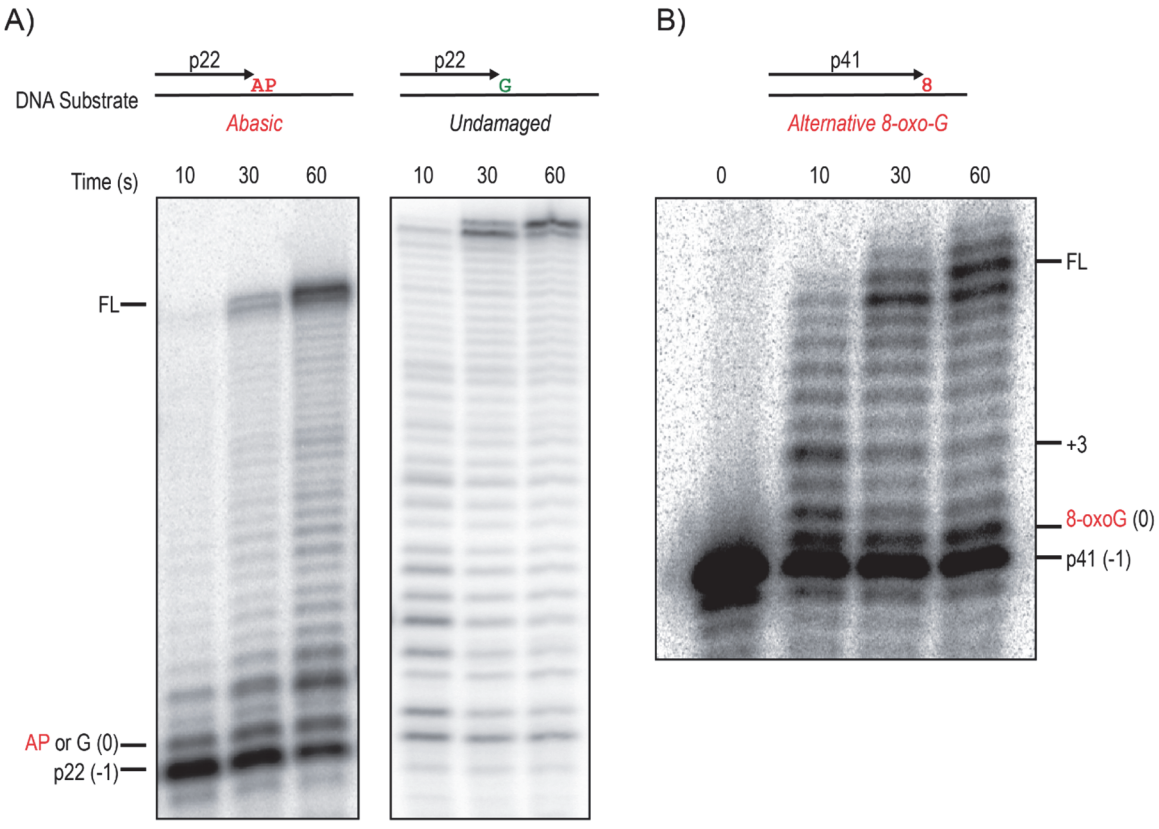

Figure 4.6: The +3 intermediate is characteristic of PolY bypass of 8-oxoG and is not an artifact of sequence context beyond the lesion.
Pre-steady-state lesion bypass kinetics reactions were performed by *Scheme i* on DNA substrates containing A) an abasic site (AP) lesion or an undamaged G. Similar reaction were also performed on an alternative 8-oxoG template with a different sequence context beyond the lesion.

8CGC), the YHE still yields an enriched +3 intermediate after 10 seconds (**Fig. 4.6B**). Taken together, these results indicate that the +3 intermediate is characteristic of PolY bypass of 8-oxoG and is not an artifact of sequence context.

Considering the disappearance of the +3 intermediate and increased extension observed in the steady-state SHE reactions (**Fig. 4.4 B and C**), it follows that addition of PolB1 into the kinetic lesion bypass assay would reduce accumulation of the +3 intermediate. To examine this, PolB1 was introduced to the pre-steady-state assay schemes through syringe B or A, opposite the location of PolY (**Fig. 4.7A**, *Scheme iii*, or **Fig. 4.7B**, *Scheme iv*), then initiated and quenched as before. When PolY is pre-loaded in syringe A, and PolB1 is introduced upon initiation in syringe B (**Fig. 4.7A**), lesion bypass proceeds at a similar rate (k_{obs} = 0.72 ± 0.08 s^{-1}) compared to when PolY is pre-loaded alone (**Fig. 4.5C**, *Scheme i*). *Schemes i* & *iii* are both initiated with a pre-loaded PolY, thus quantification of 'Total Bypass' by these schemes is representative of the catalytic step of lesion bypass by PolY. However, in response to DNA lesions, the TLS Pol must access the primer terminus after stalling of the HiFi Pol. To investigate this step, pre-steady-state assays were performed by *Scheme iv* which simulates a stalled B1HE that has encountered an 8-oxoG lesion. Wild-type PolB1 is completely stalled by the 8-oxoG lesion (**Fig. 4.1C**), so 'Total Bypass' products by this scheme require catalysis by PolY. Therefore, in *Scheme iv*, the observed rate of synthesis would be limited by rate of the first hand-off from PolB1 to PolY. Indeed, the observed rate of lesion bypass by *Scheme iv* (k_{obs} = 0.077 ± 0.009 s^{-1}) is about 10-fold slower than *Schemes i* & *iii* which contain a pre-loaded PolY. This rate is also 3-fold slower than the rate of lesion bypass when PolY is recruited to an unoccupied clamp (**Fig. 4.7B**, *Scheme iv* vs *ii*), indicating that the presence of a pre-loaded PolB1 slows

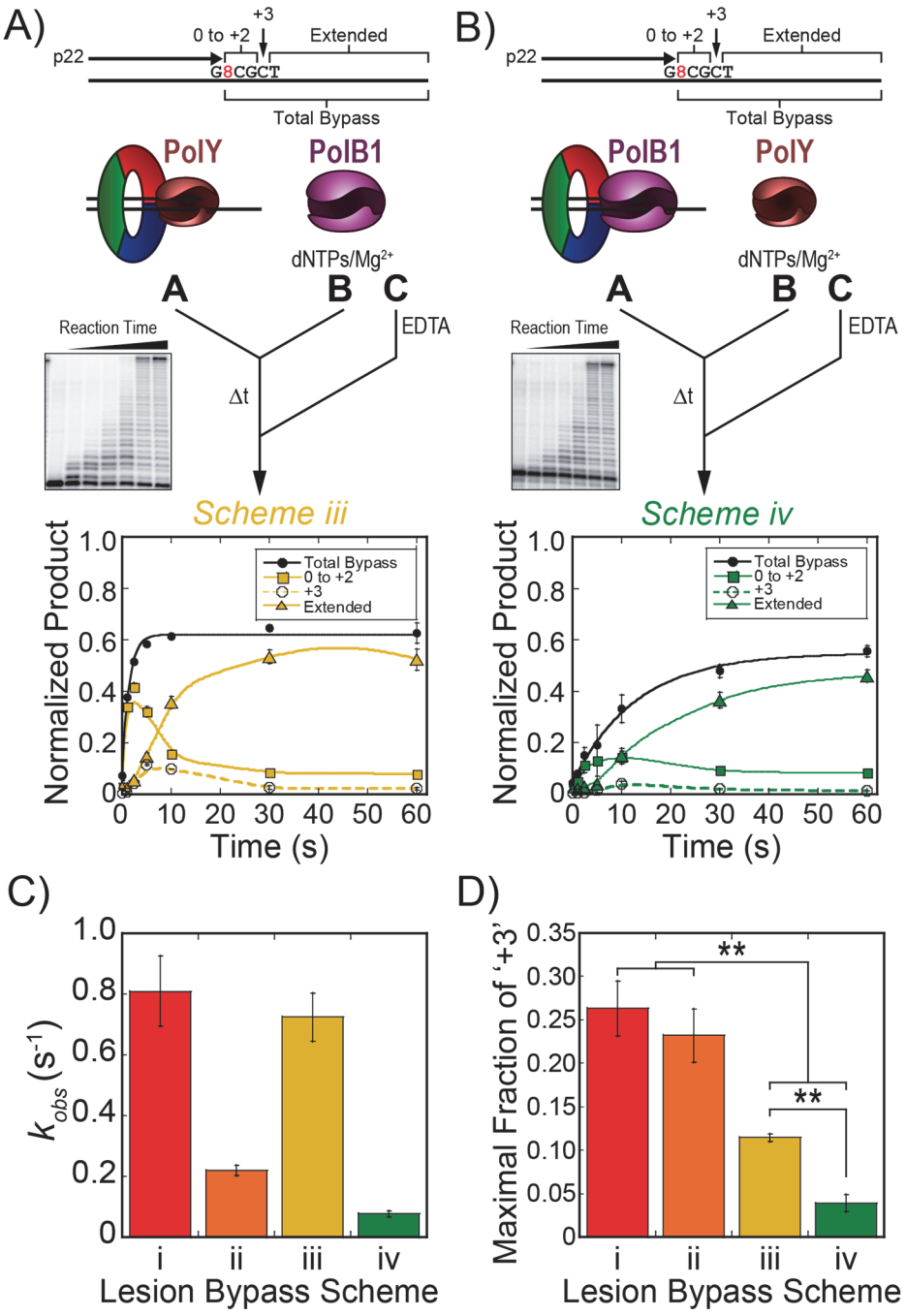

Figure 4.7: Kinetics of lesion bypass by the SHE complexes yield less +3 intermediate.
Pre-steady-state lesion bypass assays were performed by A) *Scheme iii* (yellow) and B) *Scheme iv* (green). Products by *Schemes iii* & *iv* were quantified for 'Total Bypass' (black -●-, solid line fit to **Equation 4.1**) and intermediate products '0 to +2' (-■-, smoothed solid trace), '+3' (-○-, smoothed dashed trace) and 'Extended' (-▲-, smoothed solid trace) were traced. Error bars represent standard deviation from three independent replicates of each time point. C) The observed rate constants of lesion bypass for *Schemes i - iv* were plotted (colors correspond to the respective schemes). Error bars indicate error of the regression fit. D) The maximal fraction of the '+3' intermediate products from lesion bypass of *Schemes i - iv* (dashed traces) were plotted (colors correspond to the respective schemes). Error bars represent standard deviation from three replicates for each scheme.

PolY access to the stalled primer terminus. Observed rates of lesion bypass for *Schemes i - iv* are compared in **Figure 4.7C**.

Recently, two novel accessory subunit proteins, PBP1 and PBP2, were characterized and shown to influence the activity of PolB1.[75] PBP1 contains an acidic tail which limits strand displacement activity by PolB1 during synthesis of Okazaki fragments, whereas PBP2 moderately improves catalytic activity. Given their effects on PolB1, these PBPs were included in pre-steady-state kinetic assays on undamaged DNA templates to determine whether they have an effect in regulating or displacing PolB1 upon encountering a lesion. When both PBP1 and PBP2 (400 nM) are pre-loaded with PolY in *Scheme i*, there is no apparent change in the rate of PolY catalysis (**Fig. 4.8A**). This suggests that the PBPs have no observable effect on PolY activity. Similar kinetic assays were performed using PolB1 in place of PolY (later referred to as *Scheme v* in **Fig. 4.11B**). By this scheme, reactions containing PBP1 demonstrate an inhibitory effect on the rate of catalysis by PolB1, while PBP2 alone improves PolB1 activity, as previously noted (**Fig. 4.8B**).

From its apparent inhibition of PolB1 activity, we hypothesized that PBP1 may destabilize PolB1 affinity to DNA. Upon PolB1 encountering a template lesion, PBP1-mediated displacement of PolB1 would allow faster access of PolY to the stalled primer. To investigate this, lesion bypass kinetic assays were performed by *Scheme iv* in the presence of PBP1 pre-loaded with PolB1 in syringe A. However, this did not yield any apparent change in the observed rate of exchange from PolB1 to PolY for lesion bypass (**Fig. 4.8 C and D**). The similarity in these rates suggests that PBP1 does not regulate PolB1 activity by promoting its displacement from DNA, and these accessory subunits are not directly involved in the Pol hand-off during 'on-the-fly' TLS.

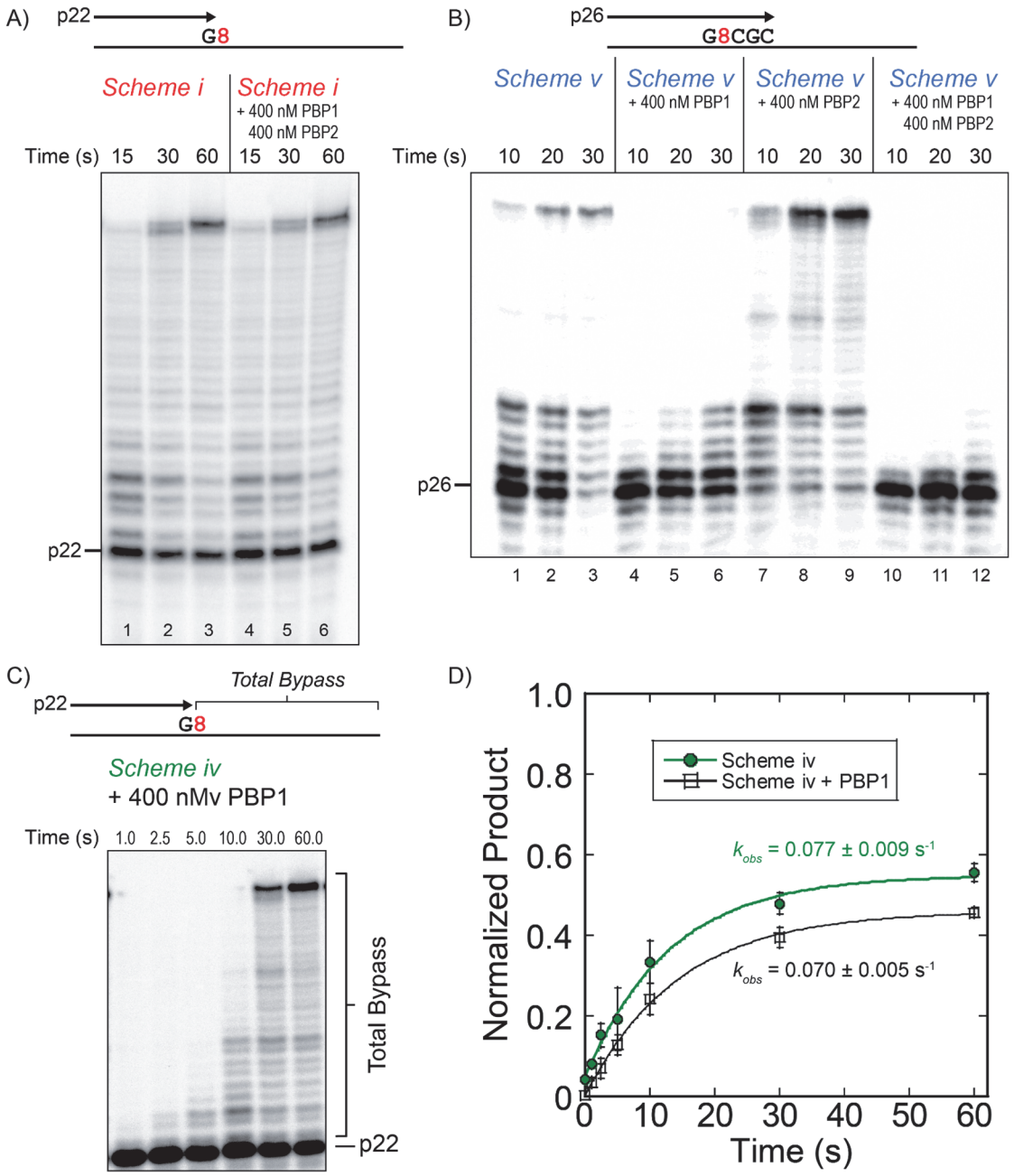

Figure 4.8: PBP1 does not increase the rate of the first hand-off from a stalled PolB1 to PolY for lesion bypass.

A) Pre-steady state lesion bypass kinetics were performed by *Scheme i* (containing pre-loaded PolY) on the indicated DNA substrate either alone (lanes 1-3) or in the presence of 400 nM PBP1 and PBP2 (lanes 4-6). B) Pre-steady-state extension kinetics assays were performed by *Scheme v* (containing pre-loaded PolB1; see **Fig. 4.11**) on the indicated DNA substrate. Reactions were performed with PolB1 alone (lanes 1-3), or in the presence of 400 nM PBP1 (lanes 4-6), 400 nM PBP2 (lanes 7-9), or 400 nM of PBP1 and PBP2 (lanes 10-12). C) Similar reactions were performed by *Scheme iv* with 400 nM PBP1 pre-loaded in syringe A and resolved by denaturing PAGE. D) 'Total Bypass' products were quantified over time (black, -□-) and fit to **Equation 4.1** to obtain the observed rate constant and compared to the rate of *Scheme iv* in the absence of PBP1 (green, -●-).Error bars represent the standard deviation of three independent replicates for each time point.

To compare the accumulation of the +3 intermediate in all lesion bypass kinetics schemes (**Figs. 4.5C, 4.7A and B**, dashed traces), we plotted the maximal signal of the +3 intermediate in the kinetic traces from each Pol complex (**Fig. 4.7D**). In schemes containing PolB1 (*iii* & *iv*), the maximal fraction of the +3 intermediate (0.11 ± 0.004 and 0.04 ± 0.01, respectively) is significantly less than the intermediate signal from reactions containing PolY alone (*Schemes i* & *ii*; 0.26 ± 0.03 and 0.23 ± 0.03, respectively). Despite the slower overall rate of lesion bypass in *Scheme iv*, the reduced fraction of +3 intermediate indicates that extension from the intermediate position is still fast. Again, this shows that PolY is capable of rapid lesion bypass up to the +3 position, but additional extension is impaired and results in accumulation of the +3 intermediate which is relieved by the presence of PolB1.

Slow Extension by the YHE Complexes from the +3 Intermediate Indicates a Perturbation in PolY Catalytic Activity at this Position

The peculiar features of this +3 lesion bypass intermediate prompted us to investigate the kinetics of extension from this position by the different Pol complexes. Reactions were assembled in the RQF-3 as described above, except a DNA substrate containing primer p26 (+3), which corresponds with the observed intermediate, was utilized. All products beyond the primer were quantified as 'Extended' products (**Fig. 4.9A**). For reactions containing PolY alone (*Schemes i* & *ii*), the apparent rates of extension are equivalent for *Schemes i* & *ii*, regardless of PolY syringe position (k_{obs} = 0.080 ± 0.008 s^{-1} and 0.078 ± 0.008 s^{-1}, respectively). The similar rates from these pre-loading schemes suggest that extension by PolY from the +3 position is not limited by its rate of association to the DNA substrate. This contrasts with the observed rates obtained for lesion bypass for

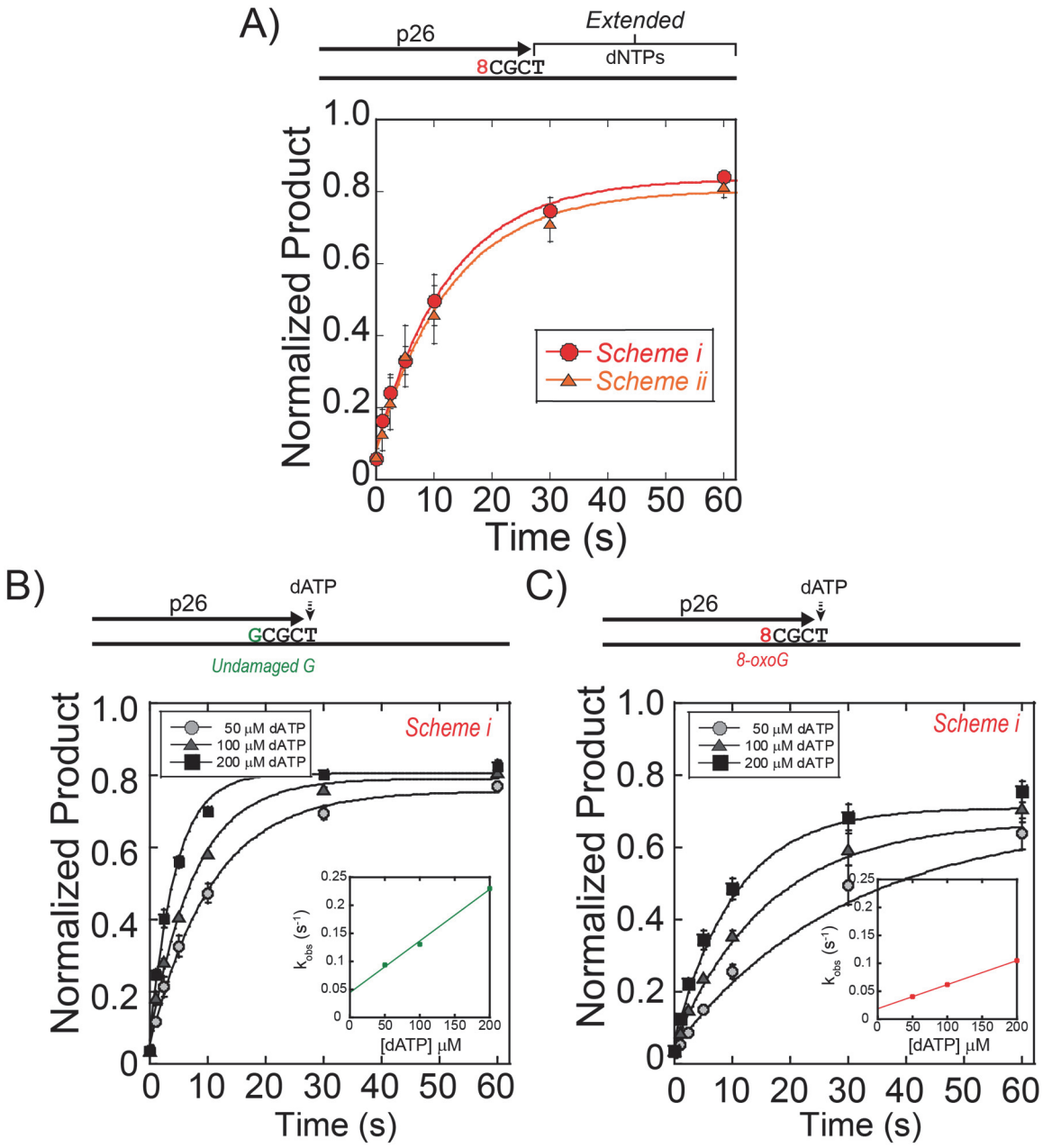

Figure 4.9: PolY conducts slow extension from the +3 intermediate.
A) Pre-steady-state extension assays were performed on DNA substrates containing primer p26 (+3) by *Schemes i & ii*. Quantification of 'Extended' products were fit to **Equation 4.1** to obtain the observed rate constants for *Scheme i* (red, -●-) and *ii* (orange, -▲-). B) Single nucleotide extension assays were performed with increasing concentrations of dATP by *Scheme i* on an undamaged or C) and 8-oxoG damaged template from the p26 (+3) primer as indicated in the legends. Quantification of 'Extended' products were fit to **Equation 4.1** to obtain the observed rate constants at indicated concentrations of dATP. Second order plots (insets) report on the kinetics of dATP insertion at +3 on undamaged (0.92 ± 0.01 $nM^{-1}s^{-1}$) or 8-oxoG damaged (0.43 ± 0.01 $nM^{-1}s^{-1}$) templates.

Schemes i & ii (**Fig. 4.5C**). These YHE extension rates are about 2.8-fold slower than the apparent rate of association for PolY (represented by lesion bypass in *Scheme ii*), indicating that the rate of PolY catalysis is limiting when extending from the +3 intermediate position. We considered the reduced rate of extension to be limited by a decrease in DNA binding affinity of PolY to the +3 extension substrate. This circumstance would effectively reduce the formation of active YHE complexes and yield a slower apparent rate of extension. However, as determined by fluorescence anisotropy, there was no apparent change in PolY binding affinity for the 8-oxoG substrate relative to the undamaged substrate with primers aligned at the -1 or +3 positions (**Fig. 4.10**). This

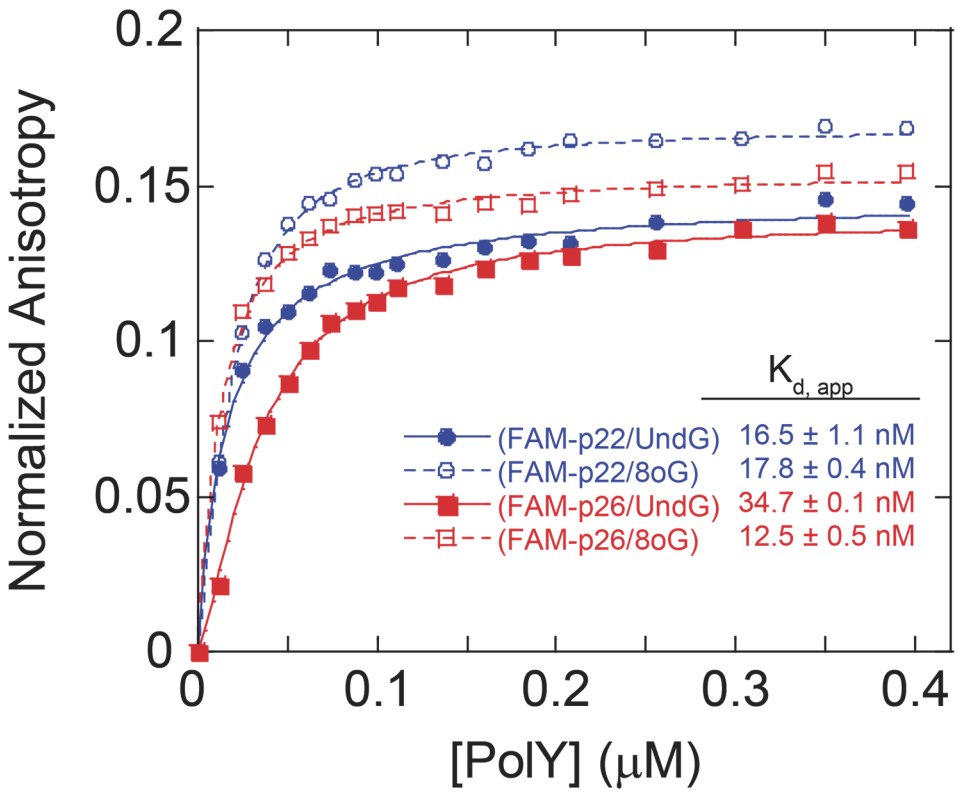

Figure 4.10: Inefficient extension of PolY from the +3 intermediate is not a result of decreased DNA binding affinity.
Fluorescence anisotropy was performed by titrating PolY into the indicated FAM-labelled DNA substrates. The binding curve was plotted and fit to **Equation 4.3** to obtain the apparent dissociation constant.

suggests that slow extension of the YHE from the +3 intermediate is not a result of destabilized DNA binding, rather it is limited by a slow elementary step which follows PolY association with the DNA substrate.

To investigate the kinetic parameter of PolY that is affected at this position, we measured the observed rates of single nucleotide incorporation by S*cheme i* as a function of dATP concentration, the next nucleotide for extension from the +3 position. On an undamaged DNA template, k_{obs} increases with elevated [dATP], as expected (**Fig. 4.9B**). However, the rate of dATP incorporation from this position on the 8-oxoG damaged template, is significantly slower (**Fig. 4.9C**). The second-order rate constant of extension from +3 position is 2.1-fold faster for the undamaged template compared to the 8-oxoG template (0.92 ± 0.01 $nM^{-1}s^{-1}$ relative to 0.43 ± 0.01 $nM^{-1}s^{-1}$), indicating a perturbation of PolY extension three nucleotides past bypass of 8-oxoG.

PolB1 Performs Rapid Extension from the +3 Intermediate Position

As observed in **Figure 4.1D**, PolB1 extension activity is highest when starting from the +3 position (purple circles), indicating kinetic efficiency for extension by PolB1. In order to investigate the role of PolB1 in extension from this intermediate position, we evaluated the kinetics of extension from the +3 position by *Schemes iii & iv*. Extension by *Scheme iii* simulates a condition that examines a switch from PolY to PolB1 at the +3 intermediate. This observed rate of extension (0.49 ± 0.05 s^{-1}, **Fig. 4.11A**, *Scheme iii*) is 6.1-fold faster than extension by the YHE complex (**Fig. 4.9**, *Schemes i & ii*). Since PolY extension is slowed at this position (**Fig. 4.9C**), the faster extension rate in *Scheme iii* is attributed to the activity of PolB1 and is representative of the second hand-off from TLS PolY to HiFi PolB1 for extension. In *Scheme iv*, PolB1 is already pre-loaded on the +3

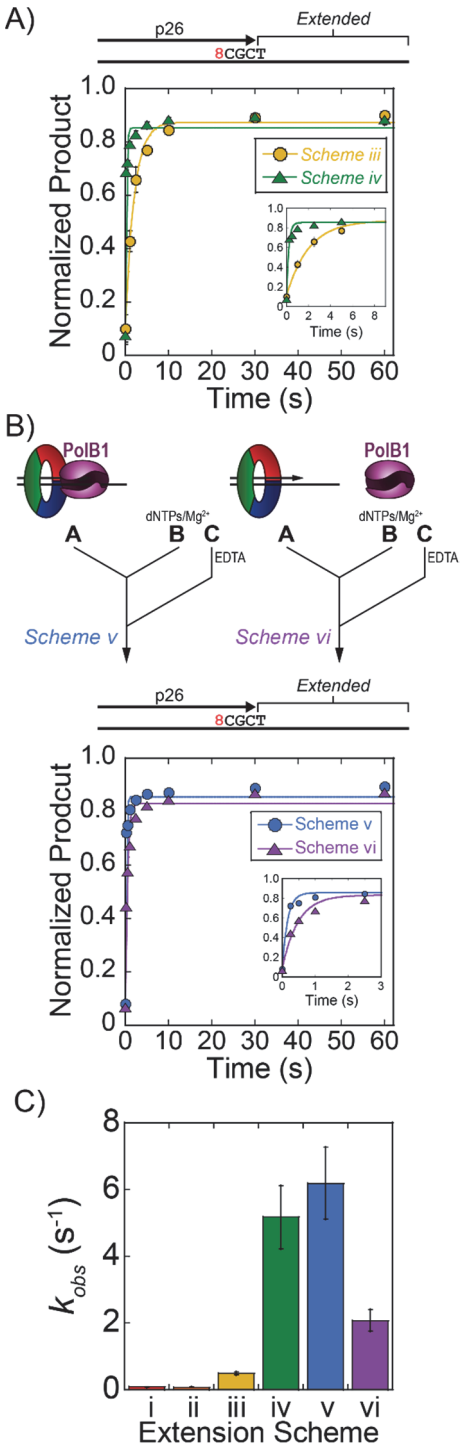

Figure 4.11: PolB1 conducts rapid extension from the +3 intermediate position.
Pre-steady-state extension kinetics were performed on a DNA substrate containing primer p26 (+3) by A) *Schemes iii* (yellow, -●-) and *iv* (green, -▲-) containing PolB1 and PolY, or B) *Schemes v* (blue, -●-) and *vi* (purple, -▲-) containing PolB1 alone. Error bars represent standard deviation from three independent replicates of each time point. Quantification of 'Extended' products were fit to **Equation 4.1** to obtain the observed rate constant for extension. Insets show the trace of 'Extended' product at a shorter time scale. C) Observed rate constants for extension were plotted; error bars indicate error of the regression fit.

extension substrate and yields a fast k_{obs} of 5.2 ± 0.9 s^{-1} (**Fig. 4.11A**, *Scheme iv*). This represents the catalytic rate of extension by a pre-loaded PolB1 and is 65-fold faster than extension by the YHE complexes from the +3 position (**Fig. 4.9A**, *Schemes i & ii*). Together, these data indicate that PolB1 can access the 3'-end from PolY at the +3 position faster than PolY can perform additional extension, and PolB1 is capable of rapid and efficient extension from this position.

Extension kinetics reactions were also performed with PolB1 alone introduced from either syringe A or B (**Fig. 4.11B**, *Schemes v & vi*, respectively). Extension by *Scheme v* resembles *Scheme iv*, containing a pre-loaded PolB1, and yields a similar rate of extension (k_{obs} = 6.2 ± 1.2 s^{-1}). When PolB1 must be recruited to the substrate upon initiation (*Scheme vi*), the rate of extension is also relatively fast (k_{obs} = 2.1 ± 0.3 s^{-1}). This observed rate likely represents the rate of association for PolB1 to an unoccupied PCNA123:DNA complex. These assays highlight the rapid extension activity of PolB1 from the +3 position. These rates (*Schemes v & vi*) are orders of magnitude faster than extension by PolY (*Schemes i & ii*) and provide kinetic evidence for the position where PolB1 resumes HiFi extension activity after PolY bypass of 8-oxoG. Observed rates of extension for *Schemes i - vi* are compared in **Figure 4.11C**.

Discussion

In this study, we have identified a novel +3 intermediate for PolY after bypass of an 8-oxoG lesion, which results from a perturbation in polymerase activity at that position. In the presence of PolB1, accumulation of the +3 intermediate is reduced and rapidly extended into longer products. Altogether, this points to an 'on-the-fly' TLS mechanism where the first hand-off (from stalled PolB1 to PolY) occurs at the -1 position (**Fig. 4.12A**

to B). PolY then performs TLS and extends to a position 3 base pairs beyond the lesion, where it becomes catalytically inefficient for extension to the +4 position (**Fig. 4.12C**). From this +3 position, the catalytic inefficiency of PolY allows for the second hand-off to restore PolB1 activity (**Fig. 4.12D to E**). This marks a distinct position beyond an 8-oxoG lesion for the second Pol hand-off which resumes HiFi replication and effectively limits error-prone TLS activity.

Previous kinetic and structural studies of PolY bypass and extension across 8-oxoG did not identify the +3 intermediate.[134, 313, 314] Accumulation of this intermediate was first apparent to us upon inclusion of spDNA trap in steady-state lesion bypass assays, which effectively amplifies sites of catalytic inefficiency during replication. In prior studies without trap DNA, multiple enzyme turnovers and distributive extension from the +3 position may have proceeded too quickly for its accumulation to be apparent. These studies also primarily focus on the kinetic steps of lesion bypass, translocation, and extension up to the +1 position by PolY; its activity was not evaluated further downstream of 8-oxoG. Finally, prior evaluations were also performed without a processivity clamp, which is a critical accessory factor that optimizes and mediates Pol and other enzymatic activities.[176, 286, 321] Our study suggests that PCNA123 mediates the complementing activities of PolY and PolB1 not only upon encountering the lesion, but also after the lesion has been bypassed. In response to other DNA lesions, the kinetics of lesion bypass by PolY have already been characterized.[124, 322-326] In some of the previous analyses, 'pause sites' were noted during PolY lesion bypass, indicating points of inefficient catalysis and extension from these lesions. However, in the absence of RFC, PCNA123, and PolB1, these pause sites cannot be directly correlated with the position of the second hand-off after lesion

bypass. This prompts additional investigation into how PolY and other TLS Pols are limited in extension after bypass of various DNA lesions, especially in the presence of a processivity clamp and HiFi Pols.

Interestingly, *E. coli* Pol IV (or DinB, a homolog of PolY)[81] demonstrates a similar +3 intermediate following bypass of N^2-dG-peptide adducts.[327] A Pol IV variant also led to identification of a +3 intermediate in response to an N^2-furfuryl-dG lesion, with a drastic reduction in catalytic efficiency from the intermediate position.[328] Additionally, human Polη was observed to become less processive at template positions one or two base pairs

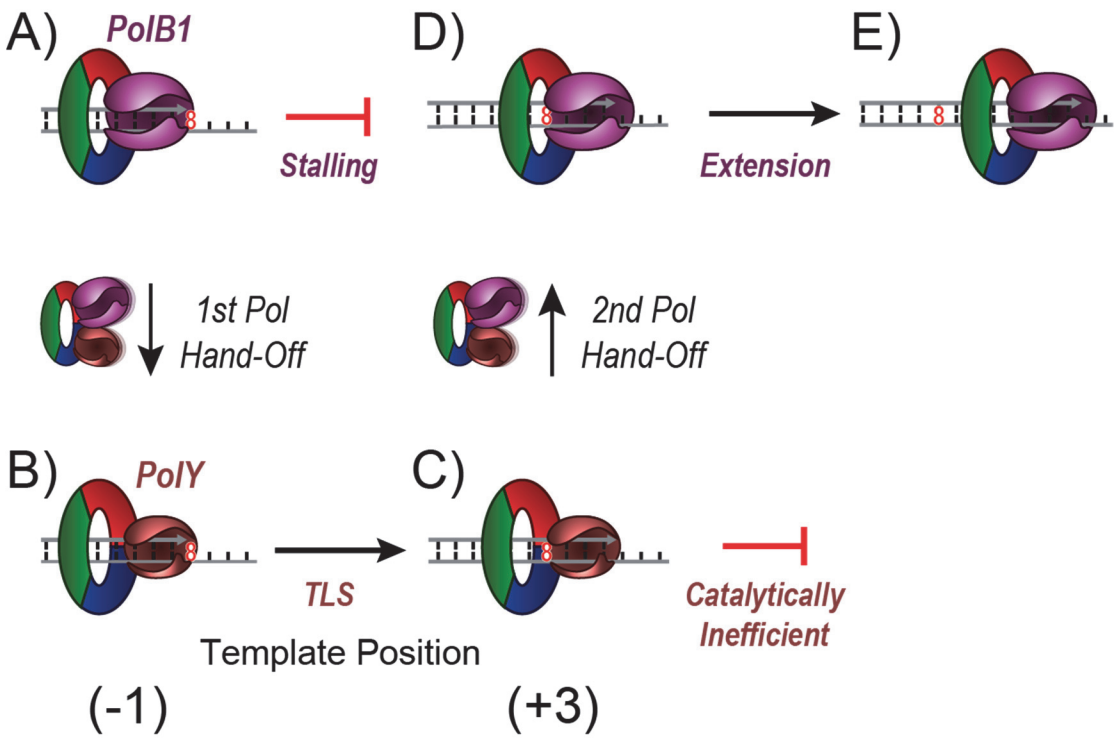

Figure 4.12: Proposed mechanism for DNA hand-offs between PolB1 and PolY in response to an 8-oxoG lesion.
A) Upon encountering 8-oxoG on the template strand, PolB1 stalls. B) Individual contacts with PCNA123 mediate the first Pol hand-off from PolB1 to PolY. C) PolY then performs translesion synthesis to the template position three base pairs beyond the 8-oxoG lesion, where it becomes catalytically inefficient for additional synthesis. D) The second Pol hand-off from PolY to PolB1 is then mediated through PCNA123 to re-establish HiFi PolB1 for E) extension and effective bypass of the lesion.

beyond a thymine-thymine dimer.[329, 330] These studies suggest the potential for structural impediments, or communication, between a bypassed template lesion and the TLS Pol active site once it has translocated to a certain position downstream, but the basis of this disruption has not been explored. We hypothesize that these observed inefficiencies correspond with a disruption in translocation. A series of positively charged residues of the PolY LF domain interact with the DNA backbone and are implicated in facilitating PolY translocation.[314] During extension from a bypassed lesion, an altered base with modifications that are oriented toward the LF may sterically disrupt interactions between template DNA and the residues involved in translocation. A disruption in translocation would prevent the Pol active site from accessing the next template base and interrupt binding of an incoming nucleotide, ultimately weakening the apparent efficiency of successive catalytic extensions. The apparent conservation of the +3 intermediate for TLS Pols from *E. coli* and *Sso,* and similar intermediates observed in humans, strengthens the hypothesis that the LF domain of Y-family Pols can sense bypassed lesions after translocating to a certain position downstream. Activation of this 'pinky trigger,' along with complementation of extension activity by a HiFi Pol and mediation through a processivity clamp may serve as the molecular signal which restores HiFi Pol activity. Though the various TLS Pols have been characterized in their bypass of a diverse set of lesions, further investigation is needed to understand the mechanisms which limit the extent of their error-prone activities.

Previously, under conditions similar to the current study, we measured the rate of association of PolY to a pre-loaded B1HE using pre-steady-state FRET.[177] This apparent rate ($0.8 \pm 0.1\ s^{-1}$) is over 10-fold faster than the apparent rate of lesion bypass by the same

pre-loading approach evaluated in *Scheme iv* (0.077 ± 0.009 s^{-1}). In that same study, we also observed that PolB1 was not displaced upon PolY association within the measured timescale, indicating that both Pols were simultaneously bound to the clamp and formed a concerted PCNA tool belt.[177] Combined with our current findings, this suggests that PolY may rapidly associate with the stalled B1HE to form a SHE complex, but the rate of the first Pol switch within the complex (involving transient dissociation of PolB1 and PolY binding to the stalled substrate) is slow and rate limiting for lesion bypass by PolY.

The apparent rate for the first Pol hand-off to PolY for TLS (0.077 ± 0.009 s^{-1}) is 6.4-fold slower than the second switch to PolB1 for extension (0.49 ± 0.05 s^{-1}; **Fig. 4.7A** *Scheme iv* vs **Fig. 4.11A** *Scheme iii*). This suggests that PolB1 is more stably bound to DNA relative to PolY, which is consistent with previous Pol:DNA binding affinity studies, [170] yet these binding affinities have not been evaluated in the presence of PCNA123. The apparent difference in hand-off rates observed in this study indicates that the fundamental basis for each hand-off is molecularly unique, and additional investigation is required to obtain direct insight into the kinetic and structural mechanisms of these Pol hand-off events.

After an 'on-the-fly' TLS event and resumption of HiFi Pol activity, the TLS Pol may remain bound to the clamp during replicative extension. This configuration allows TLS to be transiently available for subsequent encounters with DNA lesions. Yet, in the context of a more complex multi-equilibria system, dynamic exchange of HiFi Pols and other DNA processing enzymes has been observed.[265, 331, 332] PCNA123 has also been shown to coordinate an alternate arrangement of enzymes, optimizing their combined activities for Okazaki fragment maturation.[225] This indicates that an effective cellular

response would require dynamic configurations of various cellular tools in order to faithfully maintain the genome. Therefore, the mechanisms of Pol hand-offs may include aspects of distributive Pol exchange. However, this does not eliminate the possibility of switching through direct contacts between Pols by way of a transient hand-off through a PCNA tool belt scaffold, especially considering the network of direct interactions among TLS Pols[333, 334] and the sharing of accessory subunits between eukaryotic TLS Polζ and HiFi Polδ.[169, 335, 336]

Characterizing the intricacies of 'on-the-fly' TLS and its hand-off mechanisms is integral to our understanding of this early DNA damage response. Though this damage tolerance pathway benefits the cell by relieving stalled replication, unregulated TLS activity can detrimentally contribute to mutagenesis and resistance to DNA-damaging cancer therapies. Recent advances have addressed these drawbacks through identification of small molecule inhibitors which target Pol-Pol interactions and/or disrupt mutagenic TLS activity, supplementing the effectiveness of current chemotherapeutic drugs.[337-343] These studies provide a promising new approach for mitigating the role of TLS in chemoresistance and provide an exciting incentive for furthering our understanding of the kinetic and structural foundations of TLS.

CHAPTER FIVE

Characterization of Homotrimeric and Heterotrimeric Polymerase Complexes from *Saccharolobus solfataricus*

Introduction

Saccharolobus solfataricus (*Sso*) is a hyperthermic acidophile which grows at temperatures of over 80 ºC and at low pH 2-3.[344] Survival of this organism under these extreme conditions requires efficient DNA replication and repair processes in response to oxidative stress, making the *Sso* replication system a particularly interesting model for study. In *Sso*, PolB1 acts as the high-fidelity (or accurate) DNA replication polymerase (Pol)[180] and forms a holoenzyme (HE) complex with the heterotrimeric PCNA123 processivity clamp which is loaded onto DNA by the Replication Factor C (RFC) clamp loader.[345]

Though the PolB1 HE complex has a fast replication rate, it displays a low processivity of less than 200 bp.[176] This suggests that the *Sso* PolB1 HE is not stable on its own and is highly distributive (*i.e.* k_{off} is fast), meaning PolB1 bound to PCNA frequently dissociates and exchanges with other Pols from solution. This Pol exchange occurs through the C-terminal PCNA-interacting peptide (PIP). Replicative HE complexes from other domains of life exhibit highly processive replication, including gp43 from T4 phage,[17] Pol III from *E. coli*,[346] and Pol ε from yeast.[347] The eukaryotic Pol δ HE is the only other complex to possess relatively low processivity, but this is acceptable as Pol δ is implicated in the synthesis of shorter Okazaki fragments (~250 bp) on the lagging-strand.[209,210] However, as the primary high-fidelity Pol in *Sso*, PolB1 must also perform long stretches

of leading-strand synthesis. The apparent lack in processivity of the PolB1 HE requires additional investigation into how *Sso* fulfills the cellular requirement for rapid and processive DNA synthesis. To investigate this, we have evaluated how the assembly of higher-order DNA polymerase complexes contribute to replication stability, higher processivity, and efficiency of DNA synthesis by PolB1.

Homotrimeric PolB1

Sso PolB1 is a 101 kDa protein[74] which exists as a monomer in solution. In the presence of a primer/template DNA substrate, one PolB1 molecule binds the 3' end of the primed substrate with a K_d of ~150 nM. At elevated concentrations of PolB1 (> 400 nM), two additional PolB1 molecules bind cooperatively to the monomeric PolB1:DNA complex to form a PolB1 homotrimer.[18]

Formation of this trimer increases the kinetic synthesis and processivity of PolB1. Processivity of the trimer is over 50-fold higher than for monomeric PolB1, suggesting a significantly more stable replication complex. According to the proposed PolB1 trimer structure, the three Pols encircle the DNA similarly to the PCNA123 clamp. One of the Pol active sites is bound to the primer terminus for DNA synthesis while the other two enzymes stabilize the entire complex to DNA, effectively slowing the rate of dissociation (*i.e.* slower k_{off}) and increasing DNA binding affinity (*i.e.* lower K_d). According to the relationship established in **Equation 5.1**,

$$Processivity\ (bp) = \frac{Synthesis\ rate\ (bp \cdot min^{-1})}{k_{off}\ (min^{-1})} \qquad \textbf{(Equation 5.1)}$$

the slower rate of dissociation would contribute to a higher observed processivity. The PolB1 trimer also allows for a faster rate of synthesis compared to the monomer,[170] which would also contribute to greater processivity. This faster rate of synthesis may be explained

by the effective increase in concentration of PolB1 active sites at the primer terminus. By stabilizing the active Pol and tethering additional active sites nearby, the trimeric complex reduces the off-rate and increases the apparent rate of synthesis.

Additional investigation is required to understand the mechanisms of PolB1 trimer activity during processive synthesis. We propose three models by which Pols within the trimeric complex may be exchanged or switched (**Fig. 5.1**). First, by (A) "Trimer Exchange," the entire trimer may dissociate from the DNA, followed by assembly of another trimer complex from solution. Alternatively, by (B) "Monomer Exchange" an individual Pol may dissociate from the trimer complex and be replaced by another Pol from solution to restore the trimer. Lastly, the Pols may be dynamic within a bound trimer complex, allowing for (C) an "Internal Switch" of active sites among the Pols without dissociation of the trimeric complex.

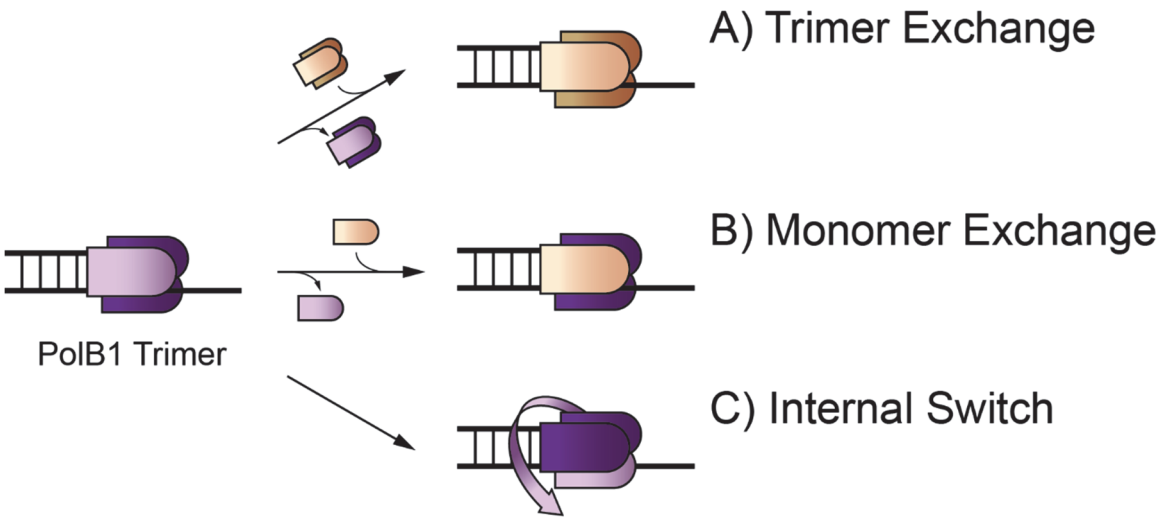

Figure 5.1: Three dynamic models for the PolB1 trimer. During synthesis by the PolB1 trimer, the active trimer (purple) may dissociate from the DNA substrate and be replaced by a new PolB1 trimer from solution (orange), as described by "Trimer Exchange" (A). Alternatively, individual PolB1 monomers within the active trimer may dissociate from the complex, followed by recruitment of a PolB1 molecule from solution to restore the trimer, as described by "Monomer Exchange" (B). Lastly, an active PolB1 trimer may be dynamic without exchange of subunits from solution by sharing the DNA substrate among the active sites within the bound complex, as described by the "Internal Switch" (C).

In this report, the elevated processivity of the PolB1 trimer is shown to be temperature dependent, consistent with the temperature dependence of trimer formation.[170] Titration of catalytically inactive PolB1 (PolB1^{cat-}) into the trimeric complex results in shorter stretches of processive synthesis, indicating the possibility of "Internal Switching" within the PolB1 trimer.

PolB1-Binding Proteins (PBP1 and PBP2)

In early biochemical characterizations, *Sso* PolB1 has been described to act as a single subunit Pol. This differs from the known multisubunit assembly of eukaryotic B-family Pols, including Polα, Polε, Polδ, and Polζ.[348, 349] However, two accessory subunits to PolB1, identified as PolB1-binding proteins (PBPs), were recently identified and shown to affect PolB1 activity.[75]

The thermostability of PolB1 is increased in the presence of PBP1 and PBP2, suggesting a physiologically relevant role of these subunits for the hyperthermophilic organism. The acidic tail of PBP1 regulates PolB1 exonuclease activity and can limit polymerase activity in the context of strand displacement during lagging strand synthesis, while PBP2 only slightly increases PolB1 polymerase activity. This is especially interesting given previous characterization of an "Okazakisome" complex which coordinates the activities of PolB1, Fen1, and Lig1 on PCNA123 for Okazaki fragment maturation.[225] The novelty of the PBPs warrants investigation into alternative functions these subunits may possess during *Sso* replication, including PolB1 HE processivity, PolB1 trimer formation, and Pol exchange within the supraholoenzyme (SHE) complex.

In this report, both PBP1 and PBP2 were successfully cloned into the pET30a expression vector, expressed and purified. Preliminary activity assays also demonstrate a concentration dependent inhibition of PolB1 polymerase activity by PBP1.

Materials and Methods

Protein Expression and Purification

Expression vectors for wild type PolB1 ($PolB1^{WT}$) and $PolB1^{cat-}$ were acquired from a previous study.[176] These proteins were expressed and purified as previously described in Chapter Three.[177] PBP1 and PBP2 were cloned, expressed, and purified as previously described in Chapter Five.

PBP Pulldowns

PBP1 and/or PBP2 were incubated with an equimolar concentration of His-tagged PolB1 in binding buffer. Protein mixtures were incubated with Ni-NTA beads (Thermo)**.** Beads were then washed with seven equivalents of binding buffer, followed by elution with an equivalent addition of buffer containing 0.5 M imidazole. The elution fraction was resolved and by SDS-PAGE and visualized by Coomasie Blue staining. As a negative control, PBP1 and/or PBP2 were incubated with Ni-NTA beads in the absence of His-tagged PolB1.

DNA Synthesis and Processivity Assays

DNA synthesis and processivity assays were performed with the circular M13 DNA template as described in Chapter Three with the following modifications. PolB1 was added at increasing concentrations and at varying ratios of WT to cat^{-}. Incubation and reaction

temperature was also changed from 60 ºC to 40 ºC, as indicated. DNA synthesis assays were also performed with the PolB1 HE (+ PCNA123, RFC, ATP) and in the presence of PBP1 and/or PBP2, as indicated.

Results

PolB1 Trimer Activity is Temperature Dependent

Previously, PolB1 replication rate and processivity were shown to be both temperature and concentration dependent.[170] This apparent increase in activity is explained by the positive correlation of both polymerization rate (increasing k_{pol}) and stabilization of PolB1 (decreasing k_{off}) with increasing temperature. Additionally, activity is further increased with elevated concentrations consistent with trimeric PolB1, suggestive of both a faster and more stable replication complex.

To directly compare the effects of PolB1 concentration and temperature on overall activity, PolB1 was titrated into replication and processivity assays at different temperatures (**Fig. 5.2A**). At 60 ºC, processivity (+ spDNA trap) of PolB1 is concentration dependent. Specifically, at monomeric PolB1 concentrations (**Fig. 5.2B**, lane 2), an average of 126 ± 80 bp were extended, whereas trimeric concentrations (lanes 2 -5) yield an 8-fold increase in processivity of over 1000 bp. These values are consistent with previous findings.[18] At 40 ºC (lanes 10 -13), the maximal processivity observed is only 122 ± 34 bp at the highest concentration of PolB1 tested (lane 13). This is only a 2.4-fold increase over the monomeric PolB1 at 40 ºC (lane 10). This difference in the concentration dependent

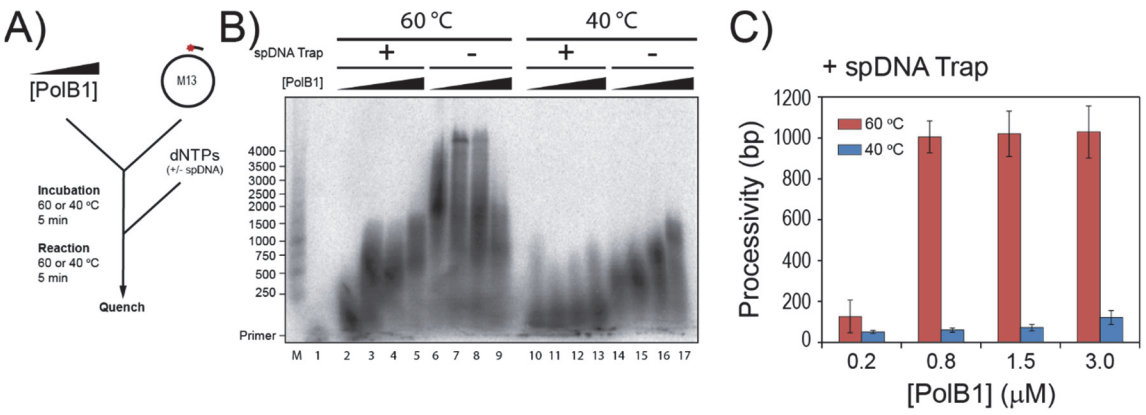

Figure 5.2: PolB1 trimer processivity is temperature dependent. DNA synthesis assays (- spDNA) and processivity assays (+ spDNA) were performed on the M13 DNA template with increasing concentrations of PolB1 at 40 ºC or 60 ºC (A). Primer extension products were resolved by denaturing alkaline agarose gel electrophoresis (B). Processivity of PolB1 complexes was quantified and compared for various concentrations of PolB1 at each temperature (C).

increase of processivity suggests a temperature dependence on PolB1 trimer activity which is limited by trimer formation.

In replication assays (- spDNA trap) at 60 ºC (lanes 6-9), PolB1 activity demonstrates an odd trend. From 0.2 μM to 0.8 μM PolB1 (lanes 6 and 7), longer replication products are observed, consistent with the faster rate of trimeric PolB1. However, at concentrations above 0.8 μM (lanes 8 and 9), there is a concentration dependent decrease in the apparent rate of synthesis. This concentration dependent decrease in rate is not reflected in the observed processivity at 60 ºC (**Fig. 5.2C**), indicating that excess PolB1 in solution may interfere with polymerase activity in a distributive context without disrupting processivity (*i.e.* the ratio of k_{pol} to k_{off}) of the PolB1 trimer.

Active Sites Within the PolB1 Trimer can Perform a Concerted Internal Switch

To investigate the dynamics of Pol exchange or switching within the PolB1 trimer, PolB1^{cat-} was introduced into replication and processivity assays. At indicated total

concentrations of PolB1, the pre-loading ratio of WT:cat^{-} PolB1 was varied, then initiated and quenched as before (**Fig. 5.3A**).

In replication assays of 0.8 μM PolB1, the apparent rate of replication decreases at higher ratios of PolB1^{cat-} (**Fig. 5.3B**, - spDNA). A similar decrease in replication rate is observed for replication assays at other concentrations of PolB1, even at 0.2 μM (blue circles) which represents the slower PolB1 monomer (**Fig. 5.3C**). This suggests that catalytically inactive Pols can access the DNA substrate and inhibit replication by active Pols. In these replication assays, the mechanism by which PolB1^{cat-} accesses the DNA substrate may proceed by any of the three dynamic mechanisms of exchange (**Fig. 5.1**).

Alternatively, in the presence of a DNA trap, distributive exchange cannot occur from solution, providing an approach to selectively monitor dynamics of the trimer through an Internal Switch (**Fig. 5.1C**). If the PolB1 trimer were to remain static during a single processive step, a trimer which assembles with an active PolB1^{WT} bound to the primer terminus will replicate for the full processive step prior to dissociation; contrarily, a static trimer which assembles with PolB1^{cat-} bound to the substrate will perform no synthesis prior to dissociation. This “all-or-nothing” result would be indicative of a static PolB1trimer.

However, processivity assays at 0.8 μM PolB1 yield a progressive decrease in processivity with increasing ratios of PolB1^{cat-} (**Fig. 5.3B**, + spDNA). This progressive decrease in processivity is also observed with higher concentrations of the PolB1 trimer. The processivity of monomeric PolB1 (red circles) is consistently low, as expected (**Fig. 5.3D**). Altogether, these results provide evidence of a dynamic complex which can perform a concerted, internal switch within an actively replicating PolB1 trimer.

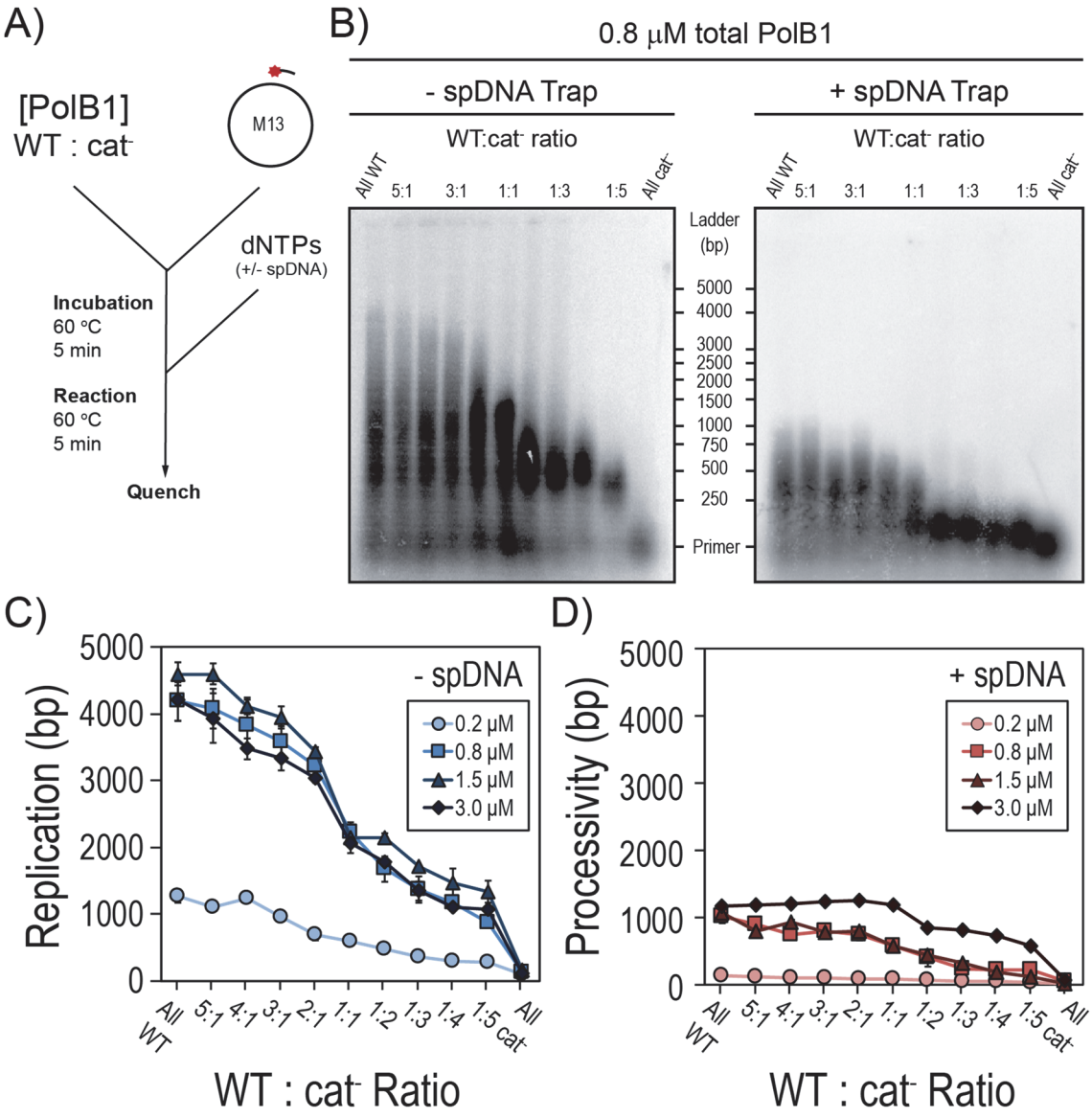

Figure 5.3: PolB1 trimer demonstrates dynamic processivity consistent with an "Internal Switch." DNA synthesis and processivity assays were performed at indicated concentrations of PolB1 containing different ratios of WT and catalytically inactive (cat-) PolB1 (A). Primer extension products were resolved by denaturing alkaline agarose gel electrophoresis (B), quantified, .and plotted as a function of WT:cat- ratio for each total concentration of PolB1.

PBP1 and PBP2 were Successfully Cloned, Expressed, and Purified

With the goal of studying the biochemical effects of the PBPs on PolB1 replication, PBP1 and PBP2 sequences were first cloned into expression vectors. The genes were amplified from *Sso* genomic DNA and cloned into pET30a using *NdeI* and *XhoI* restriction sites. A PCR screen was used to confirm the presence of each PBP in pET30a (**Fig. 5.4A**) and cloning was later confirmed by DNA sequencing. Each PBP was expressed and purified as described in Chapter Four. The expected size and purity of PBP1 and PBP2 were confirmed by SDS-PAGE analysis of purified fractions from gel filtration chromatography (**Fig. 5.4B-C**). Previously, each PBP was shown to have an independent, direct interaction with PolB1.[75] Indeed, both PBP1 and PBP2 were pulled down by His-tagged PolB1, either independently or when introduced together (**Fig. 5.4D**). Together, these results demonstrate successful cloning, expression, and purification of these novel accessory subunit proteins for PolB1.

PBP1 Decreases Activity of Different PolB1 Replication Complexes

The initial biochemical investigation of PBP1 reports a regulatory effect on PolB1 strand displacement activity on shorter oligo-based DNA substrates.[75] To investigate the PBP effects on the overall rate of PolB1 replication activity on longer substrates, we included equimolar concentration of PBP1 and/or PBP2 in replication assays of various PolB1 replication complexes. For PolB1 monomer (200 nM; **Fig. 5.5A**), a slight decrease in PolB1 replication rate is observed when PBP1 is present (arrows). Addition of PBP2 alone yields no apparent effect on PolB1 monomer activity, and it does not appear to reduce the degree of inhibition by PBP1. Similarly, for the PolB1 HE (containing PCNA123, RFC, and ATP), only reactions containing PBP1 yield a slight inhibition of PolB1 activity with

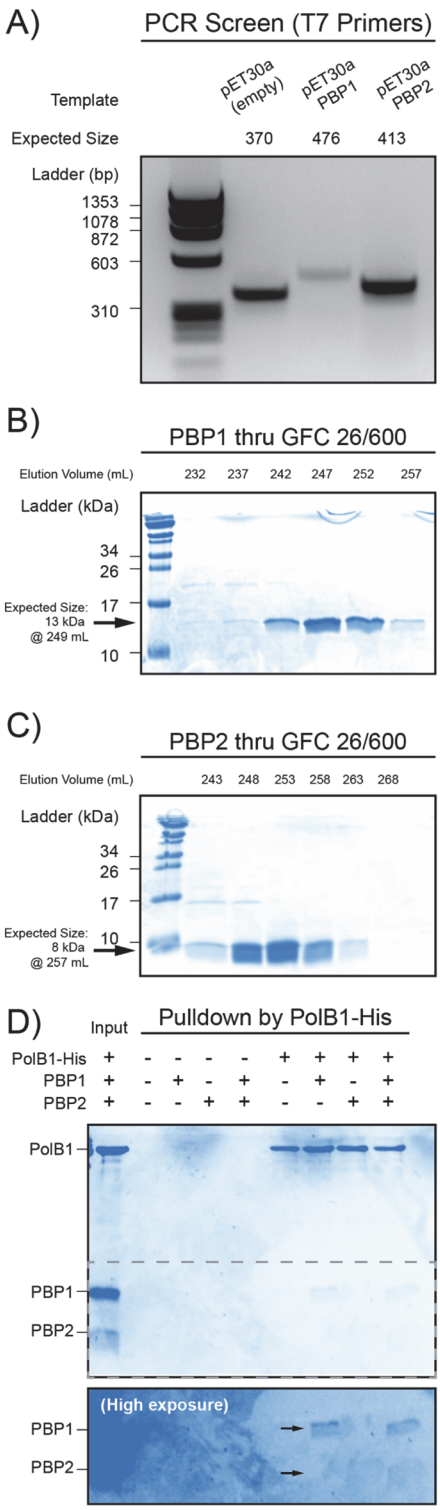

Figure 5.4: PBP1 and PBP2 were successfully cloned, expressed, and purified. PBP1 and PBP2 sequences were PCR amplified from pET30a. Expected product sizes were confirmed by agarose gel electrophoresis (A). Purification of PBP1 (B) and PBP2 (C) was confirmed after gel filtration chromatography. Interactions of PBP1 and PBP2 with PolB1 were validated by pull-down with His-PolB1 (D); dashed box indicates the region of the gel shown in high exposure.

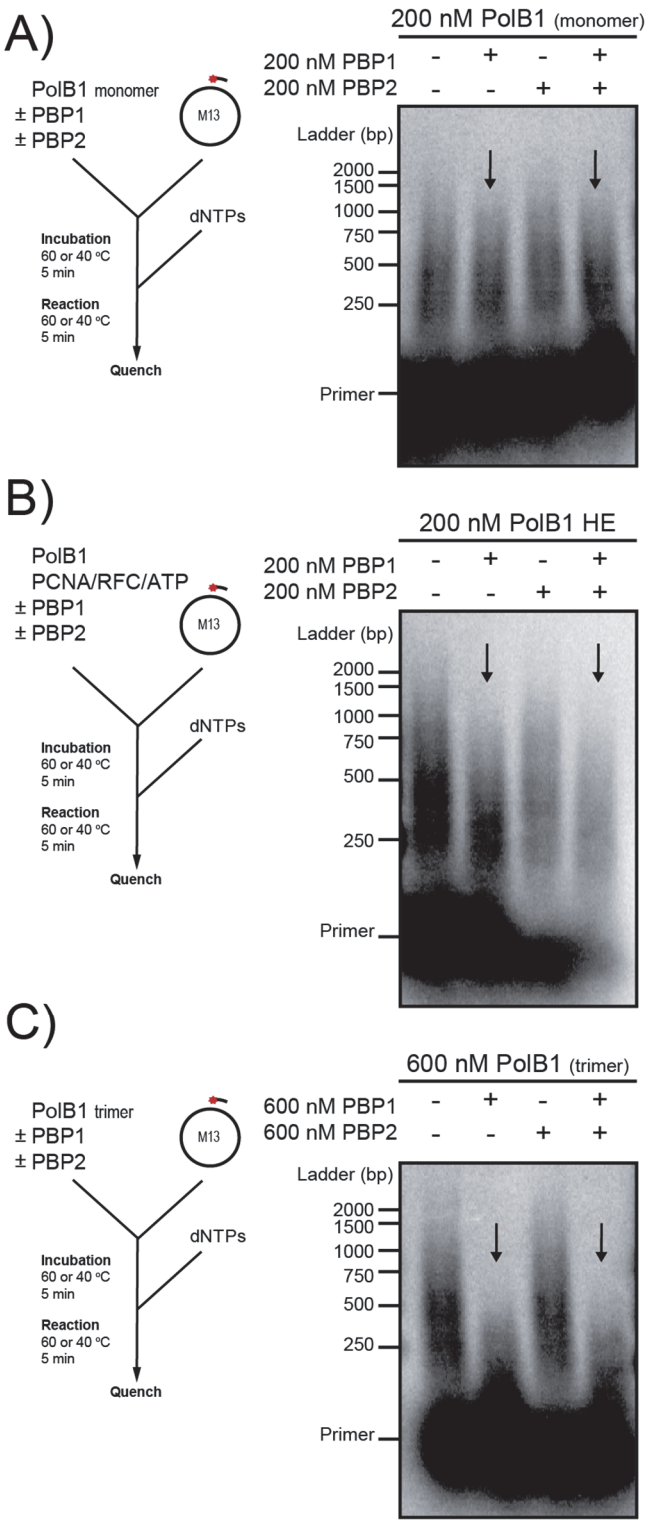

Figure 5.5: PBP1 inhibits PolB1 activity in three different replication complexes. DNA synthesis assays were performed with PBP1 and/or PBP2 at equimolar concentrations of PolB1 as a monomer (A), in the PolB1 holoenzyme (B), and in the PolB1 trimer (C). PolB1 activity was noticeably inhibited when PBP1 was included (arrows).

no apparent effect from PBP2 (**Fig. 5.5B**). Together, these results indicate a slight inhibition of PolB1 polymerase activity outside of strand displacement and Okazaki fragment maturation.

The effects of the PBPs were also monitored for the PolB1 trimer (600 nM). To maintain equimolar conditions, PBP concentrations were elevated as well. As before, only reactions containing PBP1 slowed the apparent rate of PolB1 synthesis (**Fig. 5.5C**). However, inhibition is much more apparent relative to the slight inhibition seen at 200 nM of PBP1 (arrows). Again, PBP2 had no apparent effect. This indicates a concentration dependent inhibition of PBP1 on PolB1 activity.

Discussion

PolB1 Trimer

Consistent with the temperature dependence of PolB1 trimer formation, these findings demonstrate a temperature dependence on the processivity of the complex. This lack of processivity is owed to a higher k_{off} and lower k_{pol} at lower temperatures. At elevated temperatures, the coupled increased in stability and faster polymerase activity account for the drastic elevation in processivity for this unique trimeric complex. However, additional investigation is required to understand the structural details of the PolB1 trimer. Identification of the Pol-Pol-Pol interfaces would greatly aid in our understanding of trimer formation and the basis of its stability. Biophysical investigations may also reveal conformational changes which are thermodynamically limiting for accessibility of critical residues for trimer formation. Characterizing these structural dynamics and identifying the

Pol-Pol-Pol interactions within the trimer will reveal the mechanisms which grant this complex elevated processivity.

Additionally, these results provide evidence for an "Internal Switch" within the trimeric complex. By this model, the active sites within the PolB1 trimer alternate their access to the DNA substrate without dissociation of the complex (**Fig. 5.1C**). This adds an additional layer of dynamic activity within a concerted replication complex separate from the distributive aspects of DNA replication. The details of this switching mechanism are not understood and would be clarified by a structural model of this complex.

With a faster rate of synthesis, increased stability, and high processivity, the PolB1 trimer serves as a physiologically intriguing complex. For *Sso*, an organism which grows under extreme temperatures, formation and activity of the PolB1 trimer are favored. During replication, PolB1 concentration may be localized at sites of DNA synthesis, also favoring trimer formation. Interestingly, PolB1 trimer processivity (~ 1000 bp) is higher than that of the distributive PolB1 HE (~ 200 bp).[176] This indicates that the PolB1 trimer can act efficiently and independent from PCNA123. Though its role in DNA synthesis has yet to be observed *in vivo*, the PolB1 trimer fulfills the cellular demand for processive synthesis during DNA replication.

PolB1 Binding Proteins

Here, we demonstrate the successful cloning, expression, and purification of PolB1 accessory subunits PBP1 and PBP2. Preliminary activity assays demonstrate inhibition of PolB1 activity by PBP1 with no observable effects from PBP2. Interestingly, for monomeric PolB1 complexes (200 nM), the inhibition by PBP1 is slight, while elevated concentrations (600 nM) yield a stronger inhibition of PolB1 trimer activity.

This inhibition may be explained PBP1-mediated displacement of PolB1. Previously, PBP1 regulation of strand displacement activity coincided with an increase in the total amount of substrate utilized, suggesting a role for PBP1 in PolB1 "recycling" for the synthesis of multiple Okazaki fragments on the lagging-strand.[75] This mechanism promotes a more distributive (*i.e.* less processive) replication complex, accounting for the reduction in the apparent rate of PolB1 synthesis in the presence of PBP1. PolB1 inhibition may also be explained by the C-terminal acidic tail of PBP1 which may compete with DNA for the PolB1 active site. Truncation of this acidic tail abrogated the effects of PBP1, implicating these residues in PolB1 regulation.[75]

These novel PBPs require additional investigation to characterize their roles in alternative PolB1 replication complexes. The distributive action of the PolB1 HE may be stabilized by these accessory subunits and increase processivity during replication. In the PolB1 trimer, PBP1 appears to reduce activity, but further study is needed to determine whether the basis of this inhibition strictly limits PolB1 activity or disrupts PolB1 trimer formation. Lastly, as reported in Chapter Four, the PBPs do not appear to have a role in the exchange or "hand-off" of DNA between stalled PolB1 and PolY for translesion synthesis and resumption of high-fidelity replication.

CHAPTER SIX

Conclusion

As the blueprint for vital cellular functions, the DNA code must be faithfully replicated and passed down from cell to cell. Aberrations and mutations in these instructions pose a direct threat to the health of the cell, highlighting the importance of processes which promote genomic maintenance. Given the constant chemical threat to DNA, it is extraordinary that cells have the capacity to replicate their genome, preserve their genetic code, and maintain proper cellular function for multiple generations.

However, the cellular capacity to respond to DNA damage does have its limits. Excessive exposure to genotoxic agents or defects in DNA repair pathways can overwhelm the cellular response. As a result, lesions remain in the genome and cause stalling of high-fidelity (HiFi) DNA polymerases (Pols) during replication. Translesion synthesis (TLS) Pols provide a mechanism of tolerance to unrepaired lesions by replicating across damaged DNA bases. This activity, however, comes with the potential cost of replication errors and must be regulated to minimize unnecessary mutagenesis.

DNA Damage Requires a Dynamic Response

Though the enzymatic mechanisms of TLS Pols have been widely studied, the process by which they are recruited to a stalled replication fork is still a topic of investigation.[310] According to a distributive model, a stalled Pol will dissociate from the DNA and processivity clamp prior to recruitment of a TLS Pol. In this way, the replisome stochastically selects enzymes from solution until it finds the right ‘tool’ for the job for

bypassing the lesion. Alternatively, by the concerted model, multiple Pols remain stably bound to the processivity clamp through independent contacts to form a 'tool-belt' on DNA.[178] This allows a TLS Pol to be readily available upon stalling of a replicative Pol. By switching Pol active sites within this higher-order replication complex, the combined activities of TLS and replicative Pols are mediated and optimized.

This collection of work describes the formation of a tool-belt complex in archaea, termed the 'supraholoenzyme' (SHE).[177] This complex forms through multiple contacts between the replicative PolB1, TLS PolY, and the processivity clamp PCNA123. In response to an 8-oxoguanine lesion, formation of the SHE promotes efficient TLS bypass and extension from the lesion. After lesion bypass, PolY becomes catalytically inefficient for additional synthesis at a template position three base pairs downstream of 8-oxoguanine, while PolB1 is capable of rapid extension. Given prior observations of the supraholoenzyme, it is concluded that PolB1 and PolY 'hand off' the DNA at this position within a tool-belt complex.

The tool-belt model would suggest that PolY remains stably bound to the complex, even after completion of TLS and resumption of PolB1 activity. Further study is required to determine whether the same PolY enzyme is retained within the SHE and remains available for successive TLS events. However, considering the variety of enzymes involved in the numerous DNA processing pathways, proper genomic maintenance would require dynamic configurations of enzymatic tools to efficiently complete the job at hand. This suggests a model in which DNA is handed off between Pols through a transiently concerted SHE complex. Like the passing of a relay baton, there is a brief moment when both sprinters' hands are in possession of the baton during the exchange. The baton is not

tossed or dropped between the runners; it is passed directly. Additionally, both runners are not required to maintain contact as the race proceeds. Once the first runner completes their leg of the race, they are free to let go of the baton. If obstacles are encountered, the baton can be passed to a specialized runner who traverses the hurdles and hands it back to a sprinter. In this way, the replisome remains dynamic and can hand the DNA off to the appropriate enzyme in response to the various types of genomic obstacle it may encounter.

Clinical Relevance and Therapeutic Targets of TLS

TLS Pol activity plays a clear role in proper genomic maintenance in response to DNA damage. This is highlighted by the link between mutations in human Polη and the disease xeroderma pigmentosum variant (XP-V). Upon exposure to UV light, sequential thymine bases can react to form a cyclobutanepyrimidine dimer (CPD) lesion which stalls the HiFi DNA Pol.[350] Polη is remarkably effective against this lesion by accurately incorporating two adenine bases across the damaged thymines.[351] Without a functional Polη enzyme, individuals with XP-V cannot tolerate UV-induced DNA damage and suffer from sensitivity to sunlight and elevated susceptibility to skin cancer.[352, 353]

Aside from this physiologically beneficial role, the capacity for TLS Pols to bypass DNA lesions presents a problem during chemotherapeutic treatment of cancer cells. A common feature of cancer cells is an apparent deficiency in the repair of DNA.[354] The mechanisms of several anti-cancer therapies are based on inducing damage to the DNA of cancer cells with the goal of inducing lethal genomic instability.[355, 356] For example, the drug cisplatin acts by forming crosslinks between nearby guanine bases which block DNA replication.[357] With its TLS activity, Polη can bypass cisplatin lesions and allow replication to proceed, essentially reducing the efficacy of the drug.[358, 359] Further, bypass of cisplatin

by Polη is linked to the highly error-prone extension activity of Polζ.[336] Together, these TLS Pols contribute to resistance and elevated mutagenesis in response to cisplatin treatment.

This complication has prompted emerging investigations which focus on the inhibition of TLS Pols to complement traditional chemotherapies. By countering TLS activity, the mutagenic tolerance to genomic instability would be reduced and allow for maximal effectiveness of current anti-cancer drugs.[360] Recently, inhibition of Polη was demonstrated using a small molecule which disrupts binding of an incoming nucleotide, leading to increased cellular sensitivity to cisplatin.[341] A related inhibitor was shown to selectively disrupt DNA binding by Polκ and improve the effectiveness of the anti-cancer drug temozolomide.[342] Additionally, a nucleotide analog was shown to be preferentially incorporated by TLS Pols across abasic sites, effectively acting as a chain terminator and sensitizing cells to temozolomide.[361, 362]

In addition to targeting the TLS Pol active site, advancements have been made toward inhibiting the protein-protein interactions which direct the recruitment of TLS Pols to sites of replication. Through their PCNA-interacting peptide (PIP), the TLS Pols can be directly recruited to DNA. In response to DNA damage, PCNA can be ubiquitinated, providing another point of TLS recruitment through interaction with their ubiquitin binding domains.[363] The TLS Pols also possess a Rev1-interacting region (RIR), implicating Rev1 as a platform for the recruitment of multiple TLS Pols.[334] Recent studies have identified a small molecule which binds to the C-terminus of Rev1 and competes for binding of the RIR, effectively blocking recruitment of the TLS Pols.[337] This compound sensitizes cells

to cisplatin, reduces TLS-dependent mutagenesis, and suppresses tumor growth, further validating TLS inhibition as a promising anti-cancer therapy.[339]

This network of protein-protein interactions in the human replication system suggests the formation of dynamic, higher-order replication complexes, much like the supraholoenzyme described in this study. However, there are many more polymerases involved which have a diversity of roles in response to different DNA lesions. In light of this complexity, additional study is needed to understand how DNA is handed off among the various Pols, how this process changes in response to different lesions, and how TLS activity is regulated after lesion bypass. Insight into these fundamental mechanisms and how they relate to other DNA repair pathways may present novel approaches for TLS inhibition, inspiring excitement for continued investigation in this field.

APPENDIX

APPENDIX

Curriculum Vitae

Matthew T. Cranford

1314 James Avenue, Apt. 116
Waco, TX 76706
512-750-3686
Matthew_Cranford@baylor.edu

EDUCATION

PhD **Biochemistry, Baylor University** — Fall 2020
Dissertation Title:
Investigations of Dynamic Higher-Order DNA Polymerase Complexes in Archaea
Primary Investigator: Dr. Michael A. Trakselis
GPA: 3.95

BS **Biology, University of Mary Hardin-Baylor** — Spring 2014

BS **Chemistry, University of Mary Hardin-Baylor** — Spring 2014
Summa cum laude
GPA: 4.0

TEACHING EXPERIENCE

Temporary Lecturer, Baylor University
Advanced Biochemistry Lab (4142) — Spring 2018

Teaching Assistant, Baylor University
Advanced Biochemistry Lab (4142) — Fall 2014 – Fall 2015
Biophysical Chemistry Lab (4225) — Fall 2014 – Spring 2015

Advanced Instrumentation Workshop, Baylor University — Summer 2017, 2018, and 2019
"FPLC methods for protein purification"

Undergraduate Research Mentor, Baylor University — Fall 2014-Summer 2018
Provided direct training and mentoring for seven individual undergraduate researchers in the Trakselis Research Lab

PUBLICATIONS

Cranford, M.T., *Kaszubowski, J.D., Trakselis, M.A. The second DNA polymerase hand-off to resume high-fidelity replication occurs at a discrete intermediate three bases past 8-oxoguanine (accepted).*

Trakselis, M.A., **Cranford, M.T.** and Chu, A.M. (2017) Coordination and Substitution of DNA Polymerases in Response to Genomic Obstacles. Chem Res Toxicol, 30, 1956-1971.

Cranford, M.T., Chu, A.M., Baguley, J.K., Bauer, R.J. and Trakselis, M.A. (2017) Characterization of a coupled DNA replication and translesion synthesis polymerase supraholoenzyme from archaea. Nucleic Acids Res, 45, 8329-8340.

PRESENTATIONS

2020 ACS National Meeting (San Francisco, CA)
Division of Chemical Toxicology
Abstract accepted for Young Investigators Symposium
Locating the second polymerase switch: Where resumption of replication limits the length of translesion synthesis

2020 Baylor College of Medicine Genome Instability Group (Houston, TX; via Zoom)
The replication relay: Where DNA is handed-off between high-fidelity and translesion synthesis polymerases

2018 Undergraduate Chemistry Seminar (Baylor University, Waco, TX)
Invited as a guest speaker for Undergraduate Seminar (CHE 4151)
Characterization of a coupled DNA replication and translesion synthesis polymerase supraholoenzyme from archaea

2017 Keystone Symposium (Santa Fe, NM)
Poster: DNA polymerase contacts regulate formation of a novel supraholoenzyme complex

2016 Baylor University Stone Symposium (Waco, TX)
Poster: Formation of a supraholoenzyme stabilizes the DNA replication complex, increases processivity, and provides the platform for a concerted TLS Pol switch

2015 SWRM/SERMACS Regional Meeting (Memphis, TN)
Poster: Exploring the dynamics of polymerase switching among different DNA replication complexes

Baylor University Department of Chemistry and Biochemistry

Colloquium Speaker Coffee Hour: 30-minute research presentations

Visitors hosted:

- Sheila David (University of California, Davis)
- Peng Tao (Southern Methodist University)
- Joseph Loparo (Harvard Medical School)
- Zucai Suo (Florida State University College of Medicine)
- Brandt Eichman (Vanderbilt University)
- Patrick O'Brien (University of Michigan Medical School)

HONORS AND AWARDS

Provost's Medal (University of Mary Hardin-Baylor, 2014)
Awarded to the graduating senior(s) with the highest overall grade point average for four years.

John Philip Sousa Award (Stony Point High School, 2010)
Awarded to honor the top student in the high school band, recognizing superior musicianship and outstanding dedication.

Eagle Scout (Troop 145, Round Rock, TX, 2008)
The highest achievement attainable in the Boy Scouts of America.

PERSONAL

Musician

Columbus Avenue Baptist Church (Waco, TX) — Fall 2014 – Summer 2019
Guitarist, keyboardist, bassist, and guest Worship Leader — Spring 2019

Avenue on Campus — Fall 2018 – Summer 2019
Event Organizer and Worship Leader

Spoor. (band) — Fall 2019
Keyboardist

Photographer

Baylor University Department of Chemistry and Biochemistry — Fall 2015 – Fall 2019
Professional headshots for all faculty, staff, and graduate students

Annual Trakselis Lab Photo

REFERENCES

1. Dahm, R., Friedrich Miescher and the discovery of DNA. *Dev. Biol.* **2005,** *278* (2), 274-88.

2. De Castro, M., Johann Gregor Mendel: Paragon of experimental science. *Mol. Genet. Genomic Med.* **2016,** *4* (1), 3-8.

3. Avery, O. T.; Macleod, C. M.; McCarty, M., Studies on the chemical nature of the substance iInducing transformation of pneumococcal types: Induction of transformation by a desoxyribonucleic acid fraction isolated from *Pneumococcus* type III. *J. Exp. Med.* **1944,** *79* (2), 137-58.

4. Hershey, A. D.; Chase, M., Independent functions of viral protein and nucleic acid in growth of bacteriophage. *J. Gen. Physiol.* **1952,** *36* (1), 39-56.

5. Klug, A., Rosalind Franklin and the discovery of the structure of DNA. *Nature* **1968,** *219* (5156), 808-10.

6. Watson, J. D.; Crick, F. H., The structure of DNA. *Cold Spring Harb. Symp. Quant. Biol.* **1953,** *18*, 123-31.

7. Forsdyke, D. R.; Mortimer, J. R., Chargaff's legacy. *Gene* **2000,** *261* (1), 127-37.

8. Meselson, M.; Stahl, F. W., The replication of DNA in *Escherichia coli*. *Proc. Natl. Acad. Sci. U.S.A.* **1958,** *44* (7), 671-82.

9. Steitz, T. A., DNA polymerases: Structural diversity and common mechanisms. *J. Biol. Chem.* **1999,** *274* (25), 17395-8.

10. Doublie, S.; Sawaya, M. R.; Ellenberger, T., An open and closed case for all polymerases. *Structure* **1999,** *7* (2), R31-5.

11. Vaisman, A.; Woodgate, R., Translesion DNA polymerases in eukaryotes: What makes them tick? *Crit. Rev. Biochem. Mol. Biol.* **2017,** *52* (3), 274-303.

12. Tubbs, A.; Nussenzweig, A., Endogenous DNA damage as a source of genomic instability in cancer. *Cell* **2017,** *168* (4), 644-656.

13. Cortez, D., Replication-coupled DNA repair. *Mol. Cell* **2019,** *74* (5), 866-876.

14. Kunkel, T. A., DNA replication fidelity. *J. Biol. Chem.* **2004,** *279* (17), 16895-8.

15. Boudsocq, F.; Kokoska, R. J.; Plosky, B. S.; Vaisman, A.; Ling, H.; Kunkel, T. A.; Yang, W.; Woodgate, R., Investigating the role of the little finger domain of Y-family DNA polymerases in low fidelity synthesis and translesion replication. *J. Biol. Chem.* **2004,** *279* (31), 32932-40.

16. von Hippel, P. H.; Fairfield, F. R.; Dolejsi, M. K., On the processivity of polymerases. *Ann. N.Y. Acad. Sci.* **1994,** *726*, 118-131.

17. Yang, J.; Zhuang, Z.; Roccasecca, R. M.; Trakselis, M. A.; Benkovic, S. J., The dynamic processivity of the T4 DNA polymerase during replication. *Proc. Natl. Acad. Sci. U.S.A.* **2004,** *101* (22), 8289-94.

18. Mikheikin, A. L.; Lin, H. K.; Mehta, P.; Jen-Jacobson, L.; Trakselis, M. A., A trimeric DNA polymerase complex increases the native replication processivity. *Nucleic Acids Res.* **2009,** *37* (21), 7194-7205.

19. Kath, J. E.; Jergic, S.; Heltzel, J. M.; Jacob, D. T.; Dixon, N. E.; Sutton, M. D.; Walker, G. C.; Loparo, J. J., Polymerase exchange on single DNA molecules reveals processivity clamp control of translesion synthesis. *Proc. Natl. Acad. Sci. U.S.A.* **2014,** *111* (21), 7647-52.

20. Fuchs, R. P.; Fujii, S., Translesion DNA synthesis and mutagenesis in prokaryotes. *Cold Spring Harb. Perspect. Biol.* **2013,** *5* (12), a012682.

21. Berneburg, M.; Lehmann, A. R., *Xeroderma pigmentosum* and related disorders: Defects in DNA repair and transcription. *Adv. Genet.* **2001,** *43*, 71-102.

22. Lehmann, A. R.; Niimi, A.; Ogi, T.; Brown, S.; Sabbioneda, S.; Wing, J. F.; Kannouche, P. L.; Green, C. M., Translesion synthesis: Y-family polymerases and the polymerase switch. *DNA Repair* **2007,** *6* (7), 891-9.

23. Langston, L. D.; Indiani, C.; O'Donnell, M., Whither the replisome: Emerging perspectives on the dynamic nature of the DNA replication machinery. *Cell Cycle* **2009,** *8* (17), 2686-2691.

24. Graham, J. E.; Marians, K. J.; Kowalczykowski, S. C., Independent and stochastic action of DNA polymerases in the replisome. *Cell* **2017,** *169* (7), 1201-1213 e17.

25. Spiering, M. M.; Hanoian, P.; Gannavaram, S.; Benkovic, S. J., RNA primer-primase complexes serve as the signal for polymerase recycling and Okazaki fragment initiation in T4 phage DNA replication. *Proc. Natl. Acad. Sci. U.S.A.* **2017,** *114* (22), 5635-5640.

26. Mangiameli, S. M.; Merrikh, C. N.; Wiggins, P. A.; Merrikh, H., Transcription leads to pervasive replisome instability in bacteria. *Elife* **2017,** *6*, e19848.

27. Beattie, T. R.; Kapadia, N.; Nicolas, E.; Uphoff, S.; Wollman, A. J.; Leake, M. C.; Reyes-Lamothe, R., Frequent exchange of the DNA polymerase during bacterial chromosome replication. *Elife* **2017,** *6*, e21763.

28. Lewis, J. S.; Spenkelink, L. M.; Jergic, S.; Wood, E. A.; Monachino, E.; Horan, N. P.; Duderstadt, K. E.; Cox, M. M.; Robinson, A.; Dixon, N. E.; van Oijen, A. M., Single-molecule visualization of fast polymerase turnover in the bacterial replisome. *Elife* **2017,** *6*, e23932.

29. Loparo, J. J.; Kulczyk, A. W.; Richardson, C. C.; van Oijen, A. M., Simultaneous single-molecule measurements of phage T7 replisome composition and function reveal the mechanism of polymerase exchange. *Proc. Natl. Acad. Sci. U.S.A.* **2011,** *108* (9), 3584-9.

30. Hamdan, S. M.; Johnson, D. E.; Tanner, N. A.; Lee, J. B.; Qimron, U.; Tabor, S.; van Oijen, A. M.; Richardson, C. C., Dynamic DNA helicase-DNA polymerase interactions assure processive replication fork movement. *Mol. Cell* **2007,** *27* (4), 539-549.

31. Lopez de Saro, F. J., Regulation of interactions with sliding clamps during DNA replication and repair. *Curr. Genomics* **2009,** *10* (3), 206-15.

32. Sale, J. E.; Lehmann, A. R.; Woodgate, R., Y-family DNA polymerases and their role in tolerance of cellular DNA damage. *Nat. Rev. Mol. Cell Biol.* **2012,** *13* (3), 141-52.

33. Yang, W., An overview of Y-Family DNA polymerases and a case study of human DNA polymerase eta. *Biochemistry* **2014,** *53* (17), 2793-803.

34. Pryor, J. M.; Dieckman, L. M.; Boehm, E. M.; Washington, M. T., Eukaryotic Y-family polymerases: A biochemical and structural perspective. In *Nucleic Acid Polymerases*, Murakami, K. S.; Trakselis, M. A., Eds. Springer-Verlag: Berlin, 2014; Vol. 30, pp 85-108.

35. Ito, J.; Braithwaite, D. K., Compilation and alignment of DNA polymerase sequences. *Nucleic Acids Res.* **1991,** *19* (15), 4045-4057.

36. Braithwaite, D. K.; Ito, J., Compilation, alignment, and phylogenetic relationships of DNA polymerases. *Nucleic Acids Res.* **1993,** *21* (4), 787-802.

37. Ishino, Y.; Ishino, S., DNA replication in archaea, the third domain of life. In *The Mechanisms of DNA Replication*, Stuart, D., Ed. InTech: Rijeka, 2013; p Ch. 04.

38. Filee, J.; Forterre, P.; Sen-Lin, T.; Laurent, J., Evolution of DNA polymerase families: Evidences for multiple gene exchange between cellular and viral proteins. *J. Mol. Evol.* **2002,** *54* (6), 763-773.

39. Edgell, D. R.; Klenk, H. P.; Doolittle, W. F., Gene duplications in evolution of archaeal family B DNA polymerases. *J. Bacteriol.* **1997,** *179* (8), 2632-2640.

40. Cann, I. K.; Ishino, Y., Archaeal DNA replication: Identifying the pieces to solve a puzzle. *Genetics* **1999,** *152* (4), 1249-1267.

41. Soler, N.; Marguet, E.; Cortez, D.; Desnoues, N.; Keller, J.; van Tilbeurgh, H.; Sezonov, G.; Forterre, P., Two novel families of plasmids from hyperthermophilic archaea encoding new families of replication proteins. *Nucleic Acids Res.* **2010,** *38* (15), 5088-5104.

42. Joyce, C. M.; Steitz, T. A., Function and structure relationships in DNA polymerases. *Annu. Rev. Biochem.* **1994,** *63*, 777-822.

43. Sawaya, M. R.; Pelletier, H.; Kumar, A.; Wilson, S. H.; Kraut, J., Crystal structure of rat DNA polymerase beta: Evidence for a common polymerase mechanism. *Science* **1994,** *264* (5167), 1930-1935.

44. Gao, Y.; Yang, W., Capture of a third Mg(2)(+) is essential for catalyzing DNA synthesis. *Science* **2016,** *352* (6291), 1334-7.

45. Beese, L. S.; Steitz, T. A., Structural basis for the 3'-5' exonuclease activity of *Escherichia coli* DNA polymerase I: A two metal ion mechanism. *EMBO J.* **1991,** *10* (1), 25-33.

46. Li, Y.; Korolev, S.; Waksman, G., Crystal structures of open and closed forms of binary and ternary complexes of the large fragment of *Thermus aquaticus* DNA polymerase I: Structural basis for nucleotide incorporation. *EMBO J.* **1998,** *17* (24), 7514-25.

47. Christian, T. D.; Romano, L. J.; Rueda, D., Single-molecule measurements of synthesis by DNA polymerase with base-pair resolution. *Proc. Natl. Acad. Sci. U.S.A.* **2009,** *106* (50), 21109-14.

48. Nakamura, T.; Zhao, Y.; Yamagata, Y.; Hua, Y. J.; Yang, W., Watching DNA polymerase eta make a phosphodiester bond. *Nature* **2012,** *487* (7406), 196-201.

49. Kornberg, A.; Baker, T. A., *DNA Replication*. W. H. Freeman: New York, 1992; Vol. 2.

50. Edgell, D. R.; Doolittle, W. F., Archaea and the origin(s) of DNA replication proteins. *Cell* **1997,** *89* (7), 995-998.

51. Hubscher, U.; Nasheuer, H. P.; Syvaoja, J. E., Eukaryotic DNA polymerases, a growing family. *Trends Biochem. Sci.* **2000,** *25* (3), 143-147.

52. Kelman, Z.; O'Donnell, M., DNA polymerase III holoenzyme: Structure and function of a chromosomal replicating machine. *Annu. Rev. Biochem.* **1995,** *64*, 171-200.

53. Studwell-Vaughan, P. S.; O'Donnell, M., DNA polymerase III accessory proteins. V. Theta encoded by holE. *J. Biol. Chem.* **1993,** *268* (16), 11785-11791.

54. Studwell-Vaughan, P. S.; O'Donnell, M., Constitution of the twin polymerase of DNA polymerase III holoenzyme. *J. Biol. Chem.* **1991,** *266* (29), 19833-19841.

55. McInerney, P.; Johnson, A.; Katz, F.; O'Donnell, M., Characterization of a triple DNA polymerase replisome. *Mol. Cell* **2007,** *27* (4), 527-538.

56. Dallmann, H. G.; McHenry, C. S., DnaX complex of *Escherichia coli* DNA polymerase III holoenzyme. *J. Biol. Chem.* **1995,** *270* (49), 29563-29569.

57. Glover, B. P.; Pritchard, A. E.; McHenry, C. S., tau binds and organizes *Escherichia coli* replication proteins through distinct domains: Domain III, shared by gamma and tau, oligomerizes DnaX. *J. Biol. Chem.* **2001,** *276* (38), 35842-6.

58. Stewart, J.; Hingorani, M. M.; Kelman, Z.; O'Donnell, M., Mechanism of beta clamp opening by the delta subunit of *Escherichia coli* DNA polymerase III holoenzyme. *J. Biol. Chem.* **2001,** *276* (22), 19182-19189.

59. Nevin, P.; Gabbai, C. C.; Marians, K. J., Replisome-mediated translesion synthesis by a cellular replicase. *J. Biol. Chem.* **2017,** *292* (33), 13833-13842.

60. Pursell, Z. F.; Isoz, I.; Lundstrom, E. B.; Johansson, E.; Kunkel, T. A., Yeast DNA polymerase epsilon participates in leading-strand DNA replication. *Science* **2007,** *317* (5834), 127-130.

61. Nick McElhinny, S. A.; Gordenin, D. A.; Stith, C. M.; Burgers, P. M.; Kunkel, T. A., Division of labor at the eukaryotic replication fork. *Mol. Cell* **2008,** *30* (2), 137-144.

62. Chilkova, O.; Jonsson, B. H.; Johansson, E., The quaternary structure of DNA polymerase epsilon from *Saccharomyces cerevisiae*. *J. Biol. Chem.* **2003,** *278* (16), 14082-14086.

63. Henninger, E. E.; Pursell, Z. F., DNA polymerase epsilon and its roles in genome stability. *IUBMB Life* **2014,** *66* (5), 339-51.

64. Prindle, M. J.; Loeb, L. A., DNA polymerase delta in DNA replication and genome maintenance. *Environ. Mol. Mutagen.* **2012,** *53* (9), 666-82.

65. Podust, V. N.; Chang, L. S.; Ott, R.; Dianov, G. L.; Fanning, E., Reconstitution of human DNA polymerase delta using recombinant baculoviruses: The p12 subunit potentiates DNA polymerizing activity of the four-subunit enzyme. *J. Biol. Chem.* **2002,** *277* (6), 3894-3901.

66. Eissenberg, J. C.; Ayyagari, R.; Gomes, X. V.; Burgers, P. M., Mutations in yeast proliferating cell nuclear antigen define distinct sites for interaction with DNA polymerase delta and DNA polymerase epsilon. *Mol. Cell. Biol.* **1997,** *17* (11), 6367-78.

67. Yeeles, J. T.; Janska, A.; Early, A.; Diffley, J. F., How the eukaryotic replisome achieves rapid and efficient DNA replication. *Mol. Cell* **2017,** *65* (1), 105-116.

68. Johansson, E.; Garg, P.; Burgers, P. M., The Pol32 subunit of DNA polymerase delta contains separable domains for processive replication and proliferating cell nuclear antigen (PCNA) binding. *J. Biol. Chem.* **2004,** *279* (3), 1907-1915.

69. Koc, K. N.; Stodola, J. L.; Burgers, P. M.; Galletto, R., Regulation of yeast DNA polymerase delta-mediated strand displacement synthesis by 5'-flaps. *Nucleic Acids Res.* **2015,** *43* (8), 4179-90.

70. Stodola, J. L.; Burgers, P. M., Resolving individual steps of Okazaki-fragment maturation at a millisecond timescale. *Nat. Struct. Mol. Biol.* **2016,** *23* (5), 402-8.

71. Grabowski, B.; Kelman, Z., Archeal DNA replication: Eukaryal proteins in a bacterial context. *Annu. Rev. Microbiol.* **2003,** *57*, 487-516.

72. Kelman, Z.; White, M. F., Archaeal DNA replication and repair. *Curr. Opin. Microbiol.* **2005,** *8* (6), 669-676.

73. Beattie, T. R.; Bell, S. D., Molecular machines in archaeal DNA replication. *Curr. Opin. Chem. Biol.* **2011,** *15* (5), 614-9.

74. Pisani, F. M.; De, M. C.; Rossi, M., A DNA polymerase from the archaeon *Sulfolobus solfataricus* shows sequence similarity to family B DNA polymerases. *Nucleic Acids Res.* **1992,** *20* (11), 2711-2716.

75. Yan, J.; Beattie, T. R.; Rojas, A. L.; Schermerhorn, K.; Gristwood, T.; Trinidad, J. C.; Albers, S. V.; Roversi, P.; Gardner, A. F.; Abrescia, N. G. A.; Bell, S. D., Identification and characterization of a heterotrimeric archaeal DNA polymerase holoenzyme. *Nat. Commun.* **2017,** *8*, 15075.

76. Barry, E. R.; Bell, S. D., DNA replication in the archaea. *Microbiol. Mol. Biol. Rev.* **2006,** *70* (4), 876-887.

77. Ohmori, H.; Friedberg, E. C.; Fuchs, R. P.; Goodman, M. F.; Hanaoka, F.; Hinkle, D.; Kunkel, T. A.; Lawrence, C. W.; Livneh, Z.; Nohmi, T.; Prakash, L.; Prakash, S.; Todo, T.; Walker, G. C.; Wang, Z.; Woodgate, R., The Y-family of DNA polymerases. *Mol. Cell* **2001,** *8* (1), 7-8.

78. Reuven, N. B.; Arad, G.; Maor-Shoshani, A.; Livneh, Z., The mutagenesis protein UmuC is a DNA polymerase activated by UmuD', RecA, and SSB and is specialized for translesion replication. *J. Biol. Chem.* **1999,** *274* (45), 31763-6.

79. McDonald, J. P.; Rapic-Otrin, V.; Epstein, J. A.; Broughton, B. C.; Wang, X.; Lehmann, A. R.; Wolgemuth, D. J.; Woodgate, R., Novel human and mouse homologs of *Saccharomyces cerevisiae* DNA polymerase eta. *Genomics* **1999,** *60* (1), 20-30.

80. Wagner, J.; Gruz, P.; Kim, S. R.; Yamada, M.; Matsui, K.; Fuchs, R. P.; Nohmi, T., The dinB gene encodes a novel *E. coli* DNA polymerase, DNA pol IV, involved in mutagenesis. *Mol. Cell* **1999,** *4* (2), 281-6.

81. Boudsocq, F.; Iwai, S.; Hanaoka, F.; Woodgate, R., *Sulfolobus solfataricus* P2 DNA polymerase IV (Dpo4): An archaeal DinB-like DNA polymerase with lesion-bypass properties akin to eukaryotic poleta. *Nucleic Acids Res.* **2001,** *29* (22), 4607-4616.

82. Kulaeva, O. I.; Koonin, E. V.; McDonald, J. P.; Randall, S. K.; Rabinovich, N.; Connaughton, J. F.; Levine, A. S.; Woodgate, R., Identification of a DinB/UmuC homolog in the archeon *Sulfolobus solfataricus*. *Mutat. Res.* **1996,** *357* (1-2), 245-53.

83. Washington, M. T.; Johnson, R. E.; Prakash, L.; Prakash, S., Human DINB1-encoded DNA polymerase kappa is a promiscuous extender of mispaired primer termini. *Proc. Natl. Acad. Sci. U.S.A.* **2002,** *99* (4), 1910-1914.

84. Walker, G. C., Mutagenesis and inducible responses to deoxyribonucleic acid damage in *Escherichia coli*. *Microbiol. Rev.* **1984,** *48* (1), 60-93.

85. Errol, C. F.; Graham, C. W.; Wolfram, S.; Richard, D. W.; Roger, A. S.; Tom, E., *DNA Repair and Mutagenesis, Second Edition*. American Society of Microbiology: 2006.

86. Kreuzer, K. N., DNA damage responses in prokaryotes: Regulating gene expression, modulating growth patterns, and manipulating replication forks. *Cold Spring Harb. Perspect. Biol.* **2013,** *5* (11).

87. Napolitano, R.; Janel-Bintz, R.; Wagner, J.; Fuchs, R. P., All three SOS-inducible DNA polymerases (Pol II, Pol IV and Pol V) are involved in induced mutagenesis. *EMBO J.* **2000,** *19* (22), 6259-65.

88. Gruz, P.; Pisani, F. M.; Shimizu, M.; Yamada, M.; Hayashi, I.; Morikawa, K.; Nohmi, T., Synthetic activity of *Sso* DNA polymerase Y1, an archaeal DinB-like DNA polymerase, is stimulated by processivity factors proliferating cell nuclear antigen and replication factor C. *J. Biol. Chem.* **2001,** *276* (50), 47394-47401.

89. Ling, H.; Boudsocq, F.; Woodgate, R.; Yang, W., Crystal structure of a Y-family DNA polymerase in action: A mechanism for error-prone and lesion-bypass replication. *Cell* **2001,** *107* (1), 91-102.

90. Silvian, L. F.; Toth, E. A.; Pham, P.; Goodman, M. F.; Ellenberger, T., Crystal structure of a DinB family error-prone DNA polymerase from *Sulfolobus solfataricus*. *Nat. Struct. Biol.* **2001,** *8* (11), 984-989.

91. Zhou, B. L.; Pata, J. D.; Steitz, T. A., Crystal structure of a DinB lesion bypass DNA polymerase catalytic fragment reveals a classic polymerase catalytic domain. *Mol. Cell* **2001,** *8* (2), 427-437.

92. Kokoska, R. J.; Bebenek, K.; Boudsocq, F.; Woodgate, R.; Kunkel, T. A., Low fidelity DNA synthesis by a Y-family DNA polymerase due to misalignment in the active site. *J. Biol. Chem.* **2002,** *277* (22), 19633-19638.

93. Gruz, P.; Shimizu, M.; Pisani, F. M.; De, F. M.; Kanke, Y.; Nohmi, T., Processing of DNA lesions by archaeal DNA polymerases from *Sulfolobus solfataricus*. *Nucleic Acids Res.* **2003,** *31* (14), 4024-4030.

94. Jarosz, D. F.; Beuning, P. J.; Cohen, S. E.; Walker, G. C., Y-family DNA polymerases in *Escherichia coli*. *Trends Microbiol.* **2007,** *15* (2), 70-7.

95. Prakash, S.; Johnson, R. E.; Prakash, L., Eukaryotic translesion synthesis DNA polymerases: Specificity of structure and function. *Annu. Rev. Biochem.* **2005,** *74*, 317-353.

96. Trincao, J.; Johnson, R. E.; Escalante, C. R.; Prakash, S.; Prakash, L.; Aggarwal, A. K., Structure of the catalytic core of *S. cerevisiae* DNA polymerase eta: Implications for translesion DNA synthesis. *Mol. Cell* **2001,** *8* (2), 417-26.

97. Yang, W.; Woodgate, R., What a difference a decade makes: Insights into translesion DNA synthesis. *Proc. Natl. Acad. Sci. U.S.A.* **2007,** *104* (40), 15591-8.

98. Waters, L. S.; Minesinger, B. K.; Wiltrout, M. E.; D'Souza, S.; Woodruff, R. V.; Walker, G. C., Eukaryotic translesion polymerases and their roles and regulation in DNA damage tolerance. *Microbiol. Mol. Biol. Rev.* **2009,** *73* (1), 134-54.

99. Pata, J. D., Structural diversity of the Y-family DNA polymerases. *Biochim. Biophys. Acta* **2010,** *1804* (5), 1124-1135.

100. Wilson, R. C.; Jackson, M. A.; Pata, J. D., Y-family polymerase conformation is a major determinant of fidelity and translesion specificity. *Structure* **2013,** *21* (1), 20-31.

101. Johnson, R. E.; Washington, M. T.; Haracska, L.; Prakash, S.; Prakash, L., Eukaryotic polymerases iota and zeta act sequentially to bypass DNA lesions. *Nature* **2000,** *406* (6799), 1015-1019.

102. Acharya, N.; Johnson, R. E.; Prakash, S.; Prakash, L., Complex formation with Rev1 enhances the proficiency of *Saccharomyces cerevisiae* DNA polymerase zeta for mismatch extension and for extension opposite from DNA lesions. *Mol. Cell Biol.* **2006,** *26* (24), 9555-9563.

103. Paz-Elizur, T.; Takeshita, M.; Goodman, M.; O'Donnell, M.; Livneh, Z., Mechanism of translesion DNA synthesis by DNA polymerase II. Comparison to DNA polymerases I and III core. *J. Biol. Chem.* **1996,** *271* (40), 24662-24669.

104. Yamtich, J.; Sweasy, J. B., DNA polymerase family X: Function, structure, and cellular roles. *Biochim. Biophys. Acta.* **2010,** *1804* (5), 1136-50.

105. Moon, A. F.; Garcia-Diaz, M.; Batra, V. K.; Beard, W. A.; Bebenek, K.; Kunkel, T. A.; Wilson, S. H.; Pedersen, L. C., The X family portrait: Structural insights into biological functions of X family polymerases. *DNA Repair* **2007,** *6* (12), 1709-1725.

106. Garcia-Gomez, S.; Reyes, A.; Martinez-Jimenez, M. I.; Chocron, E. S.; Mouron, S.; Terrados, G.; Powell, C.; Salido, E.; Mendez, J.; Holt, I. J.; Blanco, L., PrimPol, an archaic primase/polymerase operating in human cells. *Mol. Cell* **2013,** *52* (4), 541-53.

107. Jozwiakowski, S. K.; Borazjani Gholami, F.; Doherty, A. J., Archaeal replicative primases can perform translesion DNA synthesis. *Proc. Natl. Acad. Sci. U.S.A.* **2015,** *112* (7), E633-8.

108. Guilliam, T. A.; Doherty, A. J., PrimPol-prime time to reprime. *Genes (Basel)* **2017,** *8* (1).

109. Mouron, S.; Rodriguez-Acebes, S.; Martinez-Jimenez, M. I.; Garcia-Gomez, S.; Chocron, S.; Blanco, L.; Mendez, J., Repriming of DNA synthesis at stalled replication forks by human PrimPol. *Nat. Struct. Mol. Biol.* **2013,** *20* (12), 1383-9.

110. Guilliam, T. A.; Brissett, N. C.; Ehlinger, A.; Keen, B. A.; Kolesar, P.; Taylor, E. M.; Bailey, L. J.; Lindsay, H. D.; Chazin, W. J.; Doherty, A. J., Molecular basis for PrimPol recruitment to replication forks by RPA. *Nat. Commun.* **2017,** *8*, 15222.

111. Rechkoblit, O.; Gupta, Y. K.; Malik, R.; Rajashankar, K. R.; Johnson, R. E.; Prakash, L.; Prakash, S.; Aggarwal, A. K., Structure and mechanism of human PrimPol, a DNA polymerase with primase activity. *Sci. Adv.* **2016,** *2* (10), e1601317.

112. Guilliam, T. A.; Jozwiakowski, S. K.; Ehlinger, A.; Barnes, R. P.; Rudd, S. G.; Bailey, L. J.; Skehel, J. M.; Eckert, K. A.; Chazin, W. J.; Doherty, A. J., Human PrimPol is a highly error-prone polymerase regulated by single-stranded DNA binding proteins. *Nucleic Acids Res.* **2015,** *43* (2), 1056-68.

113. Martinez-Jimenez, M. I.; Lahera, A.; Blanco, L., Human PrimPol activity is enhanced by RPA. *Sci. Rep.* **2017,** *7*.

114. Eoff, R. L.; Choi, J. Y.; Guengerich, F. P., Mechanistic studies with DNA polymerases reveal complex outcomes following bypass of DNA damage. *J. Nucleic Acids* **2010,** *2010*.

115. Boiteux, S.; Guillet, M., Abasic sites in DNA: Repair and biological consequences in *Saccharomyces cerevisiae*. *DNA Repair* **2004,** *3* (1), 1-12.

116. Lindahl, T., Instability and decay of the primary structure of DNA. *Nature* **1993,** *362* (6422), 709-715.

117. Strauss, B. S., The "A" rule revisited: Polymerases as determinants of mutational specificity. *DNA Repair* **2002,** *1* (2), 125-35.

118. Sagher, D.; Strauss, B., Insertion of nucleotides opposite apurinic/apyrimidinic sites in deoxyribonucleic acid during in vitro synthesis: Uniqueness of adenine nucleotides. *Biochemistry* **1983,** *22* (19), 4518-26.

119. Shibutani, S.; Takeshita, M.; Grollman, A. P., Translesional synthesis on DNA templates containing a single abasic site. A mechanistic study of the "A rule". *J. Biol. Chem.* **1997,** *272* (21), 13916-22.

120. Zerbe, L. K.; Goodman, M. F.; Efrati, E.; Kuchta, R. D., Abasic template lesions are strong chain terminators for DNA primase but not for DNA polymerase alpha during the synthesis of new DNA strands. *Biochemistry* **1999,** *38* (39), 12908-12914.

121. Nair, D. T.; Johnson, R. E.; Prakash, L.; Prakash, S.; Aggarwal, A. K., Rev1 employs a novel mechanism of DNA synthesis using a protein template. *Science* **2005,** *309* (5744), 2219-2222.

122. Ling, H.; Boudsocq, F.; Woodgate, R.; Yang, W., Snapshots of replication through an abasic lesion; structural basis for base substitutions and frameshifts. *Mol. Cell* **2004,** *13* (5), 751-762.

123. Fiala, K. A.; Suo, Z., Sloppy bypass of an abasic lesion catalyzed by a Y-family DNA polymerase. *J. Biol. Chem.* **2007,** *282* (11), 8199-206.

124. Fiala, K. A.; Hypes, C. D.; Suo, Z., Mechanism of abasic lesion bypass catalyzed by a Y-family DNA polymerase. *J. Biol. Chem.* **2007,** *282* (11), 8188-98.

125. Goodman, M. F.; Woodgate, R., The biochemical basis and in vivo regulation of SOS-induced mutagenesis promoted by *Escherichia coli* DNA polymerase V (UmuD'2C). *Cold Spring Harb. Symp. Quant. Biol.* **2000,** *65*, 31-40.

126. Walsh, J. M.; Hawver, L. A.; Beuning, P. J., *Escherichia coli* Y family DNA polymerases. *Front. Biosci.* **2011,** *16*, 3164-82.

127. Tang, M.; Pham, P.; Shen, X.; Taylor, J. S.; O'Donnell, M.; Woodgate, R.; Goodman, M. F., Roles of *E. coli* DNA polymerases IV and V in lesion-targeted and untargeted SOS mutagenesis. *Nature* **2000,** *404* (6781), 1014-1018.

128. Jarosz, D. F.; Godoy, V. G.; Delaney, J. C.; Essigmann, J. M.; Walker, G. C., A single amino acid governs enhanced activity of DinB DNA polymerases on damaged templates. *Nature* **2006,** *439* (7073), 225-228.

129. Wang, Y. S.; Yuan, B. F.; Cao, H. C.; Jiang, Y.; Wang, J. S., Efficient and accurate bypass of a minor-groove DNA adduct by DinB DNA polymerase *in vitro* and *in vivo*. *Chem. Res. Toxicol.* **2008,** *21* (12), 2452-2452.

130. Ikeda, M.; Furukohri, A.; Philippin, G.; Loechler, E.; Akiyama, M. T.; Katayama, T.; Fuchs, R. P.; Maki, H., DNA polymerase IV mediates efficient and quick recovery of replication forks stalled at N2-dG adducts. *Nucleic Acids Res.* **2014,** *42* (13), 8461-72.

131. Becherel, O. J.; Fuchs, R. P., Mechanism of DNA polymerase II-mediated frameshift mutagenesis. *Proc. Natl. Acad. Sci. U.S.A.* **2001,** *98* (15), 8566-71.

132. Fiala, K. A.; Suo, Z., Mechanism of DNA polymerization catalyzed by *Sulfolobus solfataricus* P2 DNA polymerase IV. *Biochemistry* **2004,** *43* (7), 2116-25.

133. Eoff, R. L.; Sanchez-Ponce, R.; Guengerich, F. P., Conformational changes during nucleotide selection by *Sulfolobus solfataricus* DNA polymerase Dpo4. *J. Biol. Chem.* **2009,** *284* (31), 21090-21099.

134. Maxwell, B. A.; Suo, Z., Kinetic basis for the differing response to an oxidative lesion by a replicative and a lesion bypass DNA polymerase from *Sulfolobus solfataricus*. *Biochemistry* **2012,** *51* (16), 3485-96.

135. Sholder, G.; Creech, A.; Loechler, E. L., How Y-Family DNA polymerase IV is more accurate than Dpo4 at dCTP insertion opposite an N2-dG adduct of benzo[a]pyrene. *DNA Repair* **2015,** *35*, 144-53.

136. Walsh, J. M.; Ippoliti, P. J.; Ronayne, E. A.; Rozners, E.; Beuning, P. J., Discrimination against major groove adducts by Y-family polymerases of the DinB subfamily. *DNA Repair* **2013,** *12* (9), 713-22.

137. Washington, M. T.; Johnson, R. E.; Prakash, S.; Prakash, L., Accuracy of thymine-thymine dimer bypass by *Saccharomyces cerevisiae* DNA polymerase eta. *Proc. Natl. Acad. Sci. U.S.A.* **2000,** *97* (7), 3094-3099.

138. Johnson, R. E.; Washington, M. T.; Prakash, S.; Prakash, L., Fidelity of human DNA polymerase eta. *J. Biol. Chem.* **2000,** *275* (11), 7447-7450.

139. Johnson, R. E.; Haracska, L.; Prakash, S.; Prakash, L., Role of DNA polymerase eta in the bypass of a (6-4) TT photoproduct. *Mol. Cell. Biol.* **2001,** *21* (10), 3558-63.

140. Ogi, T.; Lehmann, A. R., The Y-family DNA polymerase kappa (pol kappa) functions in mammalian nucleotide-excision repair. *Nat. Cell Biol.* **2006,** *8* (6), 640-2.

141. Zhang, Y.; Yuan, F.; Wu, X.; Wang, M.; Rechkoblit, O.; Taylor, J. S.; Geacintov, N. E.; Wang, Z., Error-free and error-prone lesion bypass by human DNA polymerase kappa *in vitro*. *Nucleic Acids Res.* **2000,** *28* (21), 4138-46.

142. Choi, J. Y.; Angel, K. C.; Guengerich, F. P., Translesion synthesis across bulky N2-alkyl guanine DNA adducts by human DNA polymerase kappa. *J. Biol. Chem.* **2006,** *281* (30), 21062-21072.

143. Ohashi, E.; Murakumo, Y.; Kanjo, N.; Akagi, J.; Masutani, C.; Hanaoka, F.; Ohmori, H., Interaction of hREV1 with three human Y-family DNA polymerases. *Genes Cells* **2004,** *9* (6), 523-31.

144. Guo, C.; Sonoda, E.; Tang, T. S.; Parker, J. L.; Bielen, A. B.; Takeda, S.; Ulrich, H. D.; Friedberg, E. C., REV1 protein interacts with PCNA: Significance of the REV1 BRCT domain *in vitro* and *in vivo*. *Mol. Cell* **2006,** *23* (2), 265-71.

145. Boehm, E. M.; Washington, M. T., R.I.P. to the PIP: PCNA-binding motif no longer considered specific: PIP motifs and other related sequences are not distinct entities and can bind multiple proteins involved in genome maintenance. *Bioessays* **2016,** *38* (11), 1117-1122.

146. Nelson, J. R.; Lawrence, C. W.; Hinkle, D. C., Deoxycytidyl transferase activity of yeast REV1 protein. *Nature* **1996,** *382* (6593), 729-31.

147. Haracska, L.; Unk, I.; Johnson, R. E.; Johansson, E.; Burgers, P. M.; Prakash, S.; Prakash, L., Roles of yeast DNA polymerases delta and zeta and of Rev1 in the bypass of abasic sites. *Genes Dev.* **2001,** *15* (8), 945-954.

148. Lawrence, C. W., Cellular functions of DNA polymerase zeta and Rev1 protein. *Adv. Protein Chem.* **2004,** *69*, 167-203.

149. Guo, C.; Tang, T. S.; Bienko, M.; Parker, J. L.; Bielen, A. B.; Sonoda, E.; Takeda, S.; Ulrich, H. D.; Dikic, I.; Friedberg, E. C., Ubiquitin-binding motifs in REV1 protein are required for its role in the tolerance of DNA damage. *Mol. Cell. Biol.* **2006,** *26* (23), 8892-900.

150. Ogi, T.; Kato, T., Jr.; Kato, T.; Ohmori, H., Mutation enhancement by DINB1, a mammalian homologue of the *Escherichia coli* mutagenesis protein dinB. *Genes Cells* **1999,** *4* (11), 607-18.

151. O-Wang, J.; Kawamura, K.; Tada, Y.; Ohmori, H.; Kimura, H.; Sakiyama, S.; Tagawa, M., DNA polymerase kappa, implicated in spontaneous and DNA damage-induced mutagenesis, is overexpressed in lung cancer. *Cancer Res.* **2001,** *61* (14), 5366-5369.

152. Albertella, M. R.; Lau, A.; O'Connor, M. J., The overexpression of specialized DNA polymerases in cancer. *DNA Repair* **2005,** *4* (5), 583-93.

153. Knobel, P. A.; Marti, T. M., Translesion DNA synthesis in the context of cancer research. *Cancer Cell Int.* **2011,** *11*.

154. Mukhopadhyay, S.; Clark, D. R.; Watson, N. B.; Zacharias, W.; McGregor, W. G., REV1 accumulates in DNA damage-induced nuclear foci in human cells and is implicated in mutagenesis by benzo[a]pyrenediolepoxide. *Nucleic Acids Res.* **2004,** *32* (19), 5820-5826.

155. Tissier, A.; Kannouche, P.; Reck, M. P.; Lehmann, A. R.; Fuchs, R. P.; Cordonnier, A., Co-localization in replication foci and interaction of human Y-family members, DNA polymerase pol eta and REVl protein. *DNA Repair* **2004,** *3* (11), 1503-14.

156. Bergoglio, V.; Bavoux, C.; Verbiest, V.; Hoffmann, J. S.; Cazaux, C., Localisation of human DNA polymerase kappa to replication foci. *J. Cell Sci.* **2002,** *115* (23), 4413-4418.

157. Kannouche, P. L.; Wing, J.; Lehmann, A. R., Interaction of human DNA polymerase eta with monoubiquitinated PCNA: A possible mechanism for the polymerase switch in response to DNA damage. *Mol. Cell* **2004,** *14* (4), 491-500.

158. Kannouche, P.; Fernandez de Henestrosa, A. R.; Coull, B.; Vidal, A. E.; Gray, C.; Zicha, D.; Woodgate, R.; Lehmann, A. R., Localization of DNA polymerases eta and iota to the replication machinery is tightly co-ordinated in human cells. *EMBO J.* **2003,** *22* (5), 1223-1233.

159. Sutton, M. D.; Opperman, T.; Walker, G. C., The *Escherichia coli* SOS mutagenesis proteins UmuD and UmuD' interact physically with the replicative DNA polymerase. *Proc. Natl. Acad. Sci. U.S.A.* **1999,** *96* (22), 12373-8.

160. Murison, D. A.; Ollivierre, J. N.; Huang, Q.; Budil, D. E.; Beuning, P. J., Altering the N-terminal arms of the polymerase manager protein UmuD modulates protein interactions. *PLoS One* **2017,** *12* (3), e0173388.

161. Chaurasiya, K. R.; Ruslie, C.; Silva, M. C.; Voortman, L.; Nevin, P.; Lone, S.; Beuning, P. J.; Williams, M. C., Polymerase manager protein UmuD directly regulates *Escherichia coli* DNA polymerase III alpha binding to ssDNA. *Nucleic Acids Res.* **2013,** *41* (19), 8959-68.

162. Indiani, C.; McInerney, P.; Georgescu, R.; Goodman, M. F.; O'Donnell, M., A sliding-clamp toolbelt binds high- and low-fidelity DNA polymerases simultaneously. *Mol. Cell* **2005,** *19* (6), 805-815.

163. Furukohri, A.; Goodman, M. F.; Maki, H., A dynamic polymerase exchange with *Escherichia coli* DNA polymerase IV replacing DNA polymerase III on the sliding clamp. *J. Biol. Chem.* **2008,** *283* (17), 11260-9.

164. Scotland, M. K.; Heltzel, J. M.; Kath, J. E.; Choi, J. S.; Berdis, A. J.; Loparo, J. J.; Sutton, M. D., A genetic selection for dinB mutants reveals an interaction between DNA polymerase IV and the replicative polymerase that is required for translesion synthesis. *PLoS Genet.* **2015,** *11* (9), e1005507.

165. Kath, J. E.; Chang, S.; Scotland, M. K.; Wilbertz, J. H.; Jergic, S.; Dixon, N. E.; Sutton, M. D.; Loparo, J. J., Exchange between *Escherichia coli* polymerases II and III on a processivity clamp. *Nucleic Acids Res.* **2016,** *44* (4), 1681-90.

166. Guo, C.; Fischhaber, P. L.; Luk-Paszyc, M. J.; Masuda, Y.; Zhou, J.; Kamiya, K.; Kisker, C.; Friedberg, E. C., Mouse Rev1 protein interacts with multiple DNA polymerases involved in translesion DNA synthesis. *EMBO J.* **2003,** *22* (24), 6621-6630.

167. Friedberg, E. C.; Lehmann, A. R.; Fuchs, R. P., Trading places: How do DNA polymerases switch during translesion DNA synthesis? *Mol. Cell* **2005,** *18* (5), 499-505.

168. Johnson, R. E.; Prakash, L.; Prakash, S., Pol31 and Pol32 subunits of yeast DNA polymerase delta are also essential subunits of DNA polymerase zeta. *Proc. Natl. Acad. Sci. U.S.A.* **2012,** *109* (31), 12455-60.

169. Makarova, A. V.; Stodola, J. L.; Burgers, P. M., A four-subunit DNA polymerase zeta complex containing Pol delta accessory subunits is essential for PCNA-mediated mutagenesis. *Nucleic Acids Res.* **2012,** *40* (22), 11618-26.

170. Lin, H. K.; Chase, S. F.; Laue, T. M.; Jen-Jacobson, L.; Trakselis, M. A., Differential temperature-dependent multimeric assemblies of replication and repair polymerases on DNA increase processivity. *Biochemistry* **2012,** *51* (37), 7367-82.

171. De Felice, M.; Medagli, B.; Esposito, L.; De Falco, M.; Pucci, B.; Rossi, M.; Gruz, P.; Nohmi, T.; Pisani, F. M., Biochemical evidence of a physical interaction between *Sulfolobus solfataricus* B-family and Y-family DNA polymerases. *Extremophiles* **2007,** *11* (2), 277-282.

172. Dionne, I.; Nookala, R. K.; Jackson, S. P.; Doherty, A. J.; Bell, S. D., A heterotrimeric PCNA in the hyperthermophilic archaeon *Sulfolobus solfataricus*. *Mol. Cell* **2003,** *11* (1), 275-282.

173. Williams, G. J.; Johnson, K.; Rudolf, J.; McMahon, S. A.; Carter, L.; Oke, M.; Liu, H.; Taylor, G. L.; White, M. F.; Naismith, J. H., Structure of the heterotrimeric PCNA from *Sulfolobus solfataricus*. *Acta Crystallogr. F* **2006,** *62* (Pt 10), 944-948.

174. Xing, G.; Kirouac, K.; Shin, Y. J.; Bell, S. D.; Ling, H., Structural insight into recruitment of translesion DNA polymerase Dpo4 to sliding clamp PCNA. *Mol. Microbiol.* **2009,** *71* (3), 678-691.

175. Mayanagi, K.; Kiyonari, S.; Nishida, H.; Saito, M.; Kohda, D.; Ishino, Y.; Shirai, T.; Morikawa, K., Architecture of the DNA polymerase B-proliferating cell nuclear antigen (PCNA)-DNA ternary complex. *Proc. Natl. Acad. Sci. U.S.A.* **2011**.

176. Bauer, R. J.; Wolff, I. D.; Zuo, X.; Lin, H. K.; Trakselis, M. A., Assembly and distributive action of an archaeal DNA polymerase holoenzyme. *J. Mol. Biol.* **2013,** *425* (23), 4820-4836.

177. Cranford, M. T.; Chu, A. M.; Baguley, J. K.; Bauer, R. J.; Trakselis, M. A., Characterization of a coupled DNA replication and translesion synthesis polymerase supraholoenzyme from archaea. *Nucleic Acids Res.* **2017,** *45* (14), 8329-8340.

178. Boehm, E. M.; Spies, M.; Washington, M. T., PCNA tool belts and polymerase bridges form during translesion synthesis. *Nucleic Acids Res.* **2016,** *44* (17), 8250-60.

179. Zhang, L.; Brown, J. A.; Newmister, S. A.; Suo, Z., Polymerization fidelity of a replicative DNA polymerase from the hyperthermophilic archaeon *Sulfolobus solfataricus* P2. *Biochemistry* **2009,** *48* (31), 7492-501.

180. Choi, J. Y.; Eoff, R. L.; Pence, M. G.; Wang, J.; Martin, M. V.; Kim, E. J.; Folkmann, L. M.; Guengerich, F. P., Roles of the four DNA polymerases of the crenarchaeon *Sulfolobus solfataricus* and accessory proteins in DNA replication. *J. Biol. Chem.* **2011,** *286* (36), 31180-93.

181. Xing, X.; Zhang, L.; Guo, L.; She, Q.; Huang, L., *Sulfolobus replication* factor C stimulates the activity of DNA polymerase B1. *J. Bacteriol.* **2014,** *196* (13), 2367-75.

182. Hedglin, M.; Benkovic, S. J., Eukaryotic translesion DNA synthesis on the leading and lagging strands: Unique detours around the same obstacle. *Chem. Rev.* **2017**.

183. Sabatinos, S. A.; Forsburg, S. L., Managing single-stranded DNA during replication stress in fission yeast. *Biomolecules* **2015,** *5* (3), 2123-39.

184. Cimprich, K. A.; Cortez, D., ATR: An essential regulator of genome integrity. *Nat. Rev. Mol. Cell Biol.* **2008,** *9* (8), 616-27.

185. Edenberg, E. R.; Downey, M.; Toczyski, D., Polymerase stalling during replication, transcription and translation. *Curr. Biol.* **2014,** *24* (10), R445-52.

186. Techer, H.; Koundrioukoff, S.; Nicolas, A.; Debatisse, M., The impact of replication stress on replication dynamics and DNA damage in vertebrate cells. *Nat. Rev. Genet.* **2017,** *18* (9), 535-550.

187. Yeeles, J. T.; Poli, J.; Marians, K. J.; Pasero, P., Rescuing stalled or damaged replication forks. *Cold Spring Harb. Perspect. Biol.* **2013,** *5* (5), a012815.

188. McGlynn, P.; Lloyd, R. G., Recombinational repair and restart of damaged replication forks. *Nat. Rev. Mol. Cell Biol.* **2002,** *3* (11), 859-70.

189. Berti, M.; Vindigni, A., Replication stress: Getting back on track. *Nat. Struct. Mol. Biol.* **2016,** *23* (2), 103-9.

190. Ghosal, G.; Chen, J., DNA damage tolerance: A double-edged sword guarding the genome. *Transl. Cancer Res.* **2013,** *2* (3), 107-129.

191. Chang, D. J.; Cimprich, K. A., DNA damage tolerance: When it's OK to make mistakes. *Nat. Chem. Biol.* **2009,** *5* (2), 82-90.

192. Bi, X., Mechanism of DNA damage tolerance. *World J. Biol. Chem.* **2015,** *6* (3), 48-56.

193. Zhao, L.; Washington, M. T., Translesion synthesis: Insights into the selection and switching of DNA polymerases. *Genes (Basel)* **2017,** *8* (1).

194. Branzei, D.; Foiani, M., Maintaining genome stability at the replication fork. *Nat. Rev. Mol. Cell Biol.* **2010,** *11* (3), 208-19.

195. Klarer, A. C.; McGregor, W., Replication of damaged genomes. *Crit. Rev. Eukaryot. Gene Expr.* **2011,** *21* (4), 323-36.

196. Lehmann, A. R., Replication of damaged DNA by translesion synthesis in human cells. *FEBS letters* **2005,** *579* (4), 873-6.

197. Xu, X.; Yan, C.; Kossmann, B. R.; Ivanov, I., Secondary interaction interfaces with PCNA control conformational switching of DNA polymerase PolB from polymerization to editing. *J. Phys. Chem. B* **2016,** *120* (33), 8379-88.

198. Nishida, H.; Mayanagi, K.; Kiyonari, S.; Sato, Y.; Oyama, T.; Ishino, Y.; Morikawa, K., Structural determinant for switching between the polymerase and exonuclease modes in the PCNA-replicative DNA polymerase complex. *Proc. Natl. Acad. Sci. U.S.A.* **2009,** *106* (49), 20693-8.

199. Ishmael, F. T.; Trakselis, M. A.; Benkovic, S. J., Protein-protein interactions in the bacteriophage T4 replisome. The leading strand holoenzyme is physically linked to the lagging strand holoenzyme and the primosome. *J. Biol. Chem.* **2003,** *278* (5), 3145-52.

200. Zhang, Y.; Baranovskiy, A. G.; Tahirov, T. H.; Pavlov, Y. I., The C-terminal domain of the DNA polymerase catalytic subunit regulates the primase and polymerase activities of the human DNA polymerase alpha-primase complex. *J. Biol. Chem.* **2014,** *289* (32), 22021-34.

201. Lujan, S. A.; Williams, J. S.; Kunkel, T. A., DNA polymerases divide the labor of genome replication. *Trends Cell Biol.* **2016,** *26* (9), 640-54.

202. Hedglin, M.; Pandey, B.; Benkovic, S. J., Characterization of human translesion DNA synthesis across a UV-induced DNA lesion. *Elife* **2016,** *5*.

203. Shapiro, R. S., Antimicrobial-induced DNA damage and genomic instability in microbial pathogens. *Plos Pathog.* **2015,** *11* (3).

204. Ippoliti, P. J.; Delateur, N. A.; Jones, K. M.; Beuning, P. J., Multiple strategies for translesion synthesis in bacteria. *Cells* **2012,** *1* (4), 799-831.

205. Culyba, M. J.; Mo, C. Y.; Kohli, R. M., Targets for combating the evolution of acquired antibiotic resistance. *Biochemistry* **2015,** *54* (23), 3573-3582.

206. Georgescu, R. E.; Yao, N.; Indiani, C.; Yurieva, O.; O'Donnell, M. E., Replisome mechanics: Lagging strand events that influence speed and processivity. *Nucleic Acids Res.* **2014,** *42* (10), 6497-510.

207. Tanner, N. A.; Hamdan, S. M.; Jergic, S.; Schaeffer, P. M.; Dixon, N. E.; van Oijen, A. M., Single-molecule studies of fork dynamics in *Escherichia coli* DNA replication. *Nat. Struct. Mol. Biol.* **2008,** *15* (2), 170-176.

208. Liao, Y.; Li, Y. L.; Schroeder, J. W.; Simmons, L. A.; Biteen, J. S., Single-molecule DNA polymerase dynamics at a bacterial replisome in live cells. *Biophys. J.* **2016,** *111* (12), 2562-2569.

209. Hu, Z.; Perumal, S. K.; Yue, H.; Benkovic, S. J., The human lagging strand DNA polymerase delta holoenzyme is distributive. *J. Biol. Chem.* **2012,** *287* (46), 38442-8.

210. Hedglin, M.; Pandey, B.; Benkovic, S. J., Stability of the human polymerase delta holoenzyme and its implications in lagging strand DNA synthesis. *Proc. Natl. Acad. Sci. U.S.A.* **2016,** *113* (13), E1777-86.

211. Kim, S.; Dallmann, H. G.; McHenry, C. S.; Marians, K. J., Coupling of a replicative polymerase and helicase: A tau-DnaB interaction mediates rapid replication fork movement. *Cell* **1996,** *84* (4), 643-650.

212. Zhang, H.; Lee, S. J.; Zhu, B.; Tran, N. Q.; Tabor, S.; Richardson, C. C., Helicase-DNA polymerase interaction is critical to initiate leading-strand DNA synthesis. *Proc. Natl. Acad. Sci. U.S.A.* **2011,** *108* (23), 9372-7.

213. Pandey, M.; Patel, S. S., Helicase and polymerase move together close to the fork junction and copy DNA in one-nucleotide steps. *Cell Rep.* **2014,** *6* (6), 1129-38.

214. Georgescu, R.; Yuan, Z.; Bai, L.; de Luna Almeida Santos, R.; Sun, J.; Zhang, D.; Yurieva, O.; Li, H.; O'Donnell, M. E., Structure of eukaryotic CMG helicase at a replication fork and implications to replisome architecture and origin initiation. *Proc. Natl. Acad. Sci. U.S.A.* **2017,** *114* (5), E697-E706.

215. Sun, J.; Yuan, Z.; Georgescu, R.; Li, H.; O'Donnell, M., The eukaryotic CMG helicase pumpjack and integration into the replisome. *Nucleus* **2016,** *7* (2), 146-54.

216. Sun, J.; Shi, Y.; Georgescu, R. E.; Yuan, Z.; Chait, B. T.; Li, H.; O'Donnell, M. E., The architecture of a eukaryotic replisome. *Nat. Struct. Mol. Biol.* **2015**.

217. Langston, L. D.; Zhang, D.; Yurieva, O.; Georgescu, R. E.; Finkelstein, J.; Yao, N. Y.; Indiani, C.; O'Donnell, M. E., CMG helicase and DNA polymerase epsilon form a functional 15-subunit holoenzyme for eukaryotic leading-strand DNA replication. *Proc. Natl. Acad. Sci. U.S.A.* **2014,** *111* (43), 15390-5.

218. Plosky, B. S.; Woodgate, R., Switching from high-fidelity replicases to low-fidelity lesion-bypass polymerases. *Curr. Opin. Genet. Dev.* **2004,** *14* (2), 113-119.

219. Uchida, K.; Furukohri, A.; Shinozaki, Y.; Mori, T.; Ogawara, D.; Kanaya, S.; Nohmi, T.; Maki, H.; Akiyama, M., Overproduction of *Escherichia coli* DNA polymerase DinB (Pol IV) inhibits replication fork progression and is lethal. *Mol. Microbiol.* **2008,** *70* (3), 608-22.

220. Yuan, Q.; Dohrmann, P. R.; Sutton, M. D.; McHenry, C. S., DNA polymerase III, but not polymerase IV, must be bound to a tau-containing DnaX complex to enable exchange into replication forks. *J. Biol. Chem.* **2016,** *291* (22), 11727-35.

221. Dohrmann, P. R.; Correa, R.; Frisch, R. L.; Rosenberg, S. M.; McHenry, C. S., The DNA polymerase III holoenzyme contains gamma and is not a trimeric polymerase. *Nucleic Acids Res.* **2016,** *44* (3), 1285-97.

222. Sutton, M. D.; Duzen, J. M.; Scouten Ponticelli, S. K., A single hydrophobic cleft in the *Escherichia coli* processivity clamp is sufficient to support cell viability and DNA damage-induced mutagenesis *in vivo*. *BMC Mol. Biol.* **2010,** *11*, 102.

223. Sutton, M. D.; Farrow, M. F.; Burton, B. M.; Walker, G. C., Genetic interactions between the *Escherichia coli* umuDC gene products and the beta processivity clamp of the replicative DNA polymerase. *J. Bacteriol.* **2001,** *183* (9), 2897-909.

224. Robinson, A.; McDonald, J. P.; Caldas, V. E.; Patel, M.; Wood, E. A.; Punter, C. M.; Ghodke, H.; Cox, M. M.; Woodgate, R.; Goodman, M. F.; van Oijen, A. M., Regulation of mutagenic DNA polymerase V activation in space and time. *PLoS Genet.* **2015,** *11* (8), e1005482.

225. Beattie, T. R.; Bell, S. D., Coordination of multiple enzyme activities by a single PCNA in archaeal Okazaki fragment maturation. *EMBO J.* **2012,** *31* (6), 1556-67.

226. Aberg, C.; Duderstadt, K. E.; van Oijen, A. M., Stability versus exchange: A paradox in DNA replication. *Nucleic Acids Res.* **2016,** *44* (10), 4846-54.

227. Nossal, N. G.; Makhov, A. M.; Chastain, P. D., 2nd; Jones, C. E.; Griffith, J. D., Architecture of the bacteriophage T4 replication complex revealed with nanoscale biopointers. *J. Biol. Chem.* **2007,** *282* (2), 1098-108.

228. Tanner, N. A.; Tolun, G.; Loparo, J. J.; Jergic, S.; Griffith, J. D.; Dixon, N. E.; van Oijen, A. M., *E. coli* DNA replication in the absence of free beta clamps. *EMBO J.* **2011,** *30* (9), 1830-40.

229. Reyes-Lamothe, R.; Sherratt, D. J.; Leake, M. C., Stoichiometry and architecture of active DNA replication machinery in *Escherichia coli*. *Science* **2010,** *328* (5977), 498-501.

230. Hedglin, M.; Benkovic, S. J., Regulation of Rad6/Rad18 activity during DNA damage tolerance. *Annu. Rev. Biophys.* **2015,** *44*, 207-28.

231. Ulrich, H. D., Protein-protein interactions within an E2-RING finger complex. Implications for ubiquitin-dependent DNA damage repair. *J. Biol. Chem.* **2003,** *278* (9), 7051-8.

232. Skoneczna, A.; McIntyre, J.; Skoneczny, M.; Policinska, Z.; Sledziewska-Gojska, E., Polymerase eta is a short-lived, proteasomally degraded protein that is temporarily stabilized following UV irradiation in *Saccharomyces cerevisiae*. *J. Mol. Biol.* **2007,** *366* (4), 1074-86.

233. Masuda, Y.; Kanao, R.; Kaji, K.; Ohmori, H.; Hanaoka, F.; Masutani, C., Different types of interaction between PCNA and PIP boxes contribute to distinct cellular functions of Y-family DNA polymerases. *Nucleic Acids Res.* **2015,** *43* (16), 7898-910.

234. Plosky, B. S.; Vidal, A. E.; Fernandez de Henestrosa, A. R.; McLenigan, M. P.; McDonald, J. P.; Mead, S.; Woodgate, R., Controlling the subcellular localization of DNA polymerases iota and eta via interactions with ubiquitin. *EMBO J.* **2006,** *25* (12), 2847-55.

235. Bienko, M.; Green, C. M.; Crosetto, N.; Rudolf, F.; Zapart, G.; Coull, B.; Kannouche, P.; Wider, G.; Peter, M.; Lehmann, A. R.; Hofmann, K.; Dikic, I., Ubiquitin-binding domains in Y-family polymerases regulate translesion synthesis. *Science* **2005,** *310* (5755), 1821-4.

236. Despras, E.; Delrieu, N.; Garandeau, C.; Ahmed-Seghir, S.; Kannouche, P. L., Regulation of the specialized DNA polymerase eta: Revisiting the biological relevance of its PCNA- and ubiquitin-binding motifs. *Environ. Mol. Mutagen.* **2012,** *53* (9), 752-65.

237. Freudenthal, B. D.; Gakhar, L.; Ramaswamy, S.; Washington, M. T., Structure of monoubiquitinated PCNA and implications for translesion synthesis and DNA polymerase exchange. *Nat. Struct. Mol. Biol.* **2010,** *17* (4), 479-84.

238. Garg, P.; Burgers, P. M., Ubiquitinated proliferating cell nuclear antigen activates translesion DNA polymerases eta and REV1. *Proc. Natl. Acad. Sci. U.S.A.* **2005,** *102* (51), 18361-18366.

239. Dieckman, L. M.; Washington, M. T., PCNA trimer instability inhibits translesion synthesis by DNA polymerase eta and by DNA polymerase delta. *DNA Repair* **2013,** *12* (5), 367-76.

240. Krejci, L.; Altmannova, V.; Spirek, M.; Zhao, X., Homologous recombination and its regulation. *Nucleic Acids Res.* **2012,** *40* (13), 5795-818.

241. Zhuang, Z.; Johnson, R. E.; Haracska, L.; Prakash, L.; Prakash, S.; Benkovic, S. J., Regulation of polymerase exchange between Poleta and Poldelta by monoubiquitination of PCNA and the movement of DNA polymerase holoenzyme. *Proc. Natl. Acad. Sci. U.S.A.* **2008,** *105* (14), 5361-5366.

242. Hendel, A.; Krijger, P. H.; Diamant, N.; Goren, Z.; Langerak, P.; Kim, J.; Reissner, T.; Lee, K. Y.; Geacintov, N. E.; Carell, T.; Myung, K.; Tateishi, S.; D'Andrea, A.; Jacobs, H.; Livneh, Z., PCNA ubiquitination is important, but not essential for translesion DNA synthesis in mammalian cells. *PLoS Genet.* **2011,** *7* (9), e1002262.

243. Calzada, A.; Hodgson, B.; Kanemaki, M.; Bueno, A.; Labib, K., Molecular anatomy and regulation of a stable replisome at a paused eukaryotic DNA replication fork. *Genes Dev.* **2005,** *19* (16), 1905-19.

244. Gotter, A. L., Tipin, a novel timeless-interacting protein, is developmentally co-expressed with timeless and disrupts its self-association. *J. Mol. Biol.* **2003,** *331* (1), 167-76.

245. Unsal-Kacmaz, K.; Chastain, P. D.; Qu, P. P.; Minoo, P.; Cordeiro-Stone, M.; Sancar, A.; Kaufmann, W. K., The human Tim/Tipin complex coordinates an Intra-S checkpoint response to UV that slows replication fork displacement. *Mol. Cell. Biol.* **2007,** *27* (8), 3131-42.

246. Minca, E. C.; Kowalski, D., Replication fork stalling by bulky DNA damage: Localization at active origins and checkpoint modulation. *Nucleic Acids Res.* **2011,** *39* (7), 2610-2623.

247. Noguchi, E., Division of labor of the replication fork protection complex subunits in sister chromatid cohesion and Chk1 activation. *Cell Cycle* **2011,** *10* (13), 2055-2056.

248. Egel, R., DNA replication: Stalling a fork for imprinting and switching. *Curr. Biol.* **2004,** *14* (21), R915-R917.

249. Errico, A.; Costanzo, V., Mechanisms of replication fork protection: A safeguard for genome stability. *Crit. Rev. Biochem. Mol. Biol.* **2012,** *47* (3), 222-235.

250. Leman, A. R.; Noguchi, E., Local and global functions of Timeless and Tipin in replication fork protection. *Cell Cycle* **2012,** *11* (21), 3945-55.

251. Sabbioneda, S.; Gourdin, A. M.; Green, C. M.; Zotter, A.; Giglia-Mari, G.; Houtsmuller, A.; Vermeulen, W.; Lehmann, A. R., Effect of proliferating cell nuclear antigen ubiquitination and chromatin structure on the dynamic properties of the Y-family DNA polymerases. *Mol. Biol. Cell* **2008,** *19* (12), 5193-202.

252. Barnes, R. P.; Hile, S. E.; Lee, M. Y.; Eckert, K. A., DNA polymerases eta and kappa exchange with the polymerase delta holoenzyme to complete common fragile site synthesis. *DNA Repair* **2017,** *57*, 1-11.

253. Gohler, T.; Sabbioneda, S.; Green, C. M.; Lehmann, A. R., ATR-mediated phosphorylation of DNA polymerase eta is needed for efficient recovery from UV damage. *J. Cell Biol.* **2011,** *192* (2), 219-27.

254. Dungrawala, H.; Rose, K. L.; Bhat, K. P.; Mohni, K. N.; Glick, G. G.; Couch, F. B.; Cortez, D., The replication checkpoint prevents two types of fork collapse without regulating replisome stability. *Mol. Cell* **2015,** *59* (6), 998-1010.

255. Yu, C.; Gan, H.; Han, J.; Zhou, Z. X.; Jia, S.; Chabes, A.; Farrugia, G.; Ordog, T.; Zhang, Z., Strand-specific analysis shows protein binding at replication forks and PCNA unloading from lagging strands when forks stall. *Mol. Cell* **2014,** *56* (4), 551-63.

256. Feng, W.; Guo, Y.; Huang, J.; Deng, Y.; Zang, J.; Huen, M. S., TRAIP regulates replication fork recovery and progression via PCNA. *Cell Discov.* **2016,** *2*, 16016.

257. Lau, W. C.; Li, Y.; Zhang, Q.; Huen, M. S., Molecular architecture of the Ub-PCNA/Pol eta complex bound to DNA. *Sci. Rep.* **2015,** *5*, 15759.

258. Livneh, Z.; Ziv, O.; Shachar, S., Multiple two-polymerase mechanisms in mammalian translesion DNA synthesis. *Cell Cycle* **2010,** *9* (4), 729-35.

259. Boehm, E. M.; Powers, K. T.; Kondratick, C. M.; Spies, M.; Houtman, J. C.; Washington, M. T., The proliferating cell nuclear antigen (PCNA)-interacting protein (PIP) motif of DNA polymerase eta mediates its interaction with the C-terminal domain of Rev1. *J. Biol. Chem.* **2016,** *291* (16), 8735-44.

260. Baldeck, N.; Janel-Bintz, R.; Wagner, J.; Tissier, A.; Fuchs, R. P.; Burkovics, P.; Haracska, L.; Despras, E.; Bichara, M.; Chatton, B.; Cordonnier, A. M., FF483-484 motif of human Poleta mediates its interaction with the POLD2 subunit of Poldelta and contributes to DNA damage tolerance. *Nucleic Acids Res.* **2015,** *43* (4), 2116-25.

261. Cannone, G.; Xu, Y.; Beattie, T. R.; Bell, S. D.; Spagnolo, L., The architecture of an Okazaki fragment-processing holoenzyme from the archaeon *Sulfolobus solfataricus*. *Biochem. J.* **2015,** *465* (2), 239-45.

262. Ayyagari, R.; Gomes, X. V.; Gordenin, D. A.; Burgers, P. M., Okazaki fragment maturation in yeast. I. Distribution of functions between FEN1 AND DNA2. *J. Biol. Chem.* **2003,** *278* (3), 1618-25.

263. Riva, F.; Savio, M.; Cazzalini, O.; Stivala, L. A.; Scovassi, I. A.; Cox, L. S.; Ducommun, B.; Prosperi, E., Distinct pools of proliferating cell nuclear antigen associated to DNA replication sites interact with the p125 subunit of DNA polymerase delta or DNA ligase I. *Exp. Cell Res.* **2004,** *293* (2), 357-67.

264. Geertsema, H. J.; Kulczyk, A. W.; Richardson, C. C.; van Oijen, A. M., Single-molecule studies of polymerase dynamics and stoichiometry at the bacteriophage T7 replication machinery. *Proc. Natl. Acad. Sci. U.S.A.* **2014,** *111* (11), 4073-8.

265. Dovrat, D.; Stodola, J. L.; Burgers, P. M.; Aharoni, A., Sequential switching of binding partners on PCNA during *in vitro* Okazaki fragment maturation. *Proc. Natl. Acad. Sci. U.S.A.* **2014,** *111* (39), 14118-23.

266. Hill, T. M.; Marians, K. J., *Escherichia coli* Tus protein acts to arrest the progression of DNA replication forks in vitro. *Proc. Natl. Acad. Sci. U.S.A.* **1990,** *87* (7), 2481-5.

267. Payne, B. T.; van Knippenberg, I. C.; Bell, H.; Filipe, S. R.; Sherratt, D. J.; McGlynn, P., Replication fork blockage by transcription factor-DNA complexes in *Escherichia coli*. *Nucleic Acids Res.* **2006,** *34* (18), 5194-202.

268. Possoz, C.; Filipe, S. R.; Grainge, I.; Sherratt, D. J., Tracking of controlled *Escherichia coli* replication fork stalling and restart at repressor-bound DNA *in vivo*. *EMBO J.* **2006,** *25* (11), 2596-604.

269. Labib, K.; Hodgson, B., Replication fork barriers: Pausing for a break or stalling for time? *EMBO Rep.* **2007,** *8* (4), 346-53.

270. Dalgaard, J. Z.; Klar, A. J., A DNA replication-arrest site RTS1 regulates imprinting by determining the direction of replication at mat1 in *S. pombe*. *Genes Dev.* **2001,** *15* (16), 2060-8.

271. Brewer, B. J.; Fangman, W. L., A replication fork barrier at the 3' end of yeast ribosomal RNA genes. *Cell* **1988,** *55* (4), 637-43.

272. Paeschke, K.; Bochman, M. L.; Garcia, P. D.; Cejka, P.; Friedman, K. L.; Kowalczykowski, S. C.; Zakian, V. A., Pif1 family helicases suppress genome instability at G-quadruplex motifs. *Nature* **2013,** *497* (7450), 458-62.

273. Mirkin, E. V.; Mirkin, S. M., Replication fork stalling at natural impediments. *Microbiol. Mol. Biol. Rev.* **2007,** *71* (1), 13-35.

274. Krasilnikova, M. M.; Mirkin, S. M., Replication stalling at Friedreich's ataxia (GAA)n repeats *in vivo*. *Mol. Cell Biol.* **2004,** *24* (6), 2286-95.

275. Voineagu, I.; Narayanan, V.; Lobachev, K. S.; Mirkin, S. M., Replication stalling at unstable inverted repeats: Interplay between DNA hairpins and fork stabilizing proteins. *Proc. Natl. Acad. Sci. U.S.A.* **2008,** *105* (29), 9936-41.

276. Ketkar, A.; Voehler, M.; Mukiza, T.; Eoff, R. L., Residues in the RecQ C-terminal domain of the human Werner syndrome helicase are involved in unwinding G-quadruplex DNA. *J. Biol. Chem.* **2017,** *292* (8), 3154-3163.

277. Eddy, S.; Tillman, M.; Maddukuri, L.; Ketkar, A.; Zafar, M. K.; Eoff, R. L., Human translesion polymerase kappa exhibits enhanced activity and reduced fidelity two nucleotides from G-quadruplex DNA. *Biochemistry* **2016,** *55* (37), 5218-29.

278. Eddy, S.; Maddukuri, L.; Ketkar, A.; Zafar, M. K.; Henninger, E. E.; Pursell, Z. F.; Eoff, R. L., Evidence for the kinetic partitioning of polymerase activity on G-quadruplex DNA. *Biochemistry* **2015,** *54* (20), 3218-30.

279. Eddy, S.; Ketkar, A.; Zafar, M. K.; Maddukuri, L.; Choi, J. Y.; Eoff, R. L., Human Rev1 polymerase disrupts G-quadruplex DNA. *Nucleic Acids Res.* **2014,** *42* (5), 3272-85.

280. Helmrich, A.; Ballarino, M.; Nudler, E.; Tora, L., Transcription-replication encounters, consequences and genomic instability. *Nat. Struct. Mol. Biol.* **2013,** *20* (4), 412-8.

281. Chang, E. Y.; Stirling, P. C., Replication fork protection factors controlling R-Loop bypass and suppression. *Genes (Basel)* **2017,** *8* (1).

282. Pomerantz, R. T.; O'Donnell, M., What happens when replication and transcription complexes collide? *Cell Cycle* **2010,** *9* (13).

283. Gao, Y. Z.; Mutter-Rottmayer, E.; Zlatanou, A.; Vaziri, C.; Yang, Y., Mechanisms of post-replication DNA repair. *Genes-Basel* **2017,** *8* (2).

284. Bichara, M.; Meier, M.; Wagner, J.; Cordonnier, A.; Lambert, I. B., Postreplication repair mechanisms in the presence of DNA adducts in *Escherichia coli*. *Mutat. Res. Rev. Mutat. Res.* **2011,** *727* (3), 104-122.

285. Liu, B.; Xue, Q.; Tang, Y.; Cao, J.; Guengerich, F. P.; Zhang, H., Mechanisms of mutagenesis: DNA replication in the presence of DNA damage. *Mutat. Res. Rev. Mutat. Res.* **2016,** *768*, 53-67.

286. Boehm, E. M.; Gildenberg, M. S.; Washington, M. T., The many roles of PCNA in eukaryotic DNA replication. *Enzymes* **2016,** *39*, 231-54.

287. Maga, G.; Hubscher, U., Proliferating cell nuclear antigen (PCNA): A dancer with many partners. *J. Cell. Sci.* **2003,** *116* (Pt 15), 3051-3060.

288. Moldovan, G. L.; Pfander, B.; Jentsch, S., PCNA, the maestro of the replication fork. *Cell* **2007,** *129* (4), 665-679.

289. Matsumiya, S.; Ishino, S.; Ishino, Y.; Morikawa, K., Physical interaction between proliferating cell nuclear antigen and replication factor C from *Pyrococcus furiosus*. *Genes Cells* **2002,** *7* (9), 911-922.

290. Jeruzalmi, D.; Yurieva, O.; Zhao, Y.; Young, M.; Stewart, J.; Hingorani, M.; O'Donnell, M.; Kuriyan, J., Mechanism of processivity clamp opening by the delta subunit wrench of the clamp loader complex of *E. coli* DNA polymerase III. *Cell* **2001,** *106* (4), 417-428.

291. Lopez de Saro, F. J.; Georgescu, R. E.; Goodman, M. F.; O'Donnell, M., Competitive processivity-clamp usage by DNA polymerases during DNA replication and repair. *EMBO J.* **2003,** *22* (23), 6408-18.

292. Makarova, K. S.; Koonin, E. V., Archaeology of eukaryotic DNA replication. *Cold Spring Harb. Perspect. Biol.* **2013,** *5* (11), a012963.

293. Hug, L. A.; Baker, B. J.; Anantharaman, K.; Brown, C. T.; Probst, A. J.; Castelle, C. J.; Butterfield, C. N.; Hernsdorf, A. W.; Amano, Y.; Ise, K.; Suzuki, Y.; Dudek, N.; Relman, D. A.; Finstad, K. M.; Amundson, R.; Thomas, B. C.; Banfield, J. F., A new view of the tree of life. *Nat. Microbiol.* **2016,** *1*, 16048.

294. Dore, A. S.; Kilkenny, M. L.; Jones, S. A.; Oliver, A. W.; Roe, S. M.; Bell, S. D.; Pearl, L. H., Structure of an archaeal PCNA1-PCNA2-FEN1 complex: Elucidating PCNA subunit and client enzyme specificity. *Nucleic Acids Res.* **2006,** *34* (16), 4515-4526.

295. Studier, F. W., Protein production by auto-induction in high density shaking cultures. *Protein Expr. Purif.* **2005,** *41* (1), 207-234.

296. Brenlla, A.; Markiewicz, R. P.; Rueda, D.; Romano, L. J., Nucleotide selection by the Y-family DNA polymerase Dpo4 involves template translocation and misalignment. *Nucleic Acids Res.* **2014,** *42* (4), 2555-63.

297. Heltzel, J. M.; Maul, R. W.; Scouten Ponticelli, S. K.; Sutton, M. D., A model for DNA polymerase switching involving a single cleft and the rim of the sliding clamp. *Proc. Natl. Acad. Sci. U.S.A.* **2009,** *106* (31), 12664-12669.

298. Bunting, K. A.; Roe, S. M.; Pearl, L. H., Structural basis for recruitment of translesion DNA polymerase Pol IV/DinB to the beta-clamp. *EMBO J.* **2003,** *22* (21), 5883-5892.

299. Chang, D. J.; Lupardus, P. J.; Cimprich, K. A., Monoubiquitination of proliferating cell nuclear antigen induced by stalled replication requires uncoupling of DNA polymerase and mini-chromosome maintenance helicase activities. *J. Biol. Chem.* **2006,** *281* (43), 32081-8.

300. Davies, A. A.; Huttner, D.; Daigaku, Y.; Chen, S.; Ulrich, H. D., Activation of ubiquitin-dependent DNA damage bypass is mediated by replication protein a. *Mol. Cell* **2008,** *29* (5), 625-36.

301. Edmunds, C. E.; Simpson, L. J.; Sale, J. E., PCNA ubiquitination and REV1 define temporally distinct mechanisms for controlling translesion synthesis in the avian cell line DT40. *Mol. Cell* **2008,** *30* (4), 519-29.

302. Goodman, M. F.; Woodgate, R., Translesion DNA polymerases. *Cold Spring Harb. Perspect. Biol.* **2013,** *5* (10), a010363.

303. Yeeles, J. T.; Marians, K. J., Dynamics of leading-strand lesion skipping by the replisome. *Mol. Cell* **2013,** *52* (6), 855-65.

304. Gabbai, C. B.; Yeeles, J. T.; Marians, K. J., Replisome-mediated translesion synthesis and leading strand template lesion skipping are competing bypass mechanisms. *J. Biol. Chem.* **2014,** *289* (47), 32811-23.

305. Marians, K. J., Lesion bypass and the reactivation of stalled replication forks. *Annu. Rev. Biochem.* **2018,** *87*, 217-238.

306. Taylor, M. R. G.; Yeeles, J. T. P., The initial response of a eukaryotic replisome to DNA damage. *Mol. Cell* **2018,** *70* (6), 1067-1080 e12.

307. Chang, S.; Naiman, K.; Thrall, E. S.; Kath, J. E.; Jergic, S.; Dixon, N. E.; Fuchs, R. P.; Loparo, J. J., A gatekeeping function of the replicative polymerase controls pathway choice in the resolution of lesion-stalled replisomes. *Proc. Natl. Acad. Sci. U.S.A.* **2019,** *116* (51), 25591-25601.

308. Guilliam, T. A.; Yeeles, J. T. P., Reconstitution of translesion synthesis reveals a mechanism of eukaryotic DNA replication restart. *Nat. Struct. Mol. Biol.* **2020,** *27* (5), 450-460.

309. Khare, V.; Eckert, K. A., The proofreading 3'-->5' exonuclease activity of DNA polymerases: a kinetic barrier to translesion DNA synthesis. *Mutat. Res.* **2002,** *510* (1-2), 45-54.

310. Trakselis, M. A.; Cranford, M. T.; Chu, A. M., Coordination and substitution of DNA polymerases in response to genomic obstacles. *Chem. Res. Toxicol.* **2017,** *30* (11), 1956-1971.

311. Fujii, S.; Fuchs, R. P., Defining the position of the switches between replicative and bypass DNA polymerases. *EMBO J.* **2004,** *23* (21), 4342-52.

312. Ripley, B. M.; Gildenberg, M. S.; Washington, M. T., Control of DNA damage bypass by ubiquitylation of PCNA. *Genes (Basel)* **2020,** *11* (2).

313. Zang, H.; Irimia, A.; Choi, J. Y.; Angel, K. C.; Loukachevitch, L. V.; Egli, M.; Guengerich, F. P., Efficient and high fidelity incorporation of dCTP opposite 7,8-dihydro-8-oxodeoxyguanosine by *Sulfolobus solfataricus* DNA polymerase Dpo4. *J. Biol. Chem.* **2006,** *281* (4), 2358-72.

314. Rechkoblit, O.; Malinina, L.; Cheng, Y.; Kuryavyi, V.; Broyde, S.; Geacintov, N. E.; Patel, D. J., Stepwise translocation of Dpo4 polymerase during error-free bypass of an oxoG lesion. *PLoS Biol.* **2006,** *4* (1), e11.

315. Wu, Y.; Wilson, R. C.; Pata, J. D., The Y-family DNA polymerase Dpo4 uses a template slippage mechanism to create single-base deletions. *J. Bacteriol.* **2011,** *193* (10), 2630-6.

316. Fiala, K. A.; Suo, Z., Pre-steady-state kinetic studies of the fidelity of *Sulfolobus solfataricus* P2 DNA polymerase IV. *Biochemistry* **2004,** *43* (7), 2106-15.

317. Beard, W. A.; Batra, V. K.; Wilson, S. H., DNA polymerase structure-based insight on the mutagenic properties of 8-oxoguanine. *Mutat. Res.* **2010,** *703* (1), 18-23.

318. Eoff, R. L.; Irimia, A.; Angel, K. C.; Egli, M.; Guengerich, F. P., Hydrogen bonding of 7,8-dihydro-8-oxodeoxyguanosine with a charged residue in the little finger domain determines miscoding events in *Sulfolobus solfataricus* DNA polymerase Dpo4. *J. Biol. Chem.* **2007,** *282* (27), 19831-43.

319. Pisani, F. M.; De Felice, M.; Carpentieri, F.; Rossi, M., Biochemical characterization of a clamp-loader complex homologous to eukaryotic replication factor C from the hyperthermophilic archaeon *Sulfolobus solfataricus*. *J. Mol. Biol.* **2000,** *301* (1), 61-73.

320. Dionne, I.; Brown, N. J.; Woodgate, R.; Bell, S. D., On the mechanism of loading the PCNA sliding clamp by RFC. *Mol. Microbiol.* **2008,** *68* (1), 216-22.

321. Mondol, T.; Stodola, J. L.; Galletto, R.; Burgers, P. M., PCNA accelerates the nucleotide incorporation rate by DNA polymerase delta. *Nucleic Acids Res.* **2019,** *47* (4), 1977-1986.

322. Sherrer, S. M.; Brown, J. A.; Pack, L. R.; Jasti, V. P.; Fowler, J. D.; Basu, A. K.; Suo, Z., Mechanistic studies of the bypass of a bulky single-base lesion catalyzed by a Y-family DNA polymerase. *J. Biol. Chem.* **2009,** *284* (10), 6379-88.

323. Gadkari, V. V.; Tokarsky, E. J.; Malik, C. K.; Basu, A. K.; Suo, Z., Mechanistic investigation of the bypass of a bulky aromatic DNA adduct catalyzed by a Y-family DNA polymerase. *DNA Repair* **2014,** *21*, 65-77.

324. Gowda, A. S. P.; Krzeminski, J.; Amin, S.; Suo, Z.; Spratt, T. E., Mutagenic replication of N(2)-deoxyguanosine benzo[a]pyrene adducts by *Escherichia coli* DNA polymerase I and *Sulfolobus solfataricus* DNA polymerase IV. *Chem. Res. Toxicol.* **2017,** *30* (5), 1168-1176.

325. Zang, H.; Chowdhury, G.; Angel, K. C.; Harris, T. M.; Guengerich, F. P., Translesion synthesis across polycyclic aromatic hydrocarbon diol epoxide adducts of deoxyadenosine by *Sulfolobus solfataricus* DNA polymerase Dpo4. *Chem. Res. Toxicol.* **2006,** *19* (6), 859-67.

326. Zhang, H.; Eoff, R. L.; Kozekov, I. D.; Rizzo, C. J.; Egli, M.; Guengerich, F. P., Versatility of Y-family *Sulfolobus solfataricus* DNA polymerase Dpo4 in translesion synthesis past bulky N2-alkylguanine adducts. *J. Biol. Chem.* **2009,** *284* (6), 3563-76.

327. Minko, I. G.; Yamanaka, K.; Kozekov, I. D.; Kozekova, A.; Indiani, C.; O'Donnell, M. E.; Jiang, Q.; Goodman, M. F.; Rizzo, C. J.; Lloyd, R. S., Replication bypass of the acrolein-mediated deoxyguanine DNA-peptide cross-links by DNA polymerases of the DinB family. *Chem. Res. Toxicol.* **2008,** *21* (10), 1983-90.

328. Jarosz, D. F.; Cohen, S. E.; Delaney, J. C.; Essigmann, J. M.; Walker, G. C., A DinB variant reveals diverse physiological consequences of incomplete TLS extension by a Y-family DNA polymerase. *Proc. Natl. Acad. Sci. U.S.A.* **2009,** *106* (50), 21137-42.

329. Kusumoto, R.; Masutani, C.; Shimmyo, S.; Iwai, S.; Hanaoka, F., DNA binding properties of human DNA polymerase eta: Implications for fidelity and polymerase switching of translesion synthesis. *Genes Cells* **2004,** *9* (12), 1139-50.

330. McCulloch, S. D.; Kokoska, R. J.; Masutani, C.; Iwai, S.; Hanaoka, F.; Kunkel, T. A., Preferential cis-syn thymine dimer bypass by DNA polymerase eta occurs with biased fidelity. *Nature* **2004,** *428* (6978), 97-100.

331. Lewis, J. S.; Spenkelink, L. M.; Schauer, G. D.; Yurieva, O.; Mueller, S. H.; Natarajan, V.; Kaur, G.; Maher, C.; Kay, C.; O'Donnell, M. E.; van Oijen, A. M., Tunability of DNA polymerase stability during eukaryotic DNA replication. *Mol. Cell* **2020,** *77* (1), 17-25 e5.

332. Margara, L. M.; Fernandez, M. M.; Malchiodi, E. L.; Argarana, C. E.; Monti, M. R., MutS regulates access of the error-prone DNA polymerase Pol IV to replication sites: A novel mechanism for maintaining replication fidelity. *Nucleic Acids Res.* **2016,** *44* (16), 7700-13.

333. Pozhidaeva, A.; Pustovalova, Y.; D'Souza, S.; Bezsonova, I.; Walker, G. C.; Korzhnev, D. M., NMR structure and dynamics of the C-terminal domain from human Rev1 and its complex with Rev1 interacting region of DNA polymerase eta. *Biochemistry* **2012,** *51* (27), 5506-20.

334. Pustovalova, Y.; Magalhaes, M. T.; D'Souza, S.; Rizzo, A. A.; Korza, G.; Walker, G. C.; Korzhnev, D. M., Interaction between the Rev1 C-terminal domain and the PolD3 subunit of polzeta suggests a mechanism of polymerase exchange upon Rev1/Polzeta-dependent translesion synthesis. *Biochemistry* **2016,** *55* (13), 2043-53.

335. Baranovskiy, A. G.; Lada, A. G.; Siebler, H. M.; Zhang, Y.; Pavlov, Y. I.; Tahirov, T. H., DNA polymerase delta and zeta switch by sharing accessory subunits of DNA polymerase delta. *J. Biol. Chem.* **2012,** *287* (21), 17281-7.

336. Lee, Y. S.; Gregory, M. T.; Yang, W., Human Pol zeta purified with accessory subunits is active in translesion DNA synthesis and complements Pol eta in cisplatin bypass. *Proc. Natl. Acad. Sci. U.S.A.* **2014,** *111* (8), 2954-9.

337. Sail, V.; Rizzo, A. A.; Chatterjee, N.; Dash, R. C.; Ozen, Z.; Walker, G. C.; Korzhnev, D. M.; Hadden, M. K., Identification of small molecule translesion synthesis inhibitors that target the Rev1-CT/RIR protein-protein interaction. *ACS Chem. Biol.* **2017,** *12* (7), 1903-1912.

338. Dash, R. C.; Ozen, Z.; McCarthy, K. R.; Chatterjee, N.; Harris, C. A.; Rizzo, A. A.; Walker, G. C.; Korzhnev, D. M.; Hadden, M. K., Virtual pharmacophore screening identifies small-molecule inhibitors of the Rev1-CT/RIR protein-protein Interaction. *ChemMedChem* **2019,** *14* (17), 1610-1617.

339. Wojtaszek, J. L.; Chatterjee, N.; Najeeb, J.; Ramos, A.; Lee, M.; Bian, K.; Xue, J. Y.; Fenton, B. A.; Park, H.; Li, D.; Hemann, M. T.; Hong, J.; Walker, G. C.; Zhou, P., A small molecule targeting mutagenic translesion synthesis improves chemotherapy. *Cell* **2019,** *178* (1), 152-159 e11.

340. Berdis, A. J., Inhibiting DNA polymerases as a therapeutic intervention against cancer. *Front. Mol. Biosci.* **2017,** *4*, 78.

341. Zafar, M. K.; Maddukuri, L.; Ketkar, A.; Penthala, N. R.; Reed, M. R.; Eddy, S.; Crooks, P. A.; Eoff, R. L., A small-molecule inhibitor of human DNA polymerase eta potentiates the effects of cisplatin in tumor cells. *Biochemistry* **2018,** *57* (7), 1262-1273.

342. Ketkar, A.; Maddukuri, L.; Penthala, N. R.; Reed, M. R.; Zafar, M. K.; Crooks, P. A.; Eoff, R. L., Inhibition of human DNA polymerases eta and kappa by indole-derived molecules occurs through distinct mechanisms. *ACS Chem. Biol.* **2019,** *14* (6), 1337-1351.

343. Korzhnev, D. M.; Hadden, M. K., Targeting the translesion synthesis pathway for the development of anti-cancer chemotherapeutics. *J. Med. Chem.* **2016,** *59* (20), 9321-9336.

344. Kort, J. C.; Esser, D.; Pham, T. K.; Noirel, J.; Wright, P. C.; Siebers, B., A cool tool for hot and sour archaea: Proteomics of *Sulfolobus solfataricus*. *Proteomics* **2013,** *13* (18-19), 2831-50.

345. Indiani, C.; O'Donnell, M., The replication clamp-loading machine at work in the three domains of life. *Nat. Rev. Mol. Cell Biol.* **2006,** *7* (10), 751-61.

346. Kim, S.; Dallmann, H. G.; McHenry, C. S.; Marians, K. J., Tau couples the leading- and lagging-strand polymerases at the *Escherichia coli* DNA replication fork. *J. Biol. Chem.* **1996,** *271* (35), 21406-12.

347. Hogg, M.; Osterman, P.; Bylund, G. O.; Ganai, R. A.; Lundstrom, E. B.; Sauer-Eriksson, A. E.; Johansson, E., Structural basis for processive DNA synthesis by yeast DNA polymerase epsilon. *Nat. Struct. Mol. Biol.* **2014,** *21* (1), 49-55.

348. Burgers, P. M. J.; Kunkel, T. A., Eukaryotic DNA replication fork. *Annu. Rev. Biochem.* **2017,** *86*, 417-438.

349. Martin, S. K.; Wood, R. D., DNA polymerase zeta in DNA replication and repair. *Nucleic Acids Res.* **2019,** *47* (16), 8348-8361.

350. van Steeg, H.; Kraemer, K. H., Xeroderma pigmentosum and the role of UV-induced DNA damage in skin cancer. *Mol. Med. Today* **1999,** *5* (2), 86-94.

351. Yoon, J. H.; Prakash, L.; Prakash, S., Highly error-free role of DNA polymerase eta in the replicative bypass of UV-induced pyrimidine dimers in mouse and human cells. *Proc. Natl. Acad. Sci. U.S.A.* **2009,** *106* (43), 18219-24.

352. Masutani, C.; Kusumoto, R.; Yamada, A.; Dohmae, N.; Yokoi, M.; Yuasa, M.; Araki, M.; Iwai, S.; Takio, K.; Hanaoka, F., The XPV (*xeroderma pigmentosum* variant) gene encodes human DNA polymerase eta. *Nature* **1999,** *399* (6737), 700-4.

353. Gratchev, A.; Strein, P.; Utikal, J.; Sergij, G., Molecular genetics of Xeroderma pigmentosum variant. *Exp. Dermatol.* **2003,** *12* (5), 529-36.

354. Wood, R. D., Fifty years since DNA repair was linked to cancer. *Nature* **2018,** *557* (7707), 648-649.

355. O'Connor, M. J., Targeting the DNA damage response in cancer. *Mol. Cell* **2015,** *60* (4), 547-60.

356. Choi, J. S.; Berdis, A., Combating resistance to DNA damaging agents. *Oncoscience* **2018,** *5* (5-6), 134-136.

357. Rocha, C. R. R.; Silva, M. M.; Quinet, A.; Cabral-Neto, J. B.; Menck, C. F. M., DNA repair pathways and cisplatin resistance: An intimate relationship. *Clinics (Sao Paulo)* **2018,** *73* (suppl 1), e478s.

358. Albertella, M. R.; Green, C. M.; Lehmann, A. R.; O'Connor, M. J., A role for polymerase eta in the cellular tolerance to cisplatin-induced damage. *Cancer Res.* **2005,** *65* (21), 9799-806.

359. Zhao, Y.; Biertumpfel, C.; Gregory, M. T.; Hua, Y. J.; Hanaoka, F.; Yang, W., Structural basis of human DNA polymerase eta-mediated chemoresistance to cisplatin. *Proc. Natl. Acad. Sci. U.S.A.* **2012,** *109* (19), 7269-74.

360. Yamanaka, K.; Chatterjee, N.; Hemann, M. T.; Walker, G. C., Inhibition of mutagenic translesion synthesis: A possible strategy for improving chemotherapy? *PLoS Genet.* **2017,** *13* (8), e1006842.

361. Choi, J. S.; Kim, S.; Motea, E.; Berdis, A., Inhibiting translesion DNA synthesis as an approach to combat drug resistance to DNA damaging agents. *Oncotarget* **2017,** *8* (25), 40804-40816.

362. Choi, J. S.; Kim, C. S.; Berdis, A., Inhibition of translesion DNA synthesis as a novel therapeutic strategy to treat brain cancer. *Cancer Res.* **2018,** *78* (4), 1083-1096.

363. Hofmann, K., Ubiquitin-binding domains and their role in the DNA damage response. *DNA Repair* **2009,** *8* (4), 544-56.